Technical Report Documentation Page

1. Report No. FHWA/TX-09/5-4124-01-1	2. Government Accession No.	3. Recipient's Catalog No.
4. Title and Subtitle Implementation Project: Strengthening of a Bridge near Hondo, Texas using Post-Installed Shear Connectors		5. Report Date March 2009 6. Performing Organization Code
7. Author(s) Gunup Kwon, Michael D. Engelhardt, Richard E. Klingner		8. Performing Organization Report No. 5-4124-01-1
9. Performing Organization Name and Address Center for Transportation Research The University of Texas at Austin 3208 Red River, Suite 200 Austin, TX 78705-2650		10. Work Unit No. (TRAIS) 11. Contract or Grant No. 5-4124
12. Sponsoring Agency Name and Address Texas Department of Transportation Research and Technology Implementation Office P.O. Box 5080 Austin, TX 78763-5080		13. Type of Report and Period Covered Technical Report (10/07 – 3/09) 14. Sponsoring Agency Code

15. Supplementary Notes
Project performed in cooperation with the Texas Department of Transportation and the Federal Highway Administration.

16. Abstract

This project was an implementation of research conducted under TxDOT Research Project 0-4124 on the use of post-installed shear connectors to develop composite action in existing non-composite steel bridge girder systems. In this implementation study, an existing non-composite bridge in the San Antonio District was retrofitted with these three types of post-installed shear connectors to increase the load-carrying capacity of the bridge girders. The bridge is located near the town of Hondo, Texas, and is referred to herein as the Hondo Bridge. A detailed design for strengthening the Hondo Bridge was undertaken in this study. Potential design and construction difficulties were identified and solutions to these difficulties were suggested. The bridge consists of three identical simple spans and each span was retrofitted with a different type of post-installed shear connector. A load rating was conducted for the Hondo Bride prior to retrofit, showing an HS10.6 inventory level rating and an HS17.6 operating level rating. With the addition of the post-installed shear connectors, the load rating for the bridge increased to HS17.4 inventory level and HS29.1 operating level. Thus, both the inventory level and operating level load ratings increased 65-percent as a result of the installation of post-installed shear connectors. Field live load tests were conducted to verify the development composite action in the bridge girders after installation of the post-installed shear connectors. Installation of the shear connectors in the Hondo bridge proved more difficult than anticipated. Construction difficulties and possible solutions are discussed in the report.

17. Key Words strengthening, steel girders, retrofit, partial composite, shear studs	18. Distribution Statement No restrictions. This document is available to the public through the National Technical Information Service, Springfield, Virginia 22161; www.ntis.gov.

19. Security Classif. (of report) Unclassified	20. Security Classif. (of this page) Unclassified	21. No. of pages 122	22. Price

Form DOT F 1700.7 (8-72) Reproduction of completed page authorized

Implementation Project: Strengthening of a Bridge near Hondo, Texas using Post-Installed Shear Connectors

Gunup Kwon
Michael D. Engelhardt
Richard E. Klingner

CTR Technical Report:	5-4124-01-1
Report Date:	March 2009
Project:	5-4124
Project Title:	Implementation Project: Bridge Strengthening through the Use of Post-Installed Shear Connectors
Sponsoring Agency:	Texas Department of Transportation
Performing Agency:	Center for Transportation Research at The University of Texas at Austin

Project performed in cooperation with the Texas Department of Transportation and the Federal Highway Administration.

Center for Transportation Research
The University of Texas at Austin
3208 Red River
Austin, TX 78705

www.utexas.edu/research/ctr

Disclaimers

Author's Disclaimer: The contents of this report reflect the views of the authors, who are responsible for the facts and the accuracy of the data presented herein. The contents do not necessarily reflect the official view or policies of the Federal Highway Administration or the Texas Department of Transportation (TxDOT). This report does not constitute a standard, specification, or regulation.

Patent Disclaimer: There was no invention or discovery conceived or first actually reduced to practice in the course of or under this contract, including any art, method, process, machine manufacture, design or composition of matter, or any new useful improvement thereof, or any variety of plant, which is or may be patentable under the patent laws of the United States of America or any foreign country.

Notice: The United States Government and the State of Texas do not endorse products or manufacturers. If trade or manufacturers' names appear herein, it is solely because they are considered essential to the object of this report.

Engineering Disclaimer

NOT INTENDED FOR CONSTRUCTION, BIDDING, OR PERMIT PURPOSES.

Michael D. Engelhardt, Texas P.E. # 88934
Richard E. Klingner, Texas P.E. # 65541
Research Supervisors

Acknowledgements

The authors gratefully acknowledge the financial support provided for this project by the Texas Department of Transportation. The authors extend a special thanks to Jon Kilgore, Clara Carbajal, and Joseph Rohmer of the Texas Department of Transportation for their support, assistance, and advice throughout the entire course of this project.

Table of Contents

List of Figures

List of Tables

Chapter 1. Introduction

1.1 General

A number of older bridges are constructed with floor systems consisting of a non-composite concrete slab over steel girders. A significant number of these bridges were designed based on smaller loads than the standard design loads currently used for new bridges, as specified by the American Association of State Highway and Transportation Officials (AASHTO). The inadequate strength of these bridges can result in the need to limit truck loads on the bridge through load posting, or may require replacement of the bridge. Alternatively, strengthening measures can be undertaken to increase the load rating of the bridge.

A potentially economical means of strengthening these floor systems is to connect the existing concrete slab and steel girders to permit the development of composite action. Composite action permits the existing steel girder and concrete slab to act together more efficiently than in the original non-composite condition. To achieve the benefits of composite action, the existing steel girder must be connected to the existing concrete slab to permit the transfer of shear forces at the steel-concrete interface.

In Texas Department of Transportation (TxDOT) Research Project 0-4124, "Methods to Develop Composite Action in Non-Composite Bridge Floor Systems," extensive experimental and analytical studies were conducted on the use of post-installed shear connectors for strengthening existing non-composite bridge girders. Results of Project 0-4124 are documented in Center for Transportation Report 0-4124-1 (Kwon et al. 2007). The research results on post-installed shear connectors showed that the strength and stiffness of existing non-composite bridge girders can be improved significantly with relatively a small number of post-installed shear connectors.

Of the various types of post-installed shear connectors investigated in Project 0-4124, the most promising, from a structural performance and constructability point of view are the (1) double-nut bolt; (2) adhesive anchor; and (3) high tension friction grip bolt. These connectors consist of high strength bolts or threaded rods placed in holes that are drilled in the concrete slab and top flange of the steel girder. The holes are filled with high strength grout (double-nut bolt and high tension friction grip bolt) or structural adhesive (adhesive anchor). Installation of the double-nut bolt and high-tension friction-grip bolt require construction operations on both the top and bottom sides of the concrete slab. The adhesive anchor, on the other hand, can be completely installed from underneath the slab, thereby minimizing traffic disruptions on the bridge. Tests on these post-installed shear connectors show they have static strength values similar or greater than conventional welded shear studs, and significantly better fatigue performance. The outstanding fatigue performance of the post-installed shear connectors is attributed, in large part, to the fact that no welding is involved in their installation.

The approach developed in TxDOT Project 0-4124 for determining the number of post-installed shear connectors needed to strengthen an existing bridge girder relies on the concept of partial composite design. In new construction, conventional welded shear studs are normally used to achieve composite action. Partial composite design is not normally used for new composite bridge girders, because the number of shear studs needed to satisfy fatigue design requirements typically exceeds the number needed to satisfy static strength requirements based on full composite design. However, because of the outstanding fatigue characteristics of the post-installed shear connectors, fatigue is not likely to control the required number of shear

connectors, thereby enabling partial composite design for strengthening existing non-composite bridge girders. With partial composite design, 50 to 70-percent of the shear connectors normally needed for full composite design can be eliminated, while still achieving a 40 to 50-percent increase in load carrying capacity in positive moment regions of a girder.

Supplemental research conducted by Kwon (2008) after completion of TxDOT Project 0-4124 indicates that concentrating shear connectors near supports or zero moment regions decreases slip at the steel-concrete interface, resulting in an increase of deformation capacity of partially composite beams retrofitted with post-installed shear connectors. More detailed results of Project 0-4124 and the supplemental research studies are documented in Hungerford (2004), Schaap (2004), Kayir (2006), Kwon et al. (2007), and Kwon (2008).

1.2 Objectives and Scope of Implementation Project

An older steel bridge in the San Antonio District was strengthened by post-installing shear connectors, using the techniques developed in Project 0-4124. The specific bridge chosen by TxDOT for this project is located on FM 462 over Live Oak Creek in Medina County in the San Antonio District. The objectives of this implementation project were to demonstrate this strengthening technique on an actual bridge, to evaluate any potential difficulties in the design and construction procedures and suggest solutions, and to evaluate the structural effectiveness of this strengthening methodology. The ultimate goal is to provide a precedent for this strengthening technique that will encourage its use in other bridge rehabilitation projects.

This report consists of six chapters. Chapter 2 provides a brief summary of research findings from Project 0-4124 and from supplemental research (Kwon 2008). Three post-installed shear connection methods and corresponding design equations are introduced. In Chapter 3, design procedures to strengthen existing non-composite bridges using post-installed shear connectors are presented and applied to the case-study bridge. Installation procedures for post-installed shear connectors are also presented. In Chapter 4, the results of two load tests are reported that compare the structural behavior of the bridge before and after the retrofit. Chapter 5 summarizes some additional analytical studies conducted to evaluate the behavior of various composite beams modeled using the finite element method and to refine design recommendations. Finally, Chapter 6 concludes with a summary of the work and design recommendations for strengthening existing non-composite bridge girders using post-installed shear connectors.

Chapter 2. Background: Description of Post-Installed Shear Connectors

2.1 Introduction

The work described in this report was conducted to develop efficient and practical methods to increase the load-carrying capacity of existing non-composite steel bridge girders by using post-installed shear connectors, and to demonstrate the strengthening technique developed in Research Project 0-4124.

As background, this chapter starts with a brief review of previous research on post-installed shear connectors. This chapter also reviews methods to load-rate existing bridges according to the American Association of State Highway and Transportation Officials (AASHTO) *Manual for Condition Evaluation of Bridges* (2003) and *AASHTO Guide Manual for Condition Evaluation and Load and Resistance Factor Rating (LRFR) of Highway Bridges* (2005).

2.2 Selected Post-Installed Shear Connectors

In Project 0-4124, post-installed shear connectors were tested under static and fatigue loading. Three criteria were considered in evaluating the structural performance of the post-installed shear connectors under static loading: strength, stiffness, and slip capacity. Shear connectors were also tested under fatigue loading. Fatigue tests of post-installed shear connectors showed that the post-installed shear connectors which do not require welding have significantly higher fatigue strength than welded shear studs (Kayir 2006, Kwon 2008).

Based on the test results of shear connectors under static and fatigue loadings, three types of post-installed shear connectors were selected for retrofitting existing non-composite steel bridge girders. The three types of post-installed shear connectors are described briefly in this section. Detailed descriptions of test results of the post-installed shear connectors are provided in Hungerford (2004), Schaap (2004), Kayir (2006), and Kwon (2008). The three types of post-installed shear connectors are referred to herein as the *double-nut bolt* (DBLNB), the *high-tension friction-grip bolt* (HTFGB) and the *adhesive anchor* (HASAA). The abbreviations used for each of these post-installed shear connectors is given in parenthesis.

2.2.1 Double-Nut Bolt (DBLNB)

This connection method (Figure 2.1) uses ASTM A193 B7 threaded rod as a connector. The minimum specified ultimate strength of ASTM A193 B7 threaded rod is 125 ksi. The high strength B7 threaded rod was used to increase the capacity of the connector, and thereby reduce the number of connectors installed in a bridge. ASTM A193 B7 threaded rod has rolled threads, which are believed to have better fatigue strength than the SAE J429 – Grade 8 tap bolt with cut threads (Benac 2007).

Installation of the DBLNB connectors requires access from both the top and bottom of the slab. Drilling through both the concrete slab and the steel beam flange can be completed from the top. Tightening of the connector is done underneath the slab using an impact wrench. Two nuts are placed on the connector immediately above the girder flange to help resist twisting of the connector during installation, and to reinforce the connector.

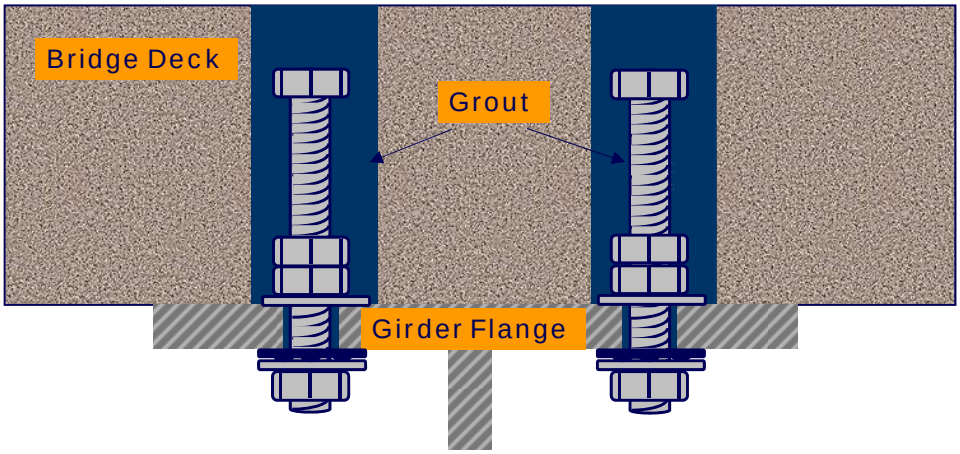

Figure 2.1: Double-Nut Bolt (DBLNB) connector

2.2.2 High-Tension Friction-Grip Bolt (HTFGB)

This shear connection method, shown in Figure 2.2, uses ASTM A325 high-strength bolts as the connector. The minimum specified ultimate strength of the connector material is 120 ksi. Installation of the HTFGB connector requires more steps than the DBLNB connector, since the HTFGB connector requires two different-size holes in the concrete slab.

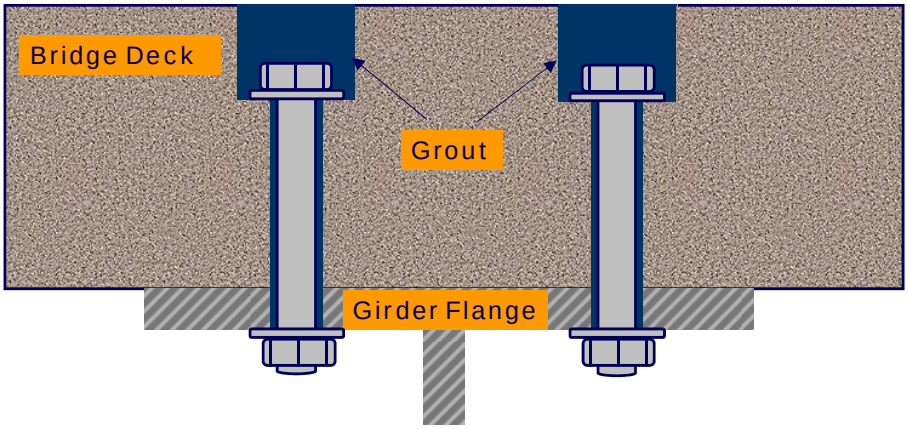

Figure 2.2: High-Tension Friction-Grip Bolt (HTFGB)

2.2.3 Adhesive Anchor (HASAA)

Like the double-nut bolt, this shear connection method (Figure 2.3) also uses ASTM A193 B7 threaded rod as the connector material. Adhesive used for this shear connection method was Hilti HY 150 (Hilti 2006), a two-component adhesive. This shear connection method requires access only from the bottom side of the slab, so that the traffic disruption can be minimized during installation of the connectors.

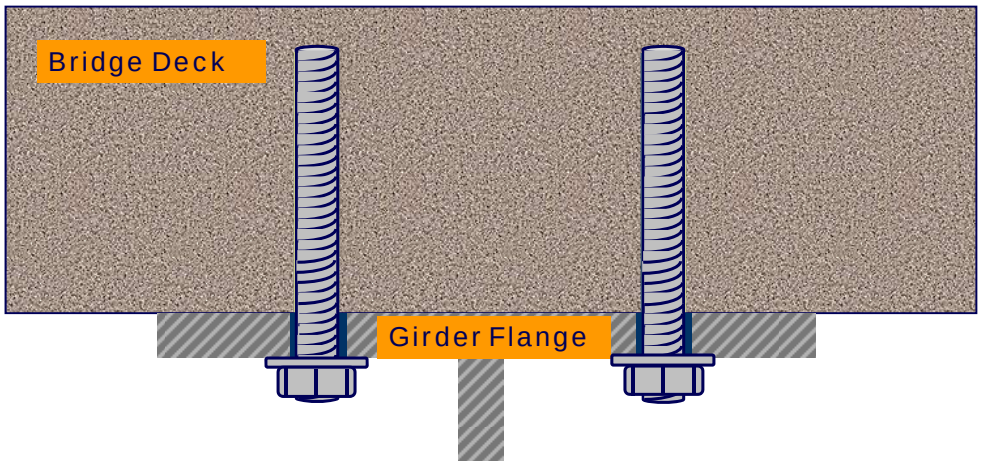

Figure 2.3: Adhesive Anchor (HASAA)

Detailed recommended installation procedures for each of these post-installed shear connectors are provided in Appendix B of this report.

2.3 Recommended Design Equations for Post-Installed Shear Connectors

In Project 0-4124 (Kwon et al. 2007), the structural behavior of post-installed shear connectors was evaluated under static and fatigue loading. Full-scale beam tests were also conducted to evaluate strength, stiffness, and deformation capacity of composite beams retrofitted with post-installed shear connectors.

2.3.1 Static Strength of Post-Installed Shear Connectors

Kayir (2006) compared static test results with current design equations to predict the ultimate strength of conventional welded shear studs and concrete anchors (AASHTO 2007, ACI 2005). None of the equations conservatively predicted the ultimate strength of the post-installed shear connectors measured in static loading tests. Alternatively, Equation 2.1 was proposed to predict the ultimate strength of post-installed shear connectors, Q_u, under static loading.

$$Q_u = 0.5 A_{sc} F_u \tag{2.1}$$

In this equation, A_{sc} is the effective shear area of the connector. The effective shear area of threaded shear connectors can be estimated as 80 percent of gross area of unthreaded connectors. F_u is the tensile strength of the shear connector material (125 ksi for ASTM A193 B7 threaded rod; 120 ksi for ASTM A325 bolts). For the DBLNB, HTFGB, and HASAA connectors, the predicted strength according to Equation 2.1 is 10 to 25% lower than the experimentally measured values. Consequently, Equation 2.1 provides a simple and conservative approach for computing shear strength of the post-installed shear connectors.

2.3.2 Fatigue Strength of Post-Installed Shear Connectors

Both the AASHTO Standard Specifications and the AASHTO LRFD Specifications define fatigue strength of conventional welded shear studs as a function of stress range. The post-installed shear connectors showed superior fatigue strength compared to conventional welded

shear studs (Kayir 2006, Kwon 2008). The fatigue endurance limit for the HTFGB and DBLNB connectors was proposed to be taken as a stress range of 35 ksi (Kwon 2008). Based on this stress range, Equation 2.2 can be used to define the endurance limit for the shear force range on the connector.

$$Z_r = 35ksi \times A_{sc} \tag{2.2}$$

where, Z_r = allowable range of shear force on the connector, kips

A_{sc} = effective shear area of the connector, in.^{2}

The HASAA connector showed lower fatigue strength than the other two shear connection methods (Kayir 2006, Kwon 2008). Based on the test results, Equation 2.3 was recommended for the design of the HASAA connector under fatigue loading (Kwon 2008).

$$Z_r = (77.8 - 8.70 \log N) \times A_{sc} \tag{2.3}$$

where, N = number of cycles of fatigue loading

Since all HASAA shear connectors except one HASAA connector specimen failed under the stress range tested by Kwon (2008), more tests with a lower stress range would be desirable to determine the endurance limit of the HASAA connector.

2.4 Design of Composite Beams

2.4.1 Shear Connection Ratio (Composite Ratio)

Composite action between the concrete slab and steel girders results in an increase in strength and stiffness of the bridge girders compared to non-composite girders. There exist two levels of composite design, fully composite and partially composite, according to the amount of shear force transferred at the steel-concrete interface (Schaap 2004, Hungerford 2004).

Fully composite design is achieved by providing enough shear connectors to transfer the interface shear force when the steel girder is fully yielded or when the concrete slab reaches its full compression capacity. A simple procedure to determine the number of shear connectors required to develop fully composite strength, N_f , is provided in the *AASHTO Standard Specifications* (2002) and the *AASHTO LRFD Specifications* (2007). The same procedure is also provided in the *Specification for Structural Steel Buildings* published by the American Institute of Steel Construction (AISC 2005). This procedure computes the force at the steel-concrete interface when the fully composite cross-section reaches its plastic capacity. In typical design practice, the transformed section is used to calculate deflection under service loads. This is based on the assumption that slip at the steel-concrete interface is negligible at service level loads for a fully composite beam.

A composite beam can be defined as *partially composite* when the number of shear connectors is less than required for fully composite design, so that the interface shear force is limited by the strength of the shear connectors. Thus, the ultimate strength of a partially composite beam is controlled by the strength of the shear connectors. In contrast to fully

composite beams, slip at the steel-concrete can be significant even at service level loads and must be considered when estimating deflections under service loads.

The shear connection ratio, N / N_f (or η) can be defined as the ratio of the number of shear connectors at the steel-concrete interface (N) to the number of shear connectors required for fully composite design (N_f). A shear connection ratio of zero corresponds to zero shear connectors at the steel-concrete interface, and hence to a non-composite beam. A shear connection ratio of 1.0 corresponds to a fully composite design. Shear connection ratios between zero and 1.0 correspond to partially composite designs.

2.4.2 Structural Behavior of Partially Composite Beams

Current AASHTO provisions require composite beams to be designed as fully composite, and have no provisions for partially composite design. In a retrofit situation, however, post-installed shear connectors are likely to be more costly and time-consuming to install than the welded shear studs used in new construction. Because of these higher installation costs, it is preferable to use the minimum number of post-installed shear connectors needed to achieve a desired level of strengthening. This, in turn, suggests the need to design such systems for partially composite action.

Stiffness of Partially Composite Beams under Service Load

The stiffness of a steel-concrete composite beam can be represented by its vertical deflection under service load. A mathematical expression of the load-deflection relationship for partially composite beams was derived by Viest *et al.* (1958). However, this closed form solution is very complex and impractical for design purposes.

A more practical solution for predicting deflection of a composite beam considering slip at the steel-concrete interface was proposed by Johnson and May (1975). For a composite beam with a shear connection ratio of η, a convenient design equation was proposed by a linear interpolation approach. The equation is:

$$v_{part} = v_{full} + \alpha \cdot \left(v_{steel} - v_{full}\right) \cdot \left(1 - \eta\right) \tag{2.4}$$

where: v_{part} = deflection of partially composite beam

v_{full} = deflection of fully composite beam

v_{steel} = deflection of bare steel beam

α = non-dimensional deflection parameter, 0.4 recommended (Oehlers 1995)

η = shear connection ratio $\left(N / N_{full}\right)$

N = number of shear connector in a shear span

N_f = number of shear connectors required for full shear connection

This equation was compared with the results from theoretical composite beam analysis by McGarraugh and Baldwin (1971). This comparison showed that the above equation provides a conservative prediction of deflections for partially composite beams.

The commentary of the AISC *Specification for Structural Steel Buildings* (AISC 2005), hereafter referred to as the *AISC Specification*, provides an equation for the effective moment of

inertia to estimate elastic deflections of partially composite beams. This equation results in the deflection of fully composite beams and bare steel beams, when $\eta = 1$ and $\eta = 0$, respectively. The equation is shown below.

$$I_{eff} = I_s + \sqrt{\left(\sum Q_n / C_f\right)}\left(I_{tr} - I_s\right) \tag{2.5}$$

where: I_s = moment of inertia of the bare steel beam

I_{tr} = moment of inertia of the fully composite beam based on a transformed section

$\sum Q_n$ = summation of the shear strengths of shear connectors between the point of maximum positive moment and the point of zero moment

C_f = compression force in concrete slab for fully composite beam, equal to the smaller of $A_s F_y$ and $0.85 f_c' A_c$

A_c = area of concrete slab within the effective width

Figure 2.4 shows the elastic stiffness of a composite beam with different shear connection ratios derived from Equation 2.5. As shown in Figure 2.4, partially composite beams are much stiffer than non-composite beams. This indicates that a significant decrease in deflection under service load is expected when even a small number of post-installed shear connectors are installed in existing non-composite steel bridge girders.

A similar equation is also provided by AISC (2005) for the effective section modulus, S_{eff}, for the tension flange of the steel section in a partially composite beam. The equation is shown below.

$$S_{eff} = S_s + \sqrt{\left(\sum Q_n / C_f\right)}\left(S_{tr} - S_s\right) \tag{2.6}$$

where: S_s = section modulus of the steel beam

S_{tr} = section modulus of the fully composite beam based on a transformed section

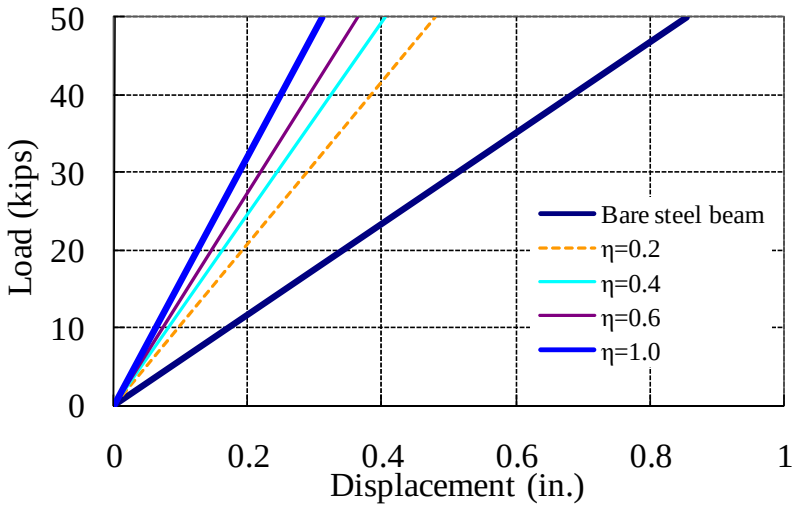

Figure 2.4: Initial stiffness of composite beams (AISC 2005)

Ultimate Load-Carrying Capacity of Composite Beams

The flexural strength of fully and partially composite beams under positive moment can be calculated by simple plastic cross-sectional analysis assuming full yielding in the steel beam and an equivalent rectangular stress block in the concrete slab (Viest 1997). The plastic stress distribution on the cross-section of a composite beam is shown in Figure 2.5. The contribution of the longitudinal reinforcement to the flexural strength of the cross-section for positive moment is normally very small, and is typically neglected.

The compression force C in the concrete slab is the smallest value among the following three equations below.

$$C_1 = A_s F_y \tag{2.7}$$

$$C_2 = 0.85 f_c' A_c \tag{2.8}$$

$$C_3 = \sum Q_n \tag{2.9}$$

where, A_s = area of steel beam

A_c = effective area of concrete slab

Flexural capacity of the composite beam cross-section can then be calculated by computing the moment of the resultant forces in Figure 2.5. For partially composite beams, Equation 2.9 controls the compression force in the concrete slab. For the design of composite beams according to current AASHTO provisions, using Equation 2.9 for the compression force is not allowed. Consequently, partially composite beams are implicitly prohibited by both the AASHTO *Standard Specifications* and the *AASHTO LRFD Specifications*.

The ultimate load-carrying capacity of a composite beam with different shear connection ratios is shown in Figure 2.8. The composite beam used in Figure 2.6 has the same geometry as the full scale beam test specimens tested as part of Project 0-4124 (Kwon et al. 2007). For this composite beam, the steel section was a W30x99 with F_y = 50 ksi; and the concrete slab was 7-ft wide by 7-inch thick with f_c' = 3ksi. A partially composite beam with a low shear connection ratio shows much higher strength than a non-composite beam. For example, a shear connection ratio as low as 30 percent results in a flexural strength increase of about 50 percent.

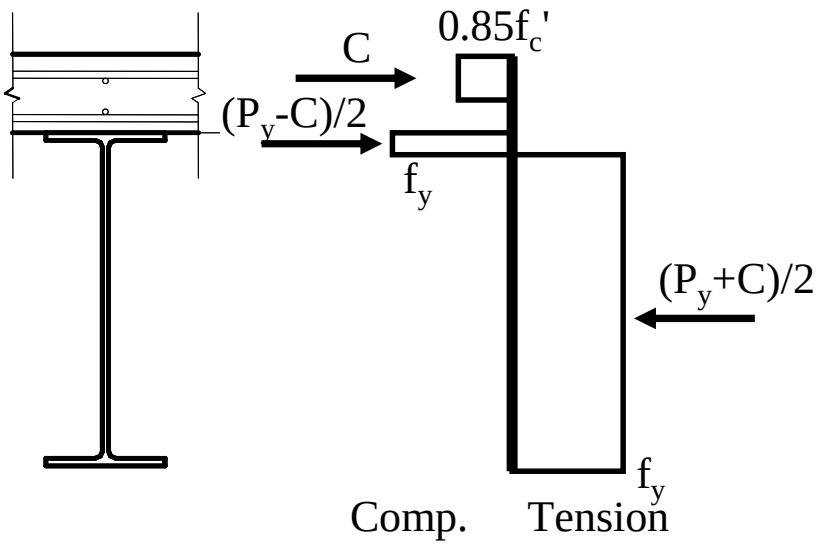

Figure 2.5: Plastic cross-section analysis for composite beams (Viest et al. 1997)

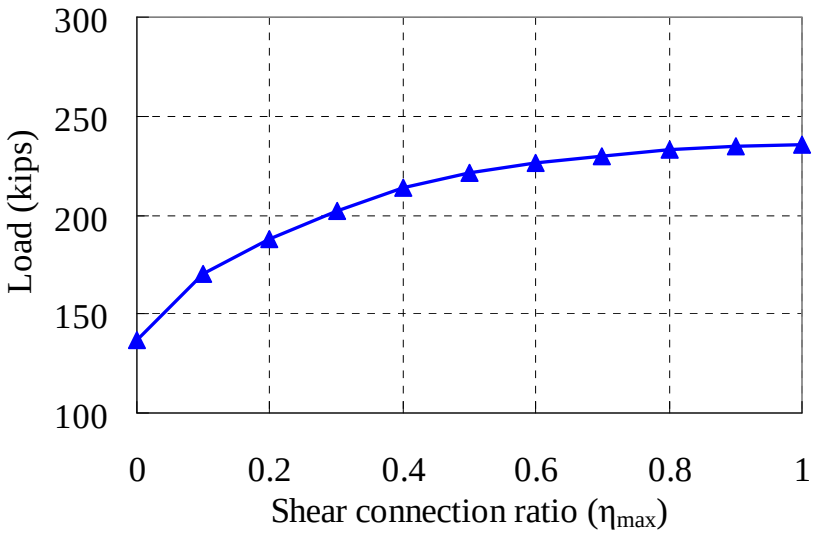

Figure 2.6: Ultimate load-carrying capacity of a composite beam

2.5 Load Rating of Existing Bridge Structures

AASHTO provides standard procedures to evaluate the load-carrying capacity of existing bridge structures. The *AASHTO Manual for Condition Evaluation of Bridges* (2003), hereafter referred to as the *AASHTO Manual for Condition Evaluation*, defines load rating as "the determination of the live load carrying capacity of an existing bridge using existing bridge plans supplemented by information gathered from a field inspection." The specific load ratings are necessary to determine the actual load-carrying capacity of existing bridges and to identify the need for load posting or bridge strengthening (AASHTO 2005). Load rating methods are briefly reviewed below, since these are pertinent to determining the number of post-installed shear connectors needed to strengthen an existing bridge to achieve a desired rating.

2.5.1 Load-Rating using ASD and LFD Methods

The *AASHTO Manual for Condition Evaluation* (AASHTO 2003) provides two levels of load-rating for existing bridges: the Inventory rating level and the Operating rating level. The Inventory rating level evaluates structural capacity corresponding to the design of a new structure, and results in a live load that can be applied for an indefinite period of time. The Operating rating level give the maximum permissible live load for the structures. An unlimited number of cycles of vehicles at the Operating rating level may shorten the life of the bridge (AASHTO 2003).

The *AASHTO Manual for Condition Evaluation* offers two methods for load rating, the allowable stress method, and the load factor method. The allowable stress method limits the stress level in a structure for the actual loadings applied, and the load factor method limits the effect of the factored loads to less than the strength of the structure and the serviceability limits.

To load-rate a bridge, the following procedure is used. The rating factor (RF) is a scale factor which gives the rating of the structure as a fraction of the rating vehicle weight. The load-rating result is usually expressed as the rating vehicle multiplied by the rating factor. For example, if an HS 20 truck loading were used for the load rating and the rating factor were 0.8, the bridge load rating would be $0.8 \times HS\,20 = HS16.0$. The rating factor is calculated using the following equation:

$$RF = \frac{C - A_1 D}{A_2 L(1+I)} \tag{2.10}$$

where, C = the capacity of the member
D = the effect of dead load
L = the effect of live load
I = the impact factor for live load
A_1 = factor for dead loads
A_2 = factor for live load

For the allowable stress method, A_1 and A_2 are equal to 1.0 for both the Inventory rating level and the Operating rating level. For the load factor method, A_1 is equal to1.3 and A_2 is equal to 2.17 for the Inventory rating level, and A_1 and A_2 are both equal to 1.3 for the Operating rating level. A rating factor must be established for all members and components of a bridge, and the lowest value among these controls the load rating.

2.5.2 Load-rating using LRFR

AASHTO also provides load rating procedures using the Load and Resistance Factor Rating method in the *Guide Manual for Condition Evaluation and Load and Resistance Factor Rating (LRFR) of Highway Bridges* (AASHTO 2005), hereafter referred to as the *AASHTO LRFR Manual for Condition Evaluation*. There are three different load-rating procedures according to the live-load model used for the load-rating: Design load rating, Legal load rating, and Permit load rating.

The Design load rating is based on the HL-93 loading and checks the strength of the structure using LRFD-based calculations. HL-93 loading consists of the design truck and design lane loads. Bridges with a Design load rating factor $RF \geq 1.0$ have satisfactory load rating for all legal loads (AASHTO 2005). The Legal load rating is the load rating for AASHTO and State legal loads. Finally, the Permit load rating evaluates the structure for safety and serviceability for vehicles above the legally established weight limitations (AASHTO 2005).

To load-rate a bridge, the following equation is used for the LRFR load rating method.

$$RF = \frac{C - (\gamma_{DC})(DC) - (\gamma_{DW})(DW) \pm (\gamma_p)(P)}{(\gamma_L)(LL + IM)} \tag{2.11}$$

For the strength limit states: $C = \varphi_c \varphi_s \varphi R_n$

For the service limit states: $C = f_R$

where, f_R = allowable stress in the *AASHTO LRFD Specifications*

R_n = nominal member resistance

DC = dead load effect due to structural components and attachments

DW = dead-load effect due to wearing surface and utilities

P = permanent loads other than dead loads

LL = live-load effect

IM =dynamic load allowance

γ_{DC} = LRFD load factor for structural components and attachments

γ_{DW} = LRFD load factor for wearing surfaces and utilities

γ_p = LRFD load factor for permanent loads

γ_L = evaluation live-load factor

φ_c = condition factor

φ_s = system factor

φ = LRFD resistance factor

The load and resistance factors are specified in the *AASHTO LRFR Manual for Condition Evaluation*. The load rating result is also reported as the product of a rating truck multiplied by the rating factor.

2.6 Need for Partial Composite for Strengthening Bridge Girders

The AASHTO composite beam design provisions are intended for new construction using welded shear studs, and are based on past research on these systems. Further, the current AASHTO specifications recognize fully composite design only, not partially composite design. The absence of provisions for partially composite design in AASHTO likely reflects the fact that fatigue design requirements for welded shear studs normally result in a large number of shear connectors that will typically lead to a fully composite beam for static strength calculations. Thus, partially composite design is not normally used for bridge girders. By contrast, partially composite design is used on a routine basis for composite beams in buildings, and the *AISC*

Specification (2005) has included detailed design provisions for partially composite beams for many years. The different approaches to composite beam design in bridges versus buildings (bridges normally use fully composite beams; buildings normally use partially composite beams) likely reflects the dominating influence of fatigue in design of the composite beams for bridges, and the absence of fatigue considerations in design of composite beams for buildings.

When considering the development of composite action in existing non-composite bridge girders, a number of changes from conventional bridge design practice are needed. The welded shear stud, commonly used in new construction, is not likely to be a practical alternative as a post-installed shear connector due to its relatively low fatigue strength. Thus, the current practice of using welded shear studs must be changed to enable the use of unconventional shear connectors.

Economical strengthening of existing non-composite beams requires adopting partially composite design. The cost of post-installed shear connectors for an existing bridge is likely to be higher than the cost of welded shear studs for new construction. Fully composite design will therefore likely be very costly for strengthening existing bridges. Thus, the economic viability of strengthening existing non-composite bridges by post-installing shear connectors will depend largely on the ability to implement partially composite design. Tests conducted in Project 0-4124 (Kayir 2006, Kwon 2008) showed that the post-installed shear connectors has significantly higher fatigue strength than conventional welded shear studs, and this high fatigue strength enables to use partially composite design for retrofitting existing non-composite bridges using post-installed shear connectors.

Full-scale beam test and supplemental finite element analysis (Kwon 2008) indicated that installation of shear connectors concentrated near zero moment regions can reduce slip at the steel-concrete interface, resulting in larger deformation capacity than the composite beams with uniformly distributed shear connectors. Concentration of shear connectors near zero moment regions is also beneficial for construction point of view, since the construction area can be minimized during the retrofit projects.

Chapter 3. Design Process and Installation of Post-Installed Shear Connectors

3.1 Introduction

From previous research on TxDOT Project 0-4124, it appears that post-installed shear connectors can be an effective means for strengthening existing non-composite bridge girders. This chapter describes design and installation procedures for strengthening the case study bridge using post-installed shear connectors. The number of shear connectors needed to achieve various target levels of strength increase considering both static and fatigue design checks on the connectors are evaluated.

This study was undertaken with the advice and assistance of TxDOT engineers to select the case study bridge, to provide drawings and other data on the bridge, and to identify target load rating levels for the retrofitted bridge.

3.2 Description of the Case Study Bridge

The specific bridge chosen for this case study is located on a two-lane rural road near the city of Hondo, Texas, and crosses a small creek. Hondo is located approximately 40 miles west of San Antonio. For purposes of this case study, the bridge will be referred to as the Hondo Bridge. Figure 3.1 shows several photographs of the bridge. The bridge was built in 1950 and the measured Average Daily Traffic (ADT) in 2006 was 900 vehicles. The bridge consists of three simple spans, and the superstructure is constructed with a non-composite concrete floor slab over rolled steel wide-flange girders. The current load ratings for this bridge were sufficiently low that load posting of the bridge may be needed. Consequently, TxDOT was interested in improving the load rating to maintain the bridge in continued service, without the need to limit vehicle weights through load posting. Because the existing concrete deck and steel girders were still in good condition, and because all spans were simply supported, this bridge was chosen as a case study for strengthening with post-installed shear connectors.

The Hondo Bridge is a steel-girder bridge with three spans: each is about 40-ft long, with simply supported girders. The bridge is skewed at an angle of 30 degrees and consists of four girders in the transverse direction (Figure 3.2). The girders are connected by periodic cross-frames. Figure 3.3 and Figure 3.4 show a typical section through the girders and slab. The steel sections used for the bridge are W26x85 and the concrete slab is approximately 6.25-in. deep. The W26x85 section is no longer produced and does not appear in modern steel manuals. The cross-section dimensions are available in older steel manuals, and are shown in Figure 3.4.

The girders are located at a 7-ft spacing. The concrete slab was cast on top of the slab without any shear connectors at the steel-concrete interface, meaning the superstructure was designed non-compositely. No. 4 reinforcing bars were placed longitudinally at an 18-in. spacing. In the transverse direction, No.6 reinforcing bars were placed at a 9-in. spacing.

The material properties of the concrete slab and the steel girders were not reported in the available drawings of the bridge. The *AASHTO Manual for Condition Evaluation* provides recommendations for the yield stress of the steel girders and the compressive strength of the concrete slab based on the year the bridge was built. The recommended yield stress of the steel girders and the compressive strength of the concrete slab for load-rating were 33 ksi and 2.5 ksi, respectively for a bridge constructed in 1950 (AASHTO 2003).

Figure 3.1: The Hondo case-study bridge

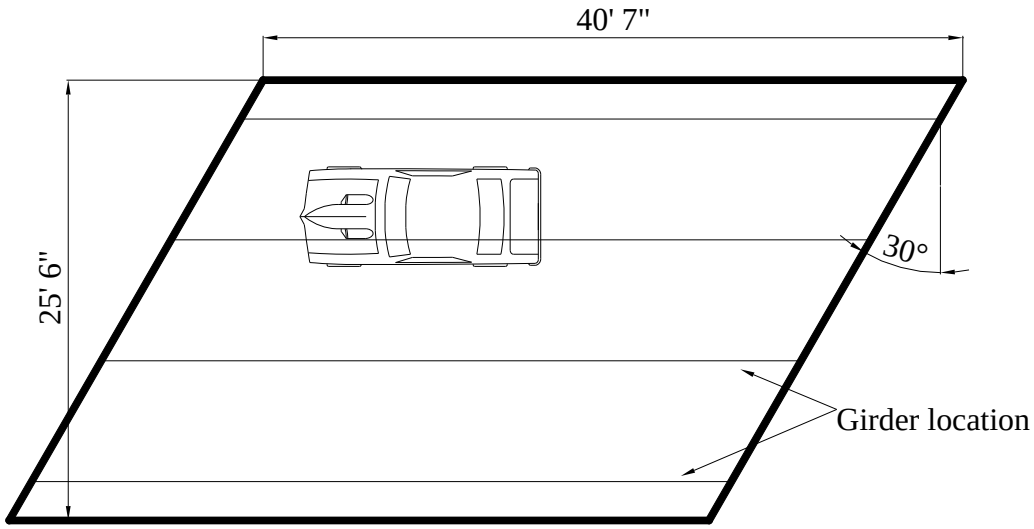

Figure 3.2: Top view of a typical span of the Hondo Bridge

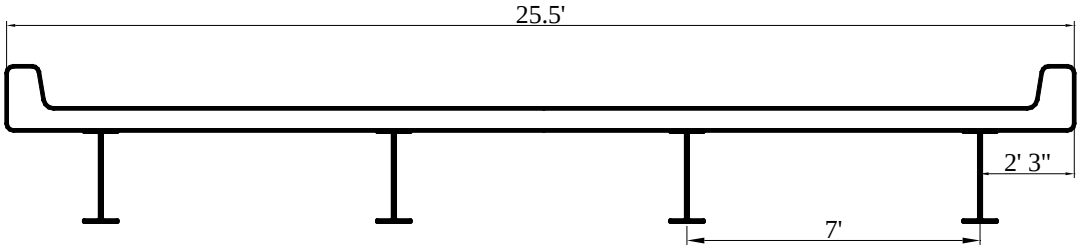

Figure 3.3: Section details for the Hondo Bridge

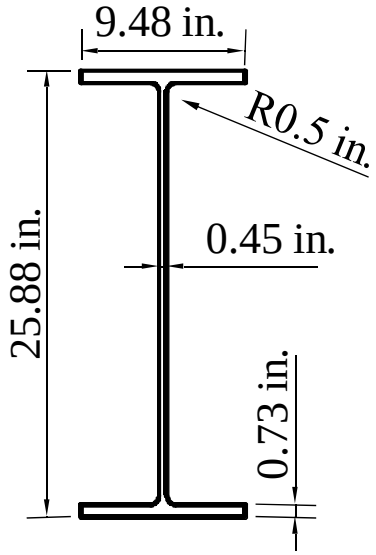

Figure 3.4: Cross-section dimensions of W26x85 bridge girder

3.3 AASHTO Load-Rating for Existing Non-Composite Bridge Girders

3.3.1 General AASHTO Load Rating Approach

The Hondo Bridge was load-rated, using an HS 20 truck load, to assess the need for strengthening. In addition to the truck load, the *AASHTO Manual for Condition Evaluation of Bridges* (AASHTO 2003) requires evaluation of the bridge with the Standard AASHTO HS lane load. However, the truck load controlled in all cases for this relatively short span bridge. Only the interior girders were load-rated since the interior girders were more severely loaded than the exterior girders.

The Hondo Bridge was load-rated using the load factor method in the *AASHTO Manual for Condition Evaluation*. As required by that method, the bridge was evaluated for both strength and serviceability criteria. As further required by that method, ratings were computed at both the Inventory and the Operating levels. The rating results shown in Table 3.1 are based on girder moments and stresses computed using conventional load rating calculation methods. Details of these calculations are presented in Appendix A. The Operating rating level is less than HS 20, indicating that the bridge is required to be posted for load.

Table 3.1: Load rating of Hondo bridge before retrofit—based on standard AASHTO calculations

Rating level		Rating results
Inventory rating	Strength	HS 12.0
	Serviceability	HS 10.6 (Controls)
Operating rating	Strength	HS 20.0
	Serviceability	HS 17.6 (Controls)

3.3.2 Load Rating based on Finite Element Analysis

Previous research (Bowen and Engelhardt 2003) has shown that conventional load rating calculations often overestimate girder moments and stresses. A more accurate assessment of bridge structural response can be obtained by developing detailed finite element models of the bridge floor system. The more accurate analysis provided by finite element models can result in higher load ratings. In the case of the Hondo Bridge, a finite element model was developed to investigate if a significantly improved load rating is possible through more accurate prediction of structural response. The superstructure of the bridge was modeled using the general purpose finite element program ABAQUS (2007). Figure 3.5(a) shows the ABAQUS model of four girders in a span. The concrete floor slab is not shown in this view for clarity. The girders were modeled using ABAQUS shell elements and the diaphragms and the cross-frames connecting the girders were modeled using the ABAQUS connector elements. Figure 3.5(b) shows the concrete slab, which was modeled using shell elements. The modeling techniques are described by Kwon (2008).

For purposes of load rating, the transverse locations of the design trucks in the ABAQUS model were determined by the lever rule. In the transverse direction, the two design trucks were placed at a 4-ft spacing. One wheel line was placed on top of the girder to be load-rated, as shown in Figure 3.6. In the longitudinal direction, the second wheel of the design truck was placed 28 in. away from the midspan of the load-rated girder. For a simply supported beam, to produce the maximum moment in the girder, the wheel loads are placed so that the centerline of the span bisects the line between the centroid of the wheel loads and the point where the central wheel load is applied (Taly 1998). To account for the effect of the dead load, the yield stress was reduced in proportion to the dead load. The maximum moment due to dead load was 146.7 ft-kips as shown in Appendix A. The load factor A_1 for load-rating is 1.3 and the plastic section modulus of the girder is 245 in.^{3}. In ABAQUS, the yield stress of the steel girder was reduced to $33-1.3\times146.7\times12/245=23.7ksi$. This method was also used to in Project 0-4124 and showed good agreement with the tests.

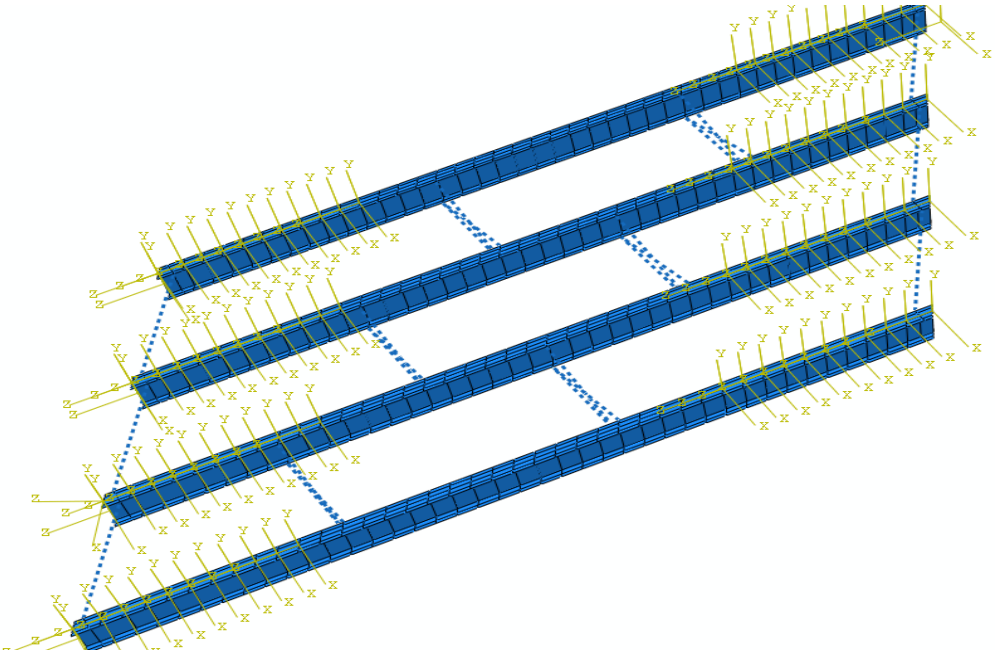

(a) Steel girders, cross-frames and diaphragms

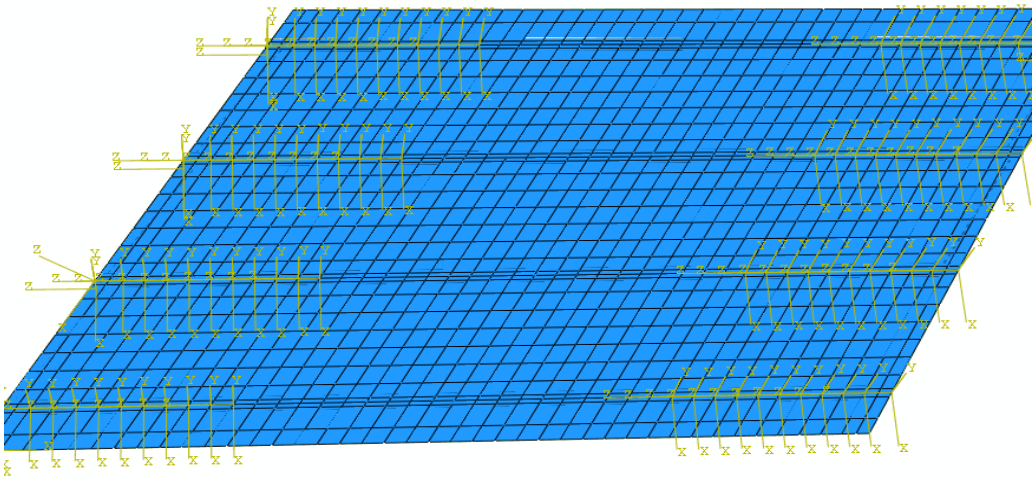

(b) Concrete slab

Figure 3.5: ABAQUS model of the Hondo Bridge

From the ABAQUS analysis, load-deflection plots of the Hondo Bridge before retrofitting are shown in Figure 3.7. The deflection was measured under the center wheel of the load-rated girder. The load factor ($A_2 \cdot (1+I) \cdot RF$) on the vertical axis is the ratio of the applied load to the standard HS 20 design truck load. The load factor 1 means the bridge is loaded with the two standard HS 20 design trucks as shown in Figure 3.6(a). The ABAQUS analysis was stopped after widespread cracking was predicted in the concrete slab elements, beyond which point the solution could not converge. This point was taken as the analytical equivalent of failure. Note from Figure 3.7 that the load-deflection curve was nearly flat at this point.

Consequently, although the finite element solution did not converge beyond the last point shown in the plot, this point likely was close to the actual maximum capacity of the bridge. Longitudinal stresses predicted by ABAQUS are shown in Figure 3.8. As expected, the neutral axis of each girder is located near mid-depth. The maximum load factor is 2.64. The load factor A_2 is 2.17 for the Inventory rating level and 1.3 for the Operating rating level. The impact factor I is 0.3 for the bridge. Based on the ABAQUS analysis, the load rating results for the AASHTO strength criterion are therefore $2.64/2.17/1.3\times(HS20)=HS18.7$ for the Inventory rating level and $2.64/1.3/1.3\times(HS20)=HS31.3$ for the Operating rating level.

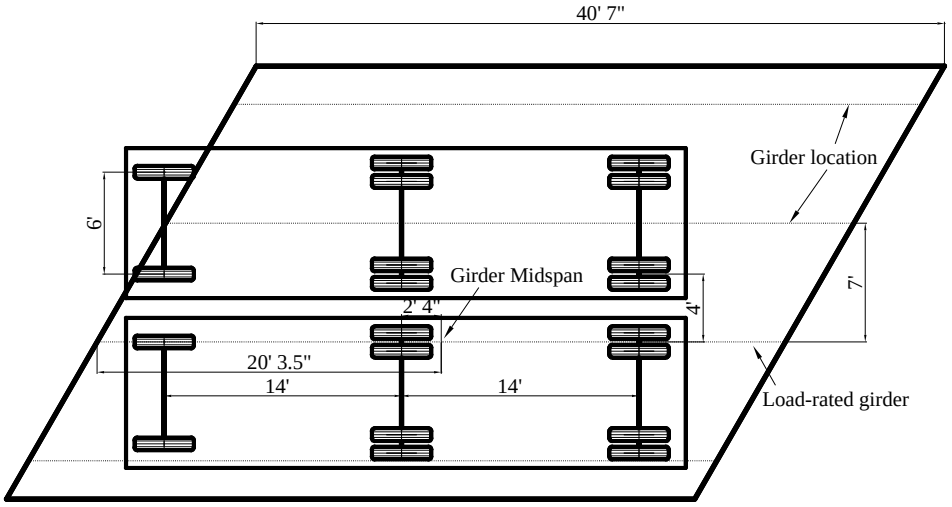

(a) Top view

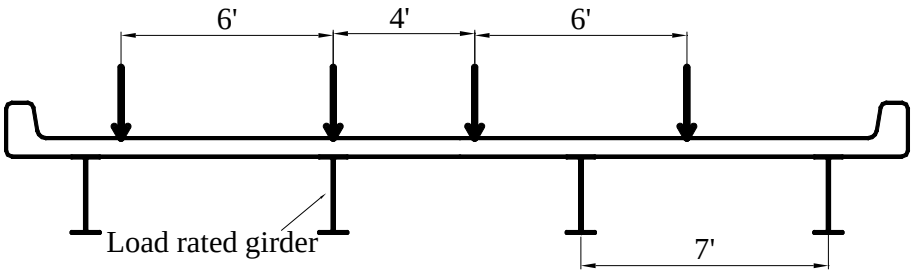

(b) Section view

Figure 3.6: Standard design truck locations for load rating using ABAQUS

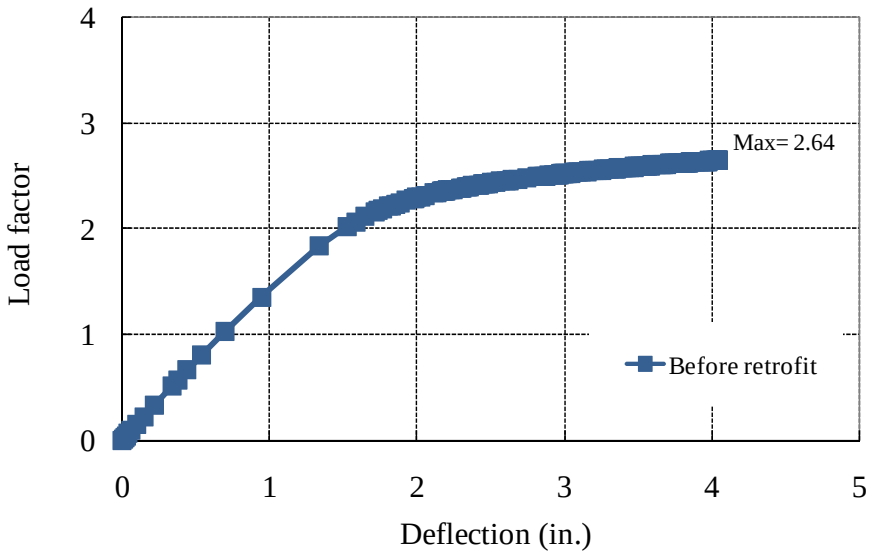

Figure 3.7: Load-deflection relations for the Hondo Bridge (before retrofitting)

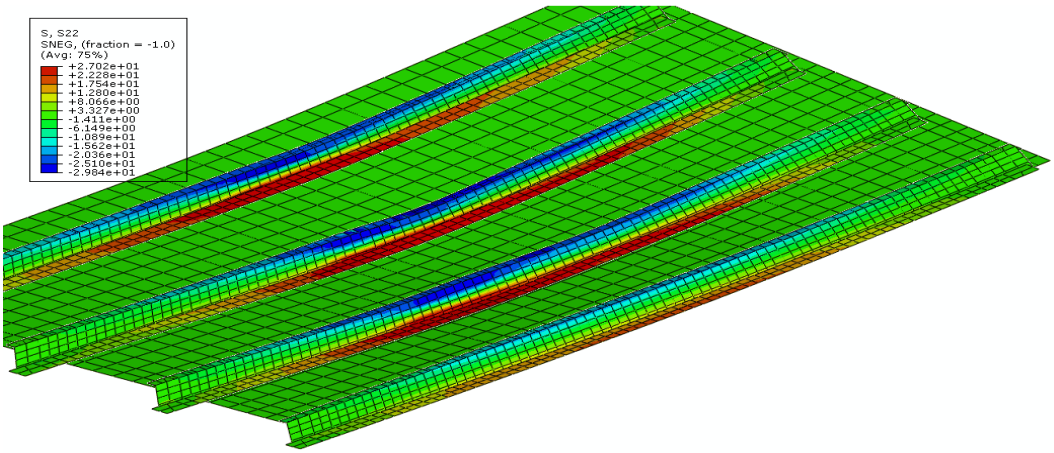

Figure 3.8: Longitudinal stress distribution of the Hondo Bridge (non-composite)

Serviceability of the bridge was also checked for overload vehicles. The AASHTO Standard Specifications require that the maximum stress in the beam flange not exceed $0.8F_y$ for non-composite beams. Since the dead load was resisted only by the steel girders, the four steel girders without the concrete slab were modeled in ABAQUS and distributed loads were applied on the steel beams representing the dead loads of the steel girders and the concrete slab. The maximum stress due to the dead loads was 8.76 ksi. Figure 3.9 shows the longitudinal stress distribution due to the dead loads in the girders. Then the live load, including the impact factor, was applied on the whole bridge model. The maximum stress due to the live load was 18.10 ksi and the structure remained in the elastic range. The rating factor for the serviceability criterion for the Operating rating level can be determined as shown below.

$$\frac{C-D}{L(1+I)} = \frac{0.8\times 33 - 8.76}{18.10} = 0.97 \qquad (3.1)$$

where, C = the capacity of the member
D = the effect of dead load
L = the effect of live load
I = the impact factor for live load

With the overload $1.67L(1+I)$ for the Inventory rating level, the sum of the stresses due to dead load and the live load was over 33 ksi, which is not acceptable. Therefore, the rating factor for the Inventory level was determined by dividing Eq. 3.1 by 1.67, which resulted in 0.58. The rating results for the serviceability criteria were HS 11.7 and HS 19.5 for the Inventory level and the Operating level, respectively. Table 3.2 compares the rating results from the general AASHTO approach with the finite element method. It is worth noting that the serviceability criterion controls the rating results. As indicated by the data in Table 3.2, by going from the standard AASHTO calculation approach to the finite element analysis, the Inventory rating increased from HS 10.6 to HS 11.7, and the Operating rating increased from HS 17.6 to HS 19.5. Thus, both the Inventory and Operating ratings increased by about 10 percent by using finite element analysis. However, even with the improved load ratings derived by the finite element analysis, the Operating rating is still below HS 20, and some strengthening measures are still needed to avoid load posting the bridge.

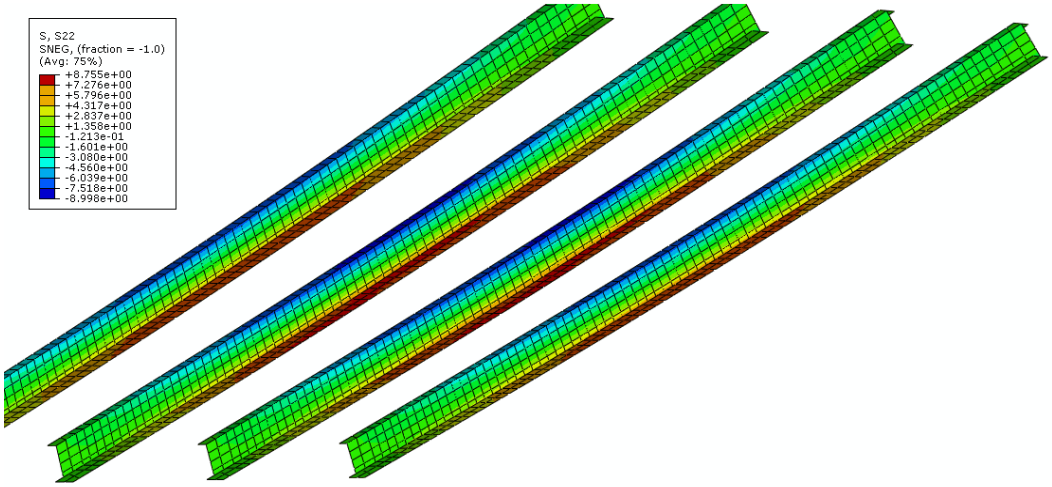

Figure 3.9: Longitudinal stress distribution due to dead load

Table 3.2: Load rating of Hondo bridge before retrofit—Comparison of standard AASHTO calculations with ABAQUS analysis

Rating method	Rating level		Rating results
Standard AASHTO approach	Inventory rating	Strength	HS 12.0
		Serviceability	HS 10.6 (Controls)
	Operating rating	Strength	HS 20.0
		Serviceability	HS 17.6 (Controls)
ABAQUS analysis	Inventory rating	Strength	HS 18.7
		Serviceability	HS 11.7 (Controls)
	Operating rating	Strength	HS 31.3
		Serviceability	HS 19.5 (Controls)

3.4 Strengthening the Hondo Bridge by Post-Installed Shear Connectors

3.4.1 General Design Approach

As noted above, according to the general AASHTO load-rating method as well as the ABAQUS analysis, the bridge showed rating results lower than HS 20 at the Operating rating level. Consequently, an increase in the load rating was desired for this bridge, and a system of post-installed shear connectors was designed to provide an increased load rating. This section describes the procedures used to determine the number and location of post-installed shear connectors required for retrofitting. Based on discussions with TxDOT personnel, the goal of this retrofit was, as a minimum, to increase the Operating level rating above HS 20. It was also desired to substantially increase the Inventory level rating, although there was no specific target for the Inventory level rating, and an HS 20 Inventory level rating was not required.

For purposes of this retrofit design, it was assumed that the post-installed shear connectors are 7/8-in. in diameter and made of high strength steel with a specified ultimate tensile strength F_u of 125 ksi. The ultimate shear strength of the connector is taken as 50 percent of the specified tensile strength, and the effective shear area is taken as 80 percent of the gross area, as recommended in Section 2.3.1. This resulted in a specified ultimate shear strength for each connector of 30.1 kips. Details of this strength calculation are provided in Appendix A.

Based on simple plastic cross-section analysis, it is possible to determine the moment capacity of a partially composite girder as a function of the shear connection ratio. Figure 3.10 shows the results for this analysis for the Hondo Bridge girders. A maximum 70-percent increase in flexural capacity can be achieved by installing shear connectors for full composite design (shear connection ratio of 1.0). To achieve this fully composite design, 56 shear connectors are

required for each girder (28 shear connectors in a shear span). For a preliminary design, it was decided to provide a sufficient number of shear connectors to achieve a 50-percent shear connection ratio, and then determine the resulting increase in the bridge load rating. A 50-percent shear connection ratio requires 28 shear connectors in a bridge girder (14 shear connectors in a shear span), and will result in an approximately 55 percent increase in its flexural capacity. The shear connectors will be installed near the supports at a 12-in. spacing to reduce slip at the steel-concrete interface, and thereby increase the ductility of the retrofitted partially composite bridge girders (Kwon 2008). The layout and the numbering of the post-installed shear connectors are shown in Figure 3.11.

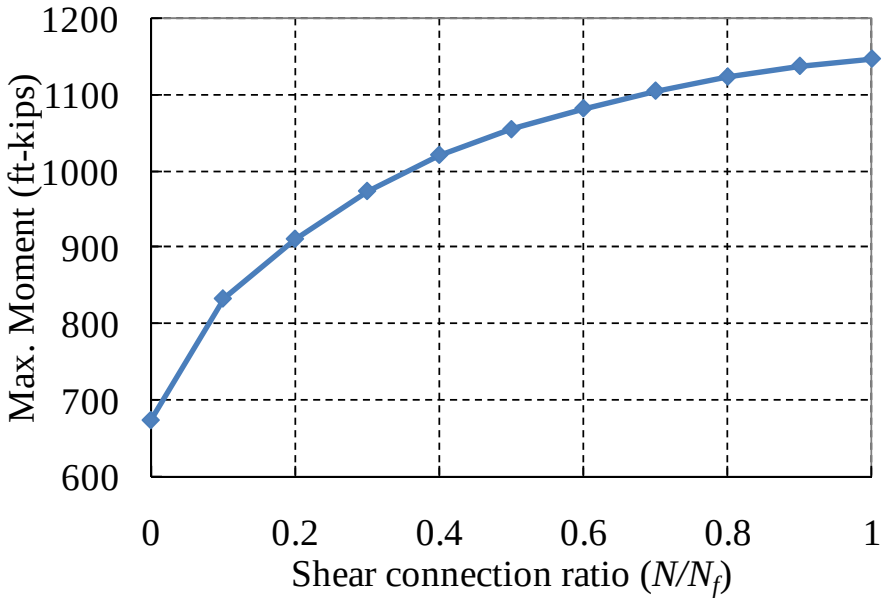

Figure 3.10: Load-carrying capacity vs. shear connection ratio for girder in Hondo Bridge

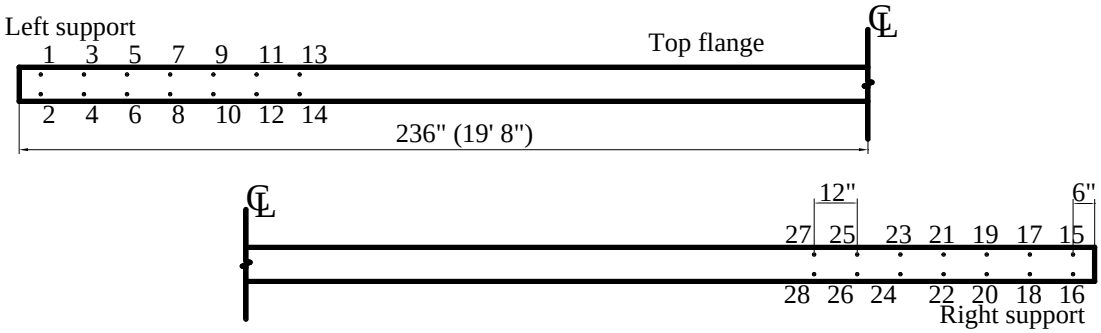

Figure 3.11: Shear connector layout for Hondo Bridge

The strengthened bridge girders were then load-rated, using procedures presented step-by-step in Appendix A. The ultimate strength of the retrofitted girder was calculated using simple plastic analysis. The flexural capacity of the girder was increased by 57 percent. Based on the AASHTO strength criterion, the load rating of the strengthened bridge girders was HS 21.5 for the Inventory rating level and HS 35.9 for the Operating rating level.

The AASHTO serviceability criterion was also checked to load-rate the strengthened bridge girders. To evaluate the serviceability of the bridge girders, it is required to calculate the beam flange stress under overload vehicles. The current AASHTO provisions (AASHTO 2002, AASHTO 2005) do not address partially composite design, and so no guidelines are available for checking the stress in the steel beam flange for partially composite beams.

In building construction, partially composite design is very common practice. The commentary of the *AISC Specification* (2005) provides an equation for the effective section modulus, S_{eff} , for partially composite beams. This equation (shown as Equation 2.6 in this report) can be used to compute the maximum stress in the steel beam flange under service load. Using the effective section modulus, the maximum stress in the steel beam flange under overload vehicles was determined for the load rating. For the serviceability criterion, the rating results were HS 17.4 for the Inventory rating level and HS 29.1 for the Operating rating level. For the original non-composite bridge, the corresponding ratings were HS 10.6 and HS 17.6 for the Inventory and Operating level ratings for the existing bridge (Table 3.1), based on standard AASHTO load rating techniques.

Fatigue strength of the shear connectors was also checked under the standard HS 20 design truck loading. For this case study, TxDOT requested that the shear connectors resist at least 2,000,000 loading cycles. For the DBLNB and HTFGB connectors, the fatigue endurance limit, 35 ksi, as shown in Equation 2.2 was used for the design check of the shear connectors under fatigue loads. For the HASAA connector, the S-N curve proposed in Equation 2.3 was used, which resulted in an allowable stress range of 23.0 ksi for 2 million cycles.

For new bridge construction, shear connectors are typically installed along the full span of the girders. To compute the stress range on the shear connectors for the fatigue design check, the HS 20 truck loads are moved along the bridge span and the shear flow is determined at various locations of the beam. Shear flow is normally calculated based on a transformed fully composite cross-section. From the shear flow, the stress on the shear connector can be computed.

For the retrofitted partially composite bridge girders, the calculation of the shear force on the connectors is not as straightforward as for conventional fully composite bridge girders, for two reasons. First, it is unclear if the conventional calculation of shear flow based on a transformed fully composite section is appropriate for a partially composite girder. Second, the shear connectors are installed only near the supports, resulting in uncertainty regarding the manner in which the shear flow is converted to shear force on the connectors. In order to provide a simple estimate of the shear force on the connectors in the partially composite girders, the shear flow was computed using a fully composite transformed section. Interface shear force at the steel-concrete interface is then computed from shear flow multiplied by the length over which the shear flow acts. The shear flow can be obtained from the shear force diagram using the transformed section. The interface shear force where shear connectors are installed is assumed to be distributed equally among the shear connectors. The interface shear force where shear connectors are not installed is assumed to be equally resisted by the shear connectors in the same shear span. Figure 3.12(a) shows the bridge girder loaded with the HS 20 design wheel load located 4 ft away from the left support. The wheel loads in Figure 3.12(a) include the impact factor and distribution factor. The corresponding shear force diagram is also shown in Figure 3.12(b) along with the shear connector locations. In the left shear span, the interface shear force corresponding to Area 1 is assumed to be resisted by the 8 shear connectors under the shear force diagram. The shear force corresponding to Area 2 is assumed to be equally distributed to the 14 shear connectors in the shear span. In the right shear span, the same design approach is applied.

Full details of the procedures used to compute shear force on the connectors and to evaluate the fatigue strength of the connectors in the strengthened partially composite bridge girders are shown in Appendix A.

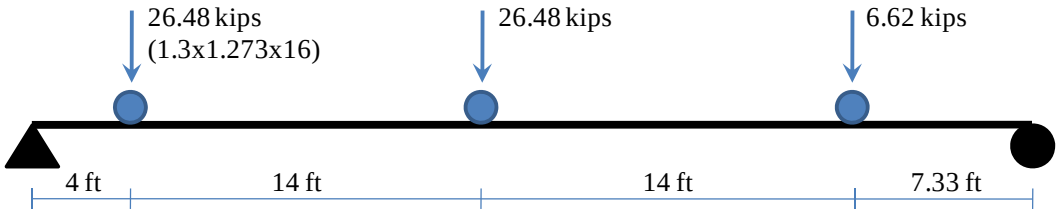

(a) HS 20 truck wheel locations

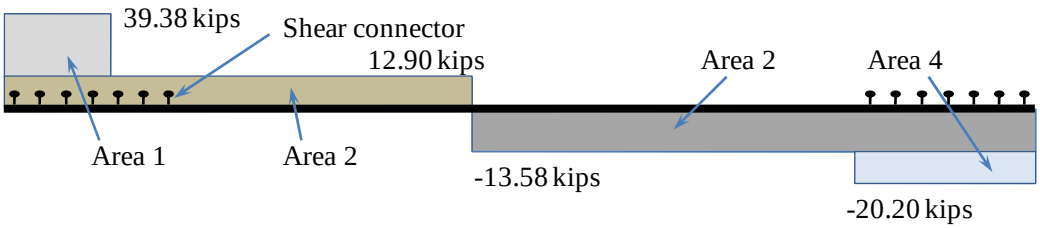

(b) Shear force diagram and connector locations

Figure 3.12: Connector force calculation for fatigue loading

The shear force on the connectors computed based on the simplified assumptions described above were compared with the shear force on the connectors predicted by the ABAQUS model of the retrofitted girder. In ABAQUS, a simply supported composite beam with the same geometry as the Hondo Bridge was modeled. Twenty-eight shear connectors were included in the ABAQUS model using the connector element. The HS 20 truck load was applied on the beam, 4 ft away from the left support. In the ABAQUS model, the load was applied and removed several times. For each load cycle, the predicted shear force at each connector changed by a small amount. This likely occurred due a small degree of inelasticity at the connectors under HS 20 loading. After about 20 cycles of loading, the predicted shear force at the connectors stabilized, and very little change occurred under further cycling. Consequently, the shear force at each connector predicted by ABAQUS after 20 cycles of loading was taken as the best analytical estimate of connector shear force.

Table 3.3 shows the force in each shear connector obtained from the finite element analysis and from the hand calculation method described above. The shear force in the connectors based on the simplified hand calculations significantly exceeded the connector shear force computed in ABAQUS for connectors near the supports. For connectors further away from the supports, the hand calculations and the ABAQUS predictions matched reasonably well. Further studies are needed to establish simple methods for computing the shear force in the connectors of a partially composite girder with connectors located only near the ends. Nonetheless, it appears that the simple hand calculations provide a conservative prediction of connector shear force.

Under fatigue loading for the Hondo Bridge, the maximum stress range that the shear connectors experienced was 30.62 ksi based on the hand calculations of connector shear force. Details of the calculations are provided in Appendix A. The computed value of 30.62 ksi is less

than the endurance limit of 35 ksi, meaning that the 14 shear connectors in a shear span satisfy fatigue strength requirement for the DBLNB and HTFGB connectors under the HS 20 design truck loading. For the HASAA connector, the maximum stress range is higher than 23.0 ksi allowable stress range for 2-million cycles, as computed from Eq. 2.3. Thus, more shear connectors are needed to reduce the stress range in the HASAA connectors. Several iterations showed that fifty-two HASAA connectors are needed for each bridge girder to satisfy the fatigue load requirements. Note that more than 120 conventional welded shear connectors in a bridge girder would be needed to satisfy the fatigue requirements for the Hondo Bridge.

If the shear force range on the HASAA connectors predicted by finite element analysis were used a basis for design, then the predicted stress range would be less than 23 ksi, and no more HASAA connectors would be needed than DBLNB or HTFGB connectors. That is, 14 connectors in a shear span (28 connectors per girder) would have been sufficient for all three types of connectors. However, for the purposes of this implementation project, the basis for checking the fatigue strength requirements for all three connectors was taken to be the simplified and conservative hand calculation method described above. This choice was made since it was assumed that finite element analysis would not normally be done for a bridge strengthening project. Consequently, it was decided to proceed with the installation of 52 HASAA connectors per girder.

Table 3.3: Connector force (kips) predicted by ABAQUS under cyclic loading

Connector Number		1, 2	3, 4	5, 6	7, 8	9, 10	11, 12	13, 14
Number of cycles	1	8.12	8.09	7.97	7.55	6.87	6.77	7.34
	5	8.10	8.10	7.97	7.52	6.75	6.74	7.35
	10	8.10	8.10	7.97	7.51	6.73	6.70	7.26
	15	8.09	8.10	7.96	7.51	6.71	6.67	7.19
	20	8.09	8.09	7.96	7.50	6.70	6.65	7.15
Hand Calculation		13.13	13.13	13.13	13.13	7.30	7.30	7.30

27, 28	25, 26	23, 24	21, 22	19, 20	17, 18	15, 16	Connector Number	
10.33	8.80	7.71	6.99	6.53	6.25	6.09	1	Number of cycles
8.97	8.86	8.08	7.26	6.73	6.41	6.22	5	
7.90	8.71	8.41	7.50	6.91	6.56	6.36	10	
7.27	8.47	8.64	7.68	7.05	6.67	6.46	15	
6.89	8.18	8.81	7.81	7.15	6.76	6.53	20	
10.62	10.62	10.62	10.62	10.62	10.62	10.62	Hand Calculation	

3.4.2 Load Rating of Retrofitted Hondo Bridge based on Finite Element Analysis

ABAQUS was also used to load-rate the strengthened girders of the Hondo Bridge. To simulate the behavior of shear connectors, the connector element in ABAQUS was used to model the shear connectors installed in the bridge girders. The three criteria, static strength, serviceability, and fatigue strength, were taken into account to load-rate the strengthened bridge girders as in the hand calculation procedure in the previous section.

A load-deflection graph for the strengthened bridge is shown in Figure 3.13 along with the graph of the non-composite bridge before the strengthening. A load factor ($A_2 \cdot (1+I) \cdot RF$) instead of the applied load value was used in the vertical axis. Failure of the loaded ABAQUS model was also defined as the development of widespread cracks in the concrete slab, resulting in failure to achieve convergence of the solution. No shear connector failure was detected in the analysis model, meaning that the load could have been increased further past the point of non-convergence. As shown in Figure 3.13, the strength of the bridge was improved significantly by installing post-installed shear connectors. The maximum load factor obtained from the analysis was 3.62, which resulted in the rating of $3.62/2.17/1.3 \times HS20 = HS25.7$ for the Inventory

rating level and $3.62/1.3/1.3\times HS20 = HS42.9$ for the Operating rating level. Figure 3.14 shows the longitudinal stress distribution in the composite girders after the strengthening. As expected, the neutral axis is located near the top flange of the beam due to partial composite action.

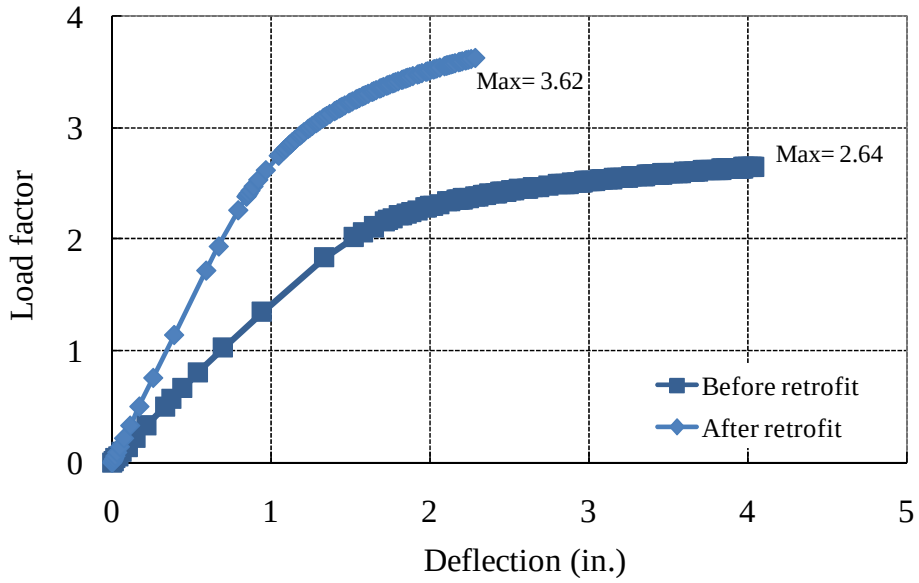

Figure 3.13: Analytically predicted load-deflection relations for Hondo Bridge (after retrofitting)

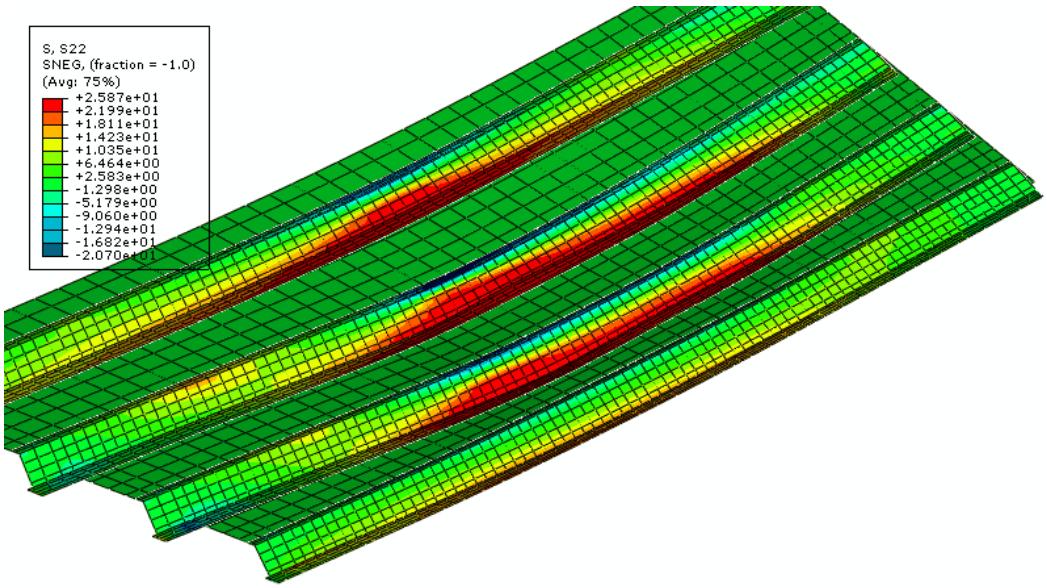

Figure 3.14: Longitudinal stress distribution of the Hondo Bridge (after retrofit)

For serviceability, the *AASHTO Standard Specifications* require that the maximum stress in the steel beam flange be less than $0.95F_y$ for overload vehicles, when composite beams are used. To load-rate the Hondo Bridge for this serviceability criterion, the HS 20 truck loading without load factor was applied to obtain the maximum stress in the steel beam flange. The maximum stress in the beam flange under the dead loads was 8.76 ksi as derived for the non-composite bridge girders. The maximum stress in the steel beam flange under the AASHTO HS 20 standard truck loads was 14.7 ksi, which resulted in a rating of $(0.95\times 33-8.76)/14.69\times HS20 = HS30.7$ for the Operating rating level and $HS30.7/1.67 = HS18.4$ for the Inventory rating level. The load rating results of the strengthened bridge girders are summarized in Table 3.4. It should be noted that the increase in load rating that is achieved by the installation of post-installed shear connectors comes from two sources. The first source of increased load rating is the increase in flexural capacity that is achieved by the development of partial composite action, resulting from the installation of shear connectors. The second source of increased load rating is the increase in allowable steel stress from $0.80F_y$ to $0.95F_y$ for the required serviceability check.

Table 3.4: Load rating of strengthened composite bridge girders

Rating method	Rating level		Rating results
Standard AASHTO approach	Inventory rating	Strength	HS 21.5
		Serviceability	HS 17.4 (Controls)
	Operating rating	Strength	HS 35.9
		Serviceability	HS 29.1 (Controls)
ABAQUS analysis	Inventory rating	Strength	HS 25.7
		Serviceability	HS 18.4 (Controls)
	Operating rating	Strength	HS 42.9
		Serviceability	HS 30.7 (Controls)

3.5 Installation of Post-Installed Shear Connectors

Constructability of post-installed shear connectors is an issue when selecting shear connection methods. Installation procedures adopted in this study could be used in other field applications or could be modified according to equipment availability and specific conditions at a bridge. A description of the shear connector installation procedures used for the Hondo Bridge is provided in the following sections and in Appendix B.

3.5.1 Shear Connection Methods and Connector Locations

The bridge consists of three simply supported spans. A different shear connection method was used for each span for the bridge in order to gain experience with each method. Figure 3.15 shows a schematic drawing of the bridge and the shear connection method applied for each span. For the first two spans from the left, 28 shear connectors were installed in each girder. The last span which was retrofitted with the HASAA connectors had 52 shear connectors for each girder. The longitudinal spacing of the shear connectors was 12 in. and the shear connectors were

installed in pairs (one on each side of the beam web) at each longitudinal section, as shown in Figure 3.16.

For the Hondo Bridge, all construction operations for the bridge strengthening were done by TxDOT maintenance personnel. Recommended installation procedures were prepared for use by TxDOT personnel. Appendix B shows the detailed installation procedures recommended for each type of post-installed shear connector. These recommended procedures were based on experiences from constructing large-scale test specimens for Project 0-4124, along with subsequent discussions with TxDOT personnel.

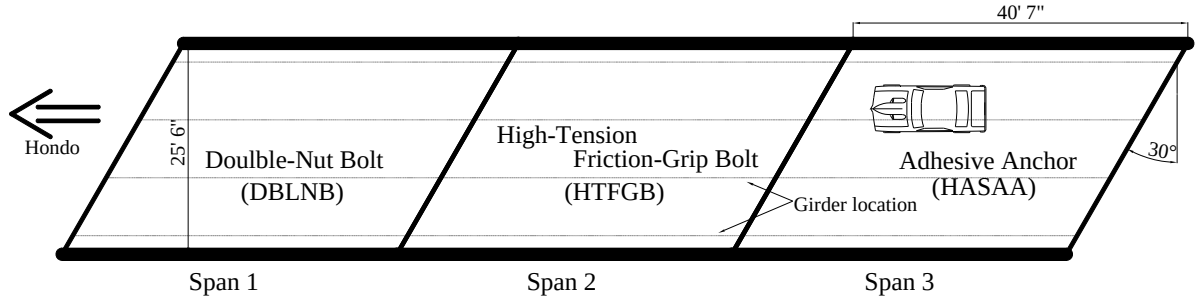

Figure 3.15: Overall layout of the Hondo Bridge

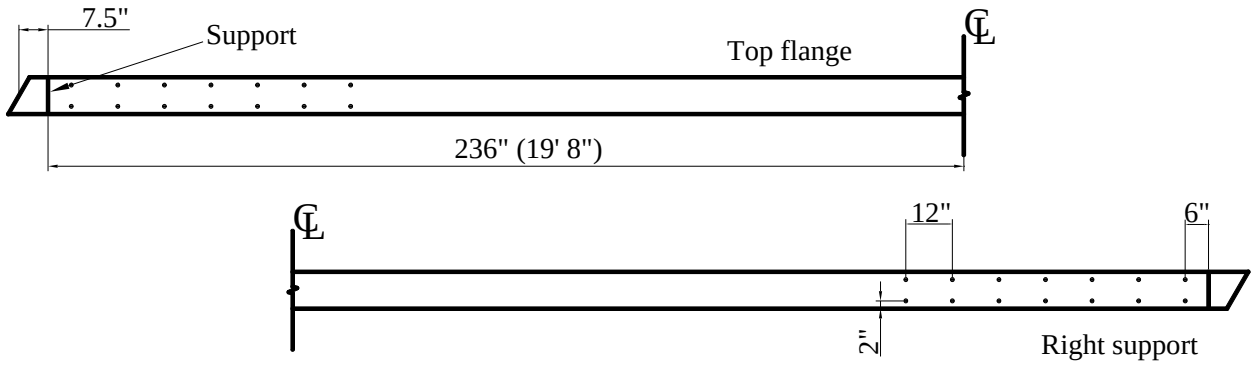

(a) Shear connector locations for the DBLNB and HTFGB connectors

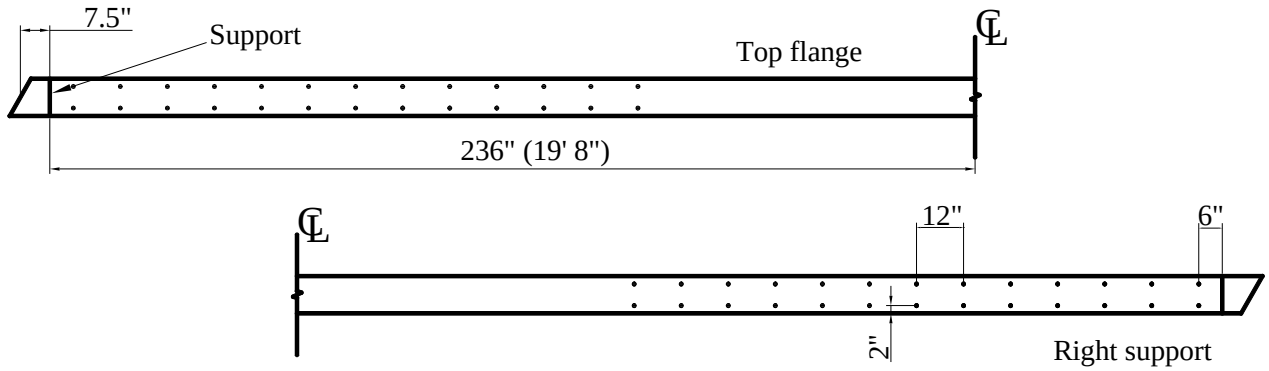

(b) Shear connector locations for the HASAA connectors

Figure 3.16: Typical shear connector locations in each girder

3.5.2 Experiences from Actual Installation

Figures 3.17 to 3.19 show several views of the Hondo Bridge after installation of the post-installed shear connectors. Figure 3.17 shows a view of the HASAA connectors installed in an interior girder in the south span of the bridge. Thirteen pairs of HASAA connectors were installed at each end of each girder in the south span (52 connectors per girder). Figure 3.18 shows the DBLNB connectors an exterior girder of the north span. Seven pairs of DBLNB connectors were installed at each end of each girder in the north span (28 connectors per girder). Finally, Figure 3.19 shows exterior girders in the north span (left portion of photo) and the center span (right portion of the photo). Thirteen pairs of HTFGB connectors were installed at each end of each girder in the center span (28 connectors per girder). Note that all three types of connectors had the same visual appearance form the bottom on the bridge. That is, the visible portion of each connector consists of a threaded fastener with a nut. As can be seen in Figure 3.18, the fasteners were located at the girder ends. The middle portion of each girder had no fasteners. As discussed earlier, locating the fasteners near the girder ends enhances the ductility of the strengthened girders.

After completion of installation of all the shear connectors at the Hondo Bridge, discussions were held with TxDOT personnel involved with the construction operations on problems encountered in the project. Following is a brief summary of key comments:

- In general, the difficulty and time required to install the shear connectors was significantly greater than anticipated before the project.
- A periodic problem that was encountered was hitting reinforcing bars in the concrete slab during drilling or coring operations. Hitting reinforcing bars was particularly problematic when drilling through the slab from underneath with a hammer drill, as was needed for the HASAA connector.
- The HASAA connector required drilling through the top flange of the steel beam. This drilling was done from underneath the bridge, using a magnetically mounted drill attached to the underside of the top flange. For the wide flange shapes used on this bridge, the underside of the top flange was tapered. Note that for modern wide-flange shapes, the underside of the top flange is flat and parallel to the top side of the flange. However, in many older steel shapes, the flanges have a slight taper, and this was the case at the Hondo Bridge. Because of the flange taper, the magnetically mounted drill was not vertical. Consequently, the drill bit was not exactly perpendicular to the top side of the top flange. This resulted in the need for the drill bit to cut though some concrete in order to complete the hole in the steel flange. This, in turn, resulted in rapid wear in drill bits, which slowed construction and increased cost.
- When the adhesive was placed in the hole for the HASAA connectors, the adhesive had a tendency to run out of the holes and onto the threads of the connector. This made it difficult subsequently to install the nuts on the connectors.
- Difficulties were encountered when installing the HTFGB connectors due to significant variability in the thickness of the concrete slab over the entire bridge deck. In cases where the slab was somewhat thinner, the bolt extended further from the bottom of the hole in the top flange. In some cases, the bolts extended far enough so that the unthreaded portion of the bolt extended beyond the underside of

the top flange. In order to properly install the nuts, it was necessary to add several washers to the bottom of the bolt.

- The construction personnel reported that they found the DBLNB connector the easiest of the three methods to install. However, they indicated that they preferred to use a standard high-strength ASTM A325 headed bolt rather than the ASTM A193 B7 all threaded rod which was called for in the recommended installation procedure (Appendix B). The installation procedure called for the use of A193 B7 all-thread rod, with a nut placed near the top to resist uplift of the deck. Two nuts (double-nuts) are also provided directly above the steel flange to reinforce the connector and to prevent rotation of the connector while the nut is installed from underneath. The experience at the Hondo Bridge was that the double-nuts did not prevent rotation of the connector during installation of the nut from underneath the bridge. Consequently, in order to prevent rotation, it was necessary to weld the nut to the top of the threaded rod, so this could be held with a wrench during tightening operations.

Based on the construction experience at the Hondo Bridge, the following suggestions are provided for future installations:

- It may be advisable to attempt to approximately locate reinforcing bars in the deck prior to installation of the shear connectors. The original bridge drawings can be used as a guide as to the general layout and spacing of reinforcing bars. This information can be augmented by the use of non-destructive reinforcing bar locator equipment. Although the reliability of “Rebar Locators” is uncertain, this equipment can likely provide some additional useful information. Finally, the use of some small pilot holes in the slab may help locate reinforcing bars.

- The HASAA connector requires drilling through the top flange of the steel beam from underneath the bridge. This is normally done using a magnetically mounted drill. When the underside of the top flange is slanted, as was the case at the Hondo Bridge, it may be possible to use taper steel shims between the magnetic mounting surface of the drill and the underside of the flange. These shims can be used to keep the drill bit perpendicular to the top side of the steel flange. This should help reduce wear on the drill bits.

- For the HASAA connector, problems with the adhesive running out of the hole can be reduced by proper selection of adhesive. It should be noted that problems with the adhesive running out of the holes were not encountered in the construction of the large-scale test specimens in Project 0-4124. However, based on discussions with TxDOT personnel, it appears that the adhesive used at the Hondo Bridge was different than that used in Project -4124 and different than was recommended in Appendix B. The adhesive used in Project 0-4124 and recommended in Appendix B was Hilti HIT HY 150 adhesive. While other adhesives are likely acceptable for this application, care should be taken in choosing alternatives, as strength, durability and installation characteristics can vary widely among adhesives.

- Adding washers to the bottom of the bolts for the HTFGB connector is not expected to have any adverse effects on the structural performance of the connector. However, it is advisable to have extra washers on hand during construction.
- For the DBLNB connector, replacing the A193 B7 threaded rod with an A325 bolt is acceptable, as long as there is sufficient thread length on the A325 bolt so that two nuts can be placed directly above the steel flange. These double-nuts are intended to prevent rotation of the connector when the nut is installed underneath the flange (a feature that apparently did not work well at the Hondo Bridge) and to help reinforce the base of the connector. Eliminating the double-nut may adversely affect fatigue life of the connector.

Figure 3.17: Post-installed shear connectors (HASAA) in an interior girder in south span of Hondo Bridge

Figure 3.18: Post-installed shear connectors (DBLNB) in an exterior girder in north span of Hondo Bridge

Figure 3.19: Post-installed shear connectors in exterior girders of north span (on left) and center span of Hondo Bridge (DBLNB in north span; HTFGB in center span)

3.6 Summary

Previous results from full-scale beam tests (Kwon 2008) in Project 0-4124v indicate that the load rating for an existing non-composite bridge can be increased substantially by the use of post-installed shear connectors. By taking advantage of partial composite design and the high strength of the post-installed shear connectors, a relatively small number of shear connectors can be highly effective in increasing the strength of the bridge. In the Hondo Bridge, 28 shear connectors were installed in each girder for the DBLNB and HTFGB connectors and 52 shear connectors in girder for the HASAA connectors. Based on standard AASHTO load rating techniques, this resulted in an increase of the Inventory level rating from HS 10.6 to HS 17.4, and an increase in the Operating level rating from HS 17.6 to HS 29.1.

A key issue when using partial composite design is the effect of fatigue design requirements on the required number of shear connectors. Because of the low fatigue life of conventional welded shear studs, partial composite design is generally not possible, since fatigue will normally control the number of required connectors. However, because of the higher fatigue life of the post-installed connectors, it is expected that fatigue will not normally control the required number of shear connectors. And even in cases where fatigue does control, the required number of shear connectors will still be substantially less than would be required with conventional welded studs.

The effect of fatigue on the required number of shear connectors was also evaluated in this case study. The results of this evaluation showed that fatigue did not control the required number of connectors for the DBLNB and HTFGB connectors. For these cases, the required number of connectors was controlled by static strength requirements, and the 28 post-installed shear connectors per girder, based on partial composite design, were adequate to achieve the load-rating increase noted above.

In the case of the HASAA connectors, fatigue controlled the required number of connectors. This is because the fatigue life of the HASAA connector is less than that for the DBLNB and HTFGB connectors, although it is still substantially better than for conventional welded studs. In the case of the HASAA connector, satisfying fatigue design requirements, 52 connectors were needed, as compared to 28 based on static strength requirements. Note that for conventional welded studs, approximately 120 shear studs per girder would be needed to satisfy AASHTO fatigue requirements. Also, as described earlier, finite element analysis indicated that 28 HASAA connectors per girder would actually have been satisfactory for fatigue. The increase from 28 to 52 was needed as a result of using conservative hand calculation methods to compute the stress range in the connectors.

An issue that requires further study is the manner in which shear force on the connector is computed in the elastic range of response, for purposes of checking fatigue. For conventional fully composite bridge girders, shear flow at the steel-concrete interface is computed based on a transformed fully composite cross-section. In the case of a partially composite girder, the use of a transformed cross-section may not provide an accurate estimate of shear flow. Further, the post-installed shear connectors are installed near the girder ends only, with no connectors in the center portion of the girder. For this arrangement of connectors, it is unclear how to compute connector shear force from the shear flow.

For the Hondo Bridge, shear flow was computed using a transformed cross-section, and a simplified method was adopted for computing the resulting shear force on each connector. Comparisons with an ABAQUS model of the bridge indicated that the actual shear force on the connectors was significantly less than that calculated by this simplified procedure. Further

studies are needed to develop a more accurate method of computing connector shear force for fatigue design. As indicated above, the availability of more accurate methods for computing the connector shear force would have permitted reducing the number of HASAA connectors in each girder from 52 to 28.

The actual installation of the post-installed shear connectors on the Hondo Bridge proved more difficult than anticipated prior to construction and based on the connector installation experiences in Project 0-4124. Problems encountered during the construction are described in this chapter, along with suggestions for mitigating these problems in future installations.

Chapter 4. Live Load Tests of the Hondo Bridge

4.1 Introduction

The structural behavior of the Hondo Bridge was evaluated from load tests. The bridge was loaded using TxDOT dump trucks, and strain and deflection of the bridge were measured during the load tests. Tests were conducted before and after the bridge strengthening, so the behavior of the bridge after the retrofit could be compared with that of the bridge before the retrofit. The first test was conducted on March 24, 2008 before the retrofit, and the second test was conducted on January 8, 2009 after the retrofit.

4.2 Load Test Program

4.2.1 Load Test Trucks

Two dump trucks provided by TxDOT were used for the load tests (Figure 4.1). The two trucks were loaded with gravel, and the front and tandem axles were weighed at truck scales before the tests. Since the two tests were conducted several months apart, the dump trucks did not have the same weights for the two tests. The configuration and weights of the trucks are shown in Figure 4.2.

Figure 4.1: Dump trucks used for the field test

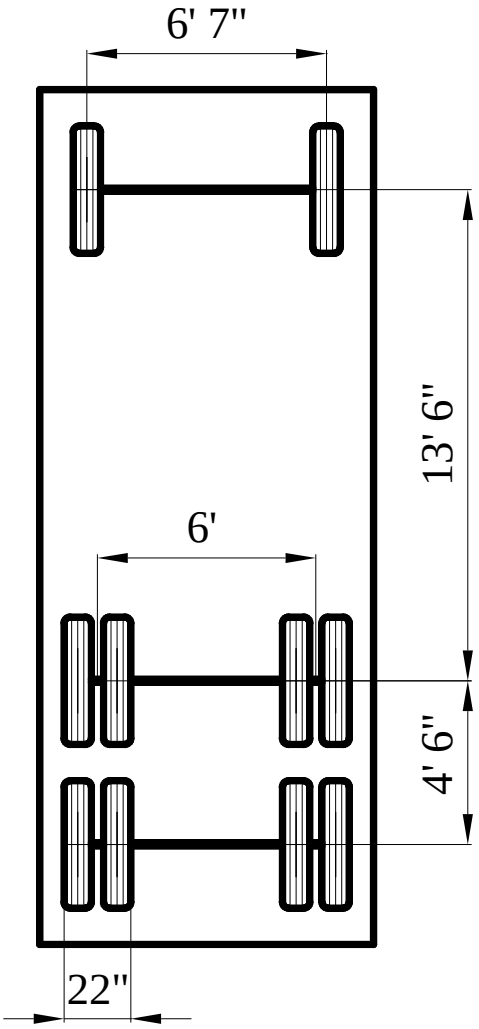

Test 1 (Before retrofit)		Test 2 (After retrofit)	
Truck 1	Truck 2	Truck 1	Truck 2
11.30 kips	9.58 kips	9.30 kips	11.06 kips
23.98 kips	25.18 kips	31.36 kips	30.74 kips
Total 35.28 kips	Total 35.02 kips	Total 40.67 kips	Total 41.80 kips

Figure 4.2: Weight of dump trucks

The load tests were conducted on only one of the three spans of the bridge. The span that was chosen was the south exterior span, which was retrofitted with HASAA connectors. This span was chosen because it provided the best access for installation of strain gages and displacement transducers underneath the bridge. Only one span was tested because the three spans of the bridge were identical before retrofit, and research conducted in project 0-4124 showed that all three connection methods showed very similar performance under static loading.

During the tests, the trucks were positioned in various locations on the span and test runs were conducted to measure deflections at mid-span and strains in the bridge girders under the truck loadings. Five different truck locations, identified as Tests A to E, are shown in Figure 4.3. The locations of the trucks were chosen to produce significant strain and deflection response at the mid-span of the bridge girders.

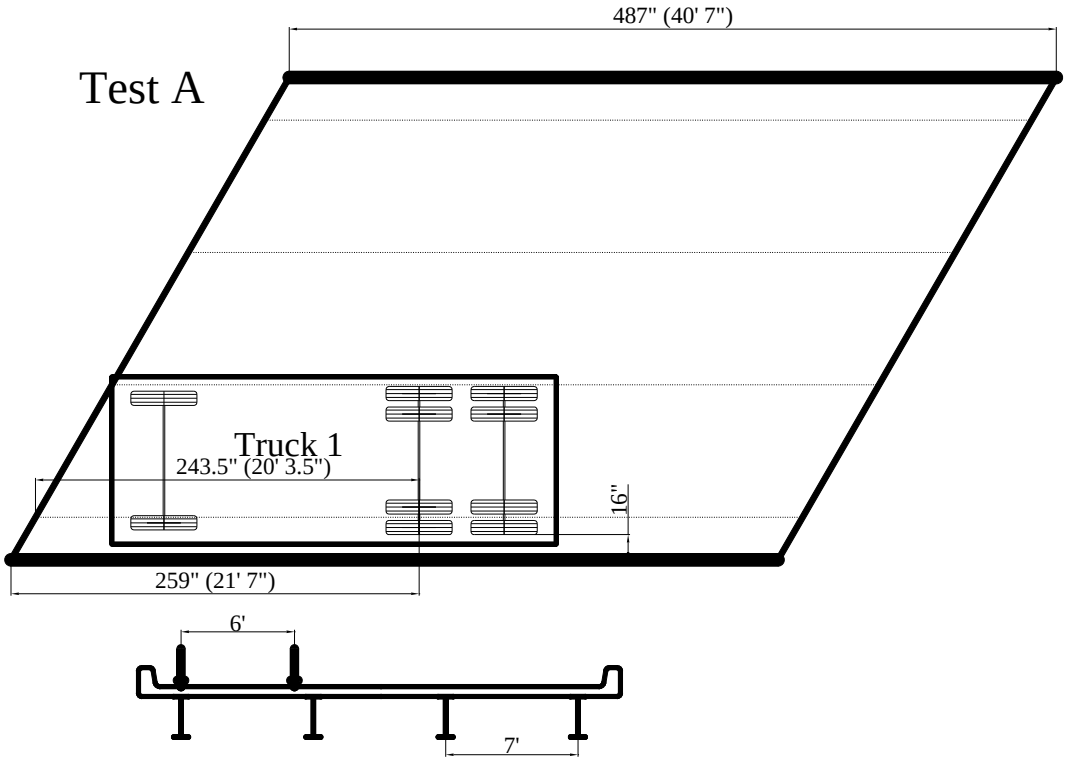

(a) Truck location for Test A

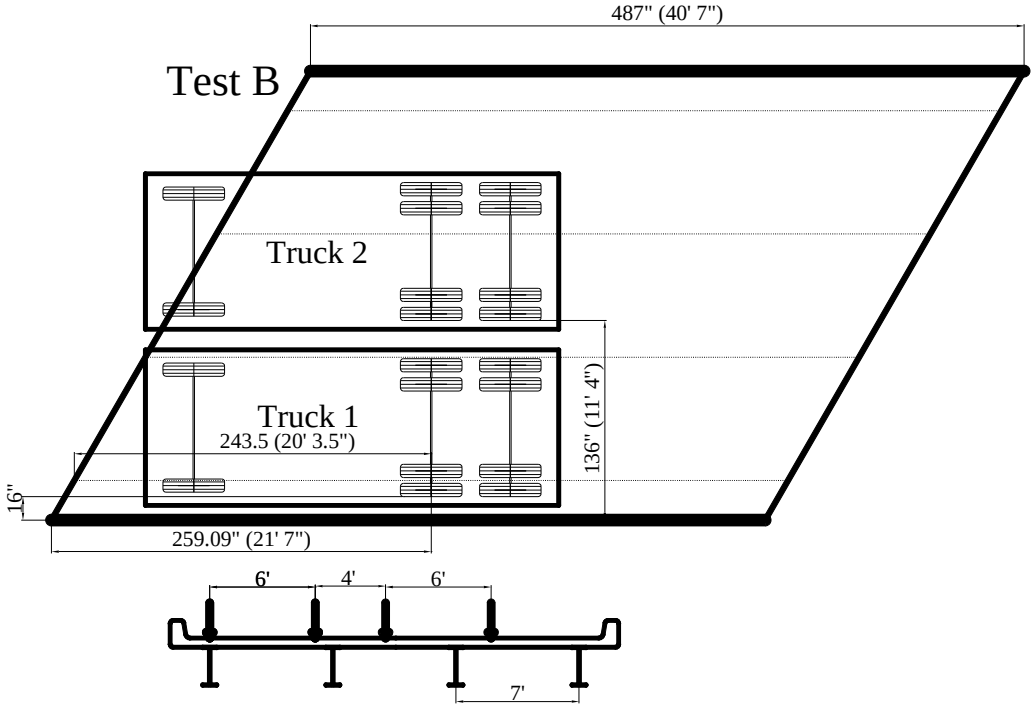

(b)Truck location for Test B

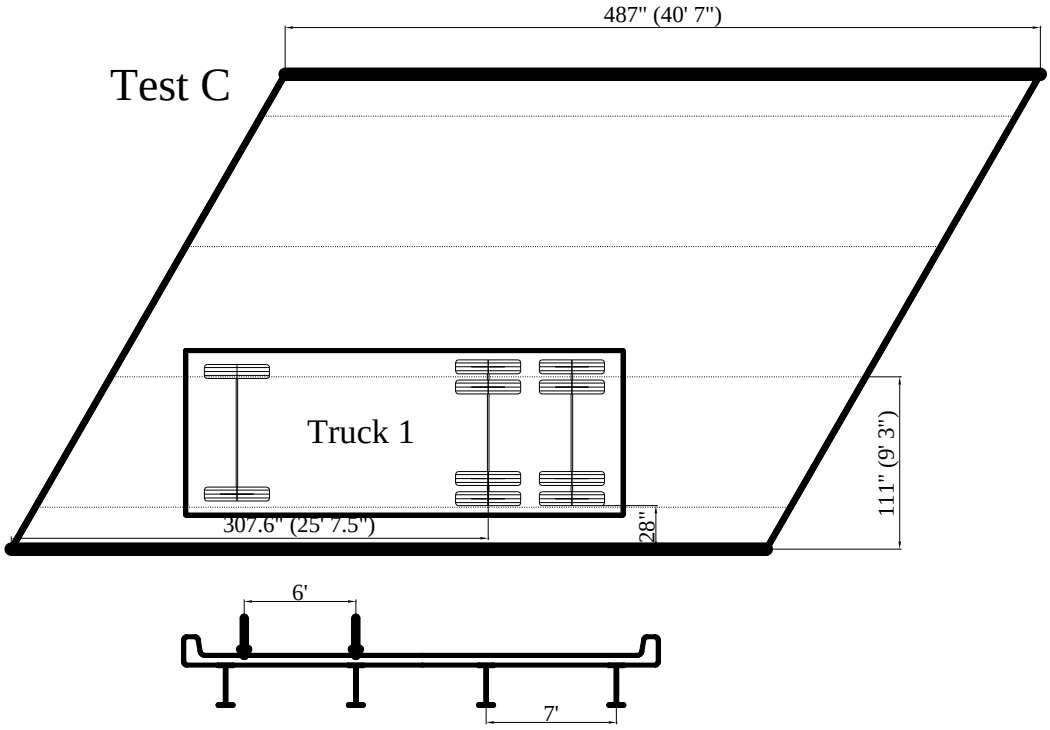

(c) Truck location for Test C

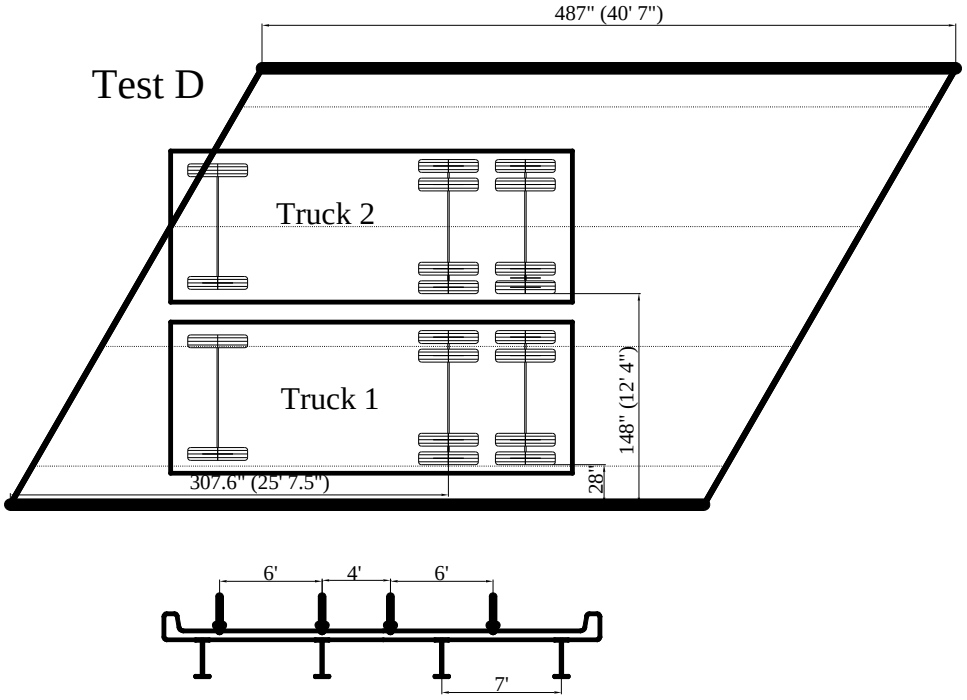

(d) Truck location for Test D

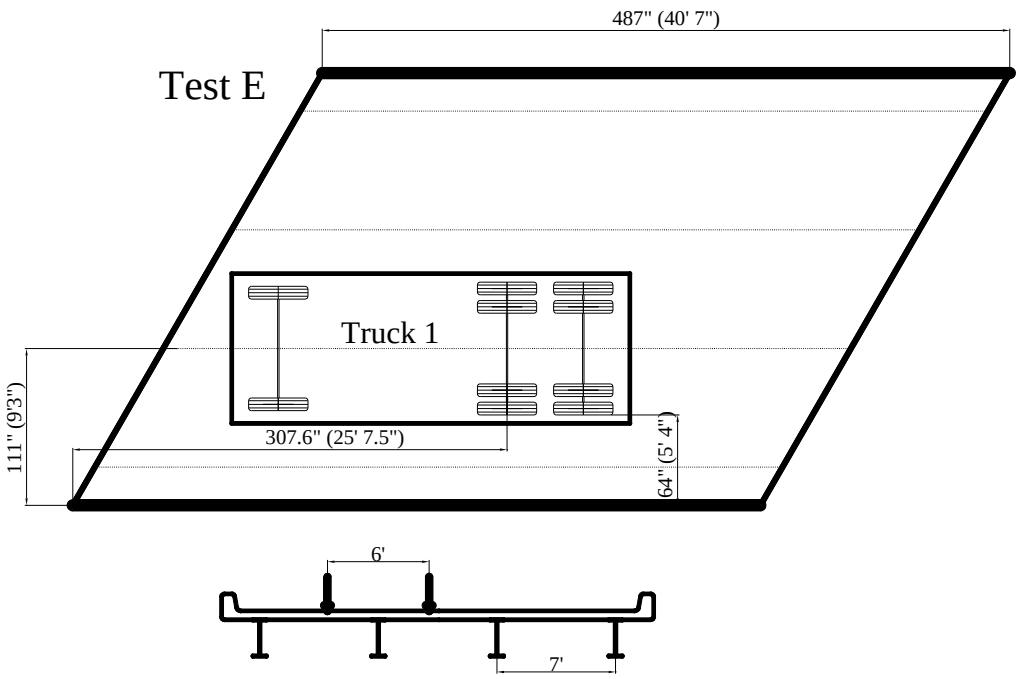

(e) Truck location for Test E

Figure 4.3: TxDOT dump truck locations for field tests

4.2.2 Instrumentation

By achieving composite action, a significant increase in the stiffness and strength of the bridge girders is expected. The increase in elastic stiffness of the bridge girders resulting from the installation of shear connectors can be evaluated by measuring deflections under truck loads before and after retrofit. The increase in strength of the bridge girders resulting from the installation of shear connectors cannot be determined directly from the field load test, since this would require testing to failure of the girders. However, the development of composite action between the concrete slab and the steel girders resulting from installation of shear connectors can be evaluated by measuring the location of the neutral axis in the steel beam by the use of strain gages. Consequently, the two measurements made during the load tests was vertical deflection of the girders, and the strain profile over the depth of the girders.

The deflections of the bridge girders were measured at two locations of the bridge to evaluate the stiffness of the bridge girder under the truck loadings. Strains in the bridge girders were measured using strain gages to locate neutral axis during the field tests. Two girders were instrumented for the load tests. The locations of displacement transducers (string potentiometers) and strain gages are shown in Figure 4.4.

The data acquisition system used for the field tests was a Cambell Scientific Inc. CR 500 unit (Figure 4.5). The data acquisition unit was connected to a laptop. During the tests, the TxDOT dump trucks were located in the predetermined positions (Figure 4.3) and held in place for several minutes while data readings were taken. The data were read at a rate of 1/5 Hz, meaning the strain and deflection data were measured every 5 seconds.

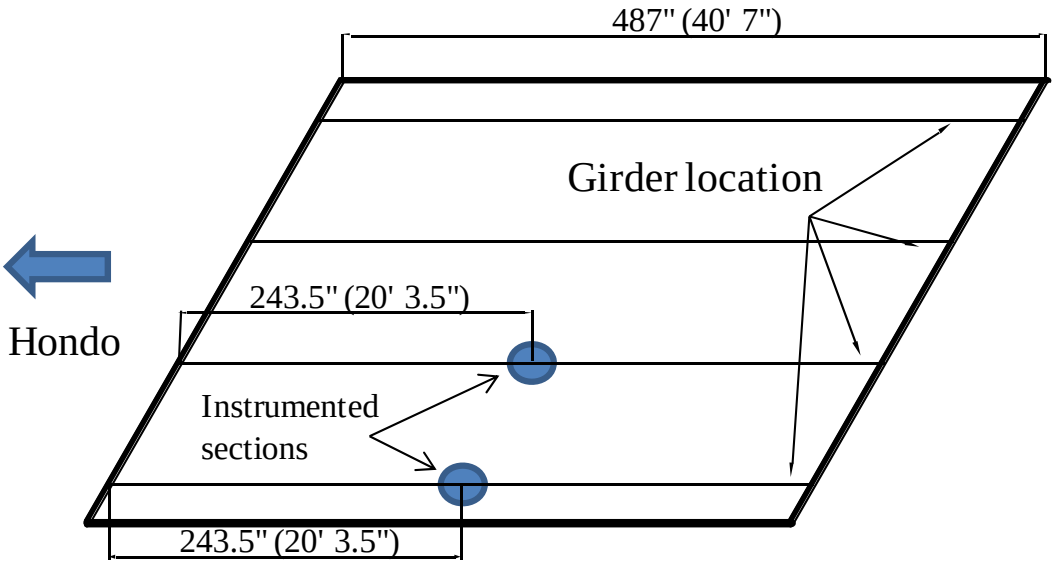

(a) Instrumented sections

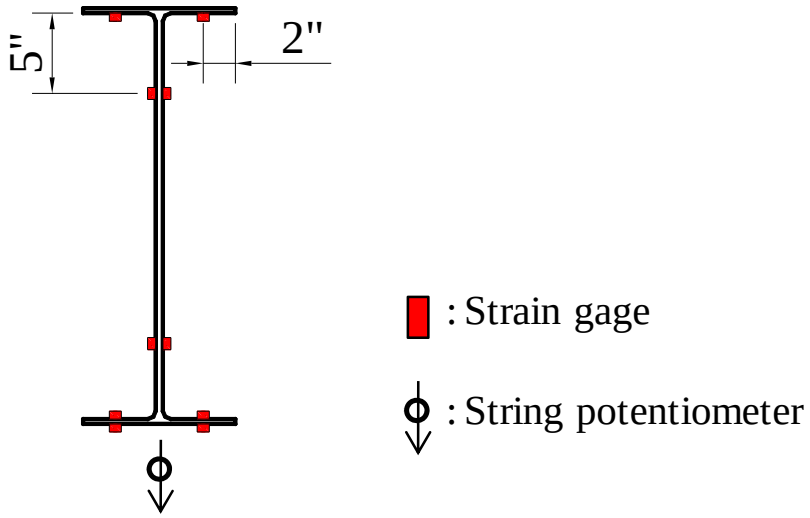

(b) Locations of strain gages and string potentiometers

Figure 4.4: Instrumentation for the field tests

Figure 4.5: CR 500 data logger used for field tests

4.3 Test Results and Discussion

Two tests, referred to as Test No.1 and Test No.2, were conducted before and after the retrofit, respectively. Strain and deflection data were collected for each test and the results before and after the retrofit were compared. Each test run was identified in alphabetical order, from A to E. For example, Test 1-B refers to the test run conducted before the retrofit with trucks located as shown in Figure 4.3(b).

4.3.1 Test No.1 (Before Retrofit)

The first field test was conducted on March 24, 2008 before the bridge was retrofitted. As discussed in the previous section, the trucks were placed at the predetermined positions as shown in Figure 4.6 and the data from the string potentiometers and strain gages were read. Table 4.1 shows the neutral axis locations for the bridge girders computed from strain gage measurements and the measured deflections. The neutral axis locations in the steel girders were obtained by interpolating strain data. Figure 4.7 shows the strain profile in the bridge girders for each test run.

For non-composite beams, the neutral axis is expected to be at the mid-height of the beam section assuming no interaction between the concrete slab and the steel girders. Theoretically, the neutral axis of the bridge girder is 12.94 in. from the bottom of the steel girder for the non-composite case. Assuming fully composite action at the steel-concrete interface, the neutral axis would be 23.37 in. from the bottom flange for elastic behavior. Note that the girders remained well within the elastic range during the load tests.

Figure 4.6: TxDOT trucks located on bridge

Table 4.1: Field test results (Test No. 1, before retrofit)

Test No.	Test 1-A		Test 1-B		Test 1-C		Test 1-D		Test 1-E	
	Ext.	Int.	Ext.	Int.	Ext.	Int.	Ext.	Int.	Ext.	Int.
N.A. from the bottom flange (in.)	16.45	14.26	16.47	13.51	18.04	14.65	18.13	14.10	19.63	14.31
Deflection (in.)	0.16	0.13	0.18	0.25	0.14	0.14	0.15	0.26	0.07	0.16

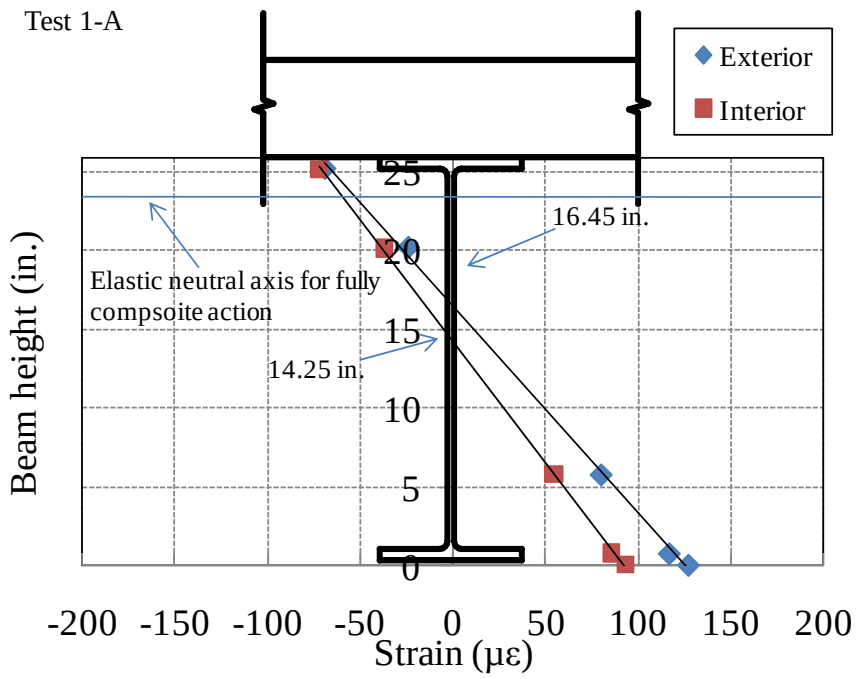

(a) Test 1-A

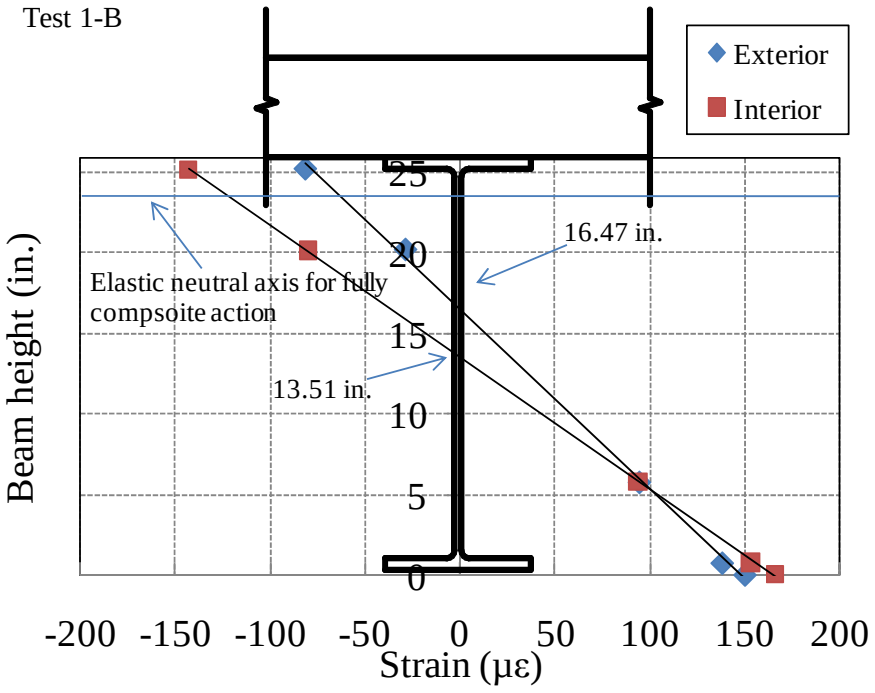

(b) Test 1-B

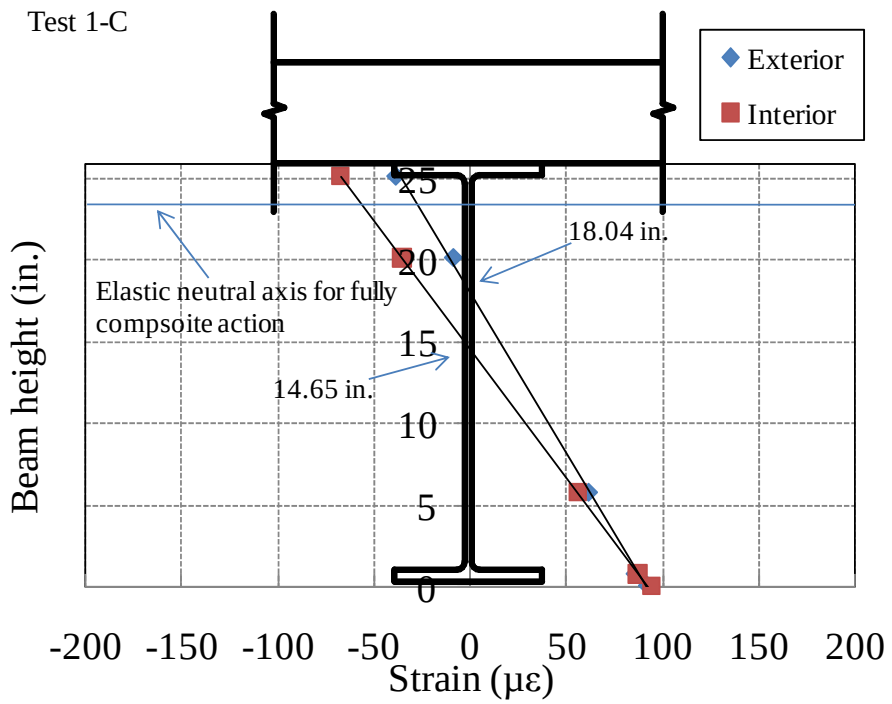

(c) Test 1-C

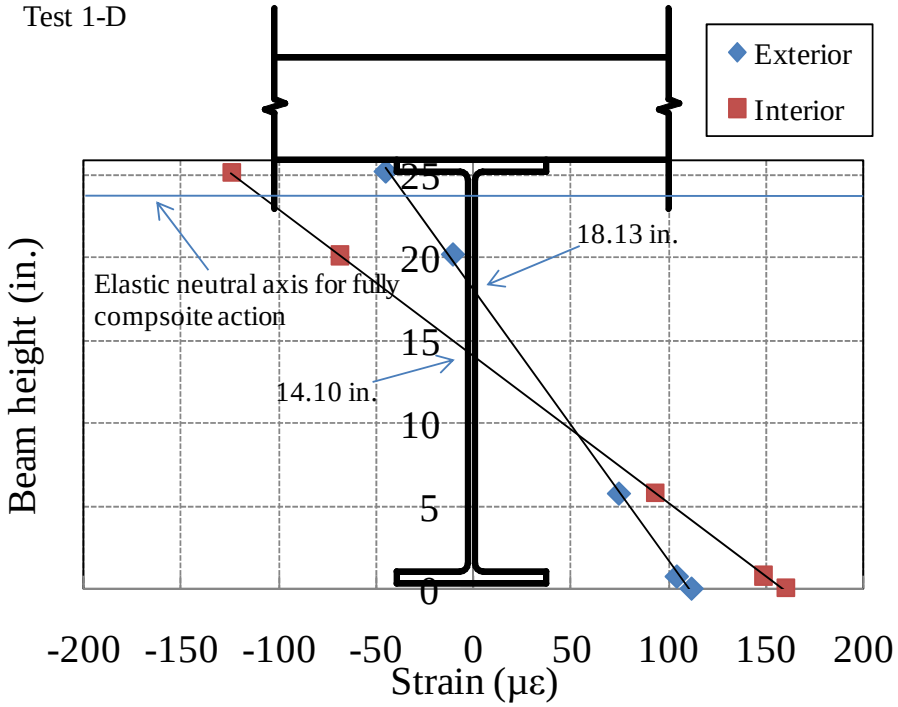

(d) Test 1-D

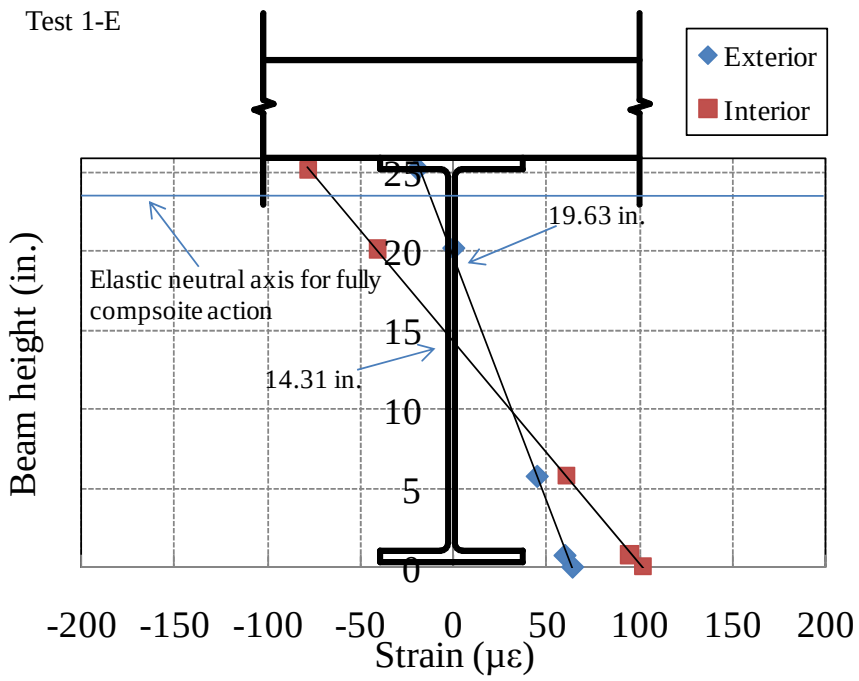

(e) Test 1-E

Figure 4.7: Strain profile in the girders (Test No.1)

As shown in Table 4.1 and Figure 4.7, the neutral axis was located higher in than mid-height of the steel girder, and therefore was higher than the theoretical neutral axis location for a completely non-composite girder. For the interior girder, the neutral axis was higher than the theoretical location by only a small amount. However, for the exterior girder, the measured neutral axis location was significantly higher than the theoretical location. This can likely be attributed to unintended composite action due to the friction and adhesion at the steel-concrete interface. For the interior girder, which was more heavily loaded than the exterior girder, the neutral axes were located closer to mid-height of the girder, indicating little composite action at the steel-concrete interface. These measurements suggest that unintended composite action deceases as load levels increase. Similar observations were made in load tests conducted on non-composite floor systems in truss bridges (Bowen and Engelhardt 2003).

4.3.2 Test No. 2 (After Retrofit)

The field test after the retrofit was conducted on January 8, 2009. The span tested under the TxDOT trucks was retrofitted with the HASAA connectors. Truck locations were the same as for the first test, and the locations are shown in Figure 4.3.

Table 4.2 lists the neutral axis locations computed from strain gage measurements and the measured deflections for each truck location. Measured strain profiles in the bridge girders are shown in Figure 4.8. As noted in the previous section, the theoretical neutral axis location for fully composite action without any slip is 23.37 in. from the bottom flange for elastic behavior. Recall, however, that the retrofitted girders were not designed for fully composite behavior.

As expected, the bridge girders showed significantly less deflection after the retrofit than before the retrofit. Note that the truck loads for Test No. 2 were higher than the truck loads for Test No.1 before the retrofit. Also, as expected for composite girders, the neutral axis in the steel beam section was significantly higher as compared to the first field test.

Table 4.2: Field test results (Test No. 2, after retrofit)

Test No.	Test 1-A		Test 1-B		Test 1-C		Test 1-D		Test 1-E	
	Ext.	Int.	Ext.	Int.	Ext.	Int.	Ext.	Int.	Ext.	Int.
N.A. from the bot. flange (in.)	22.96	19.28	22.66	19.55	23.58	19.18	23.18	19.94	22.35	20.28
Deflection (in.)	0.13	0.11	0.15	0.19	0.13	0.12	0.15	0.21	0.07	0.14

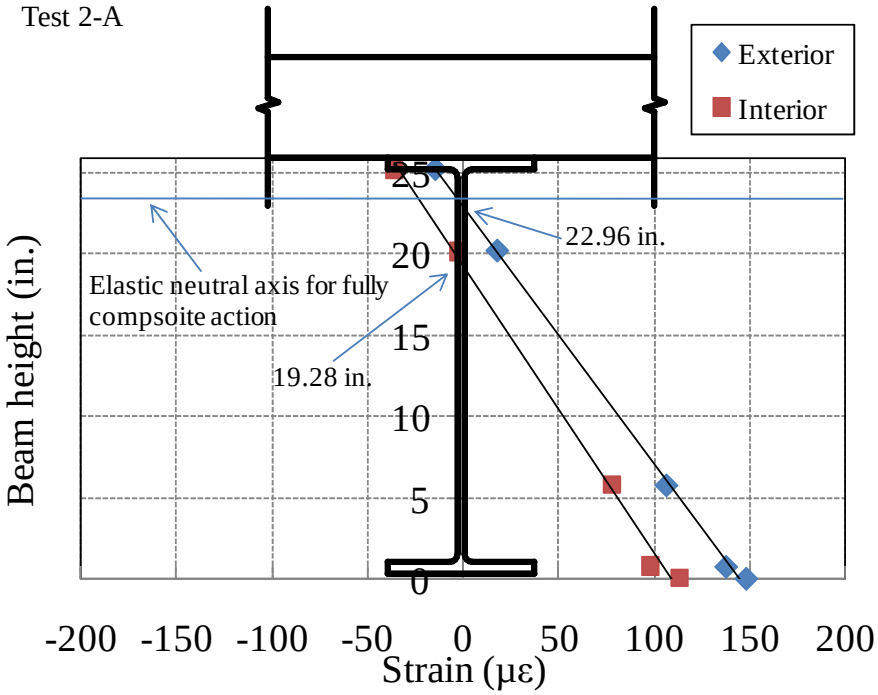

(a) Test 2-A

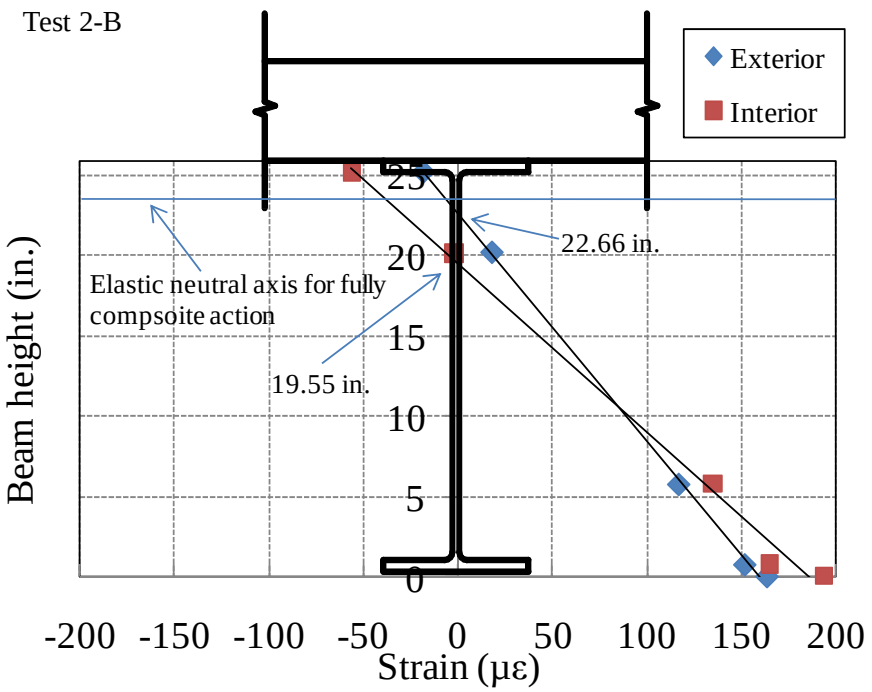

(b) Test 2-B

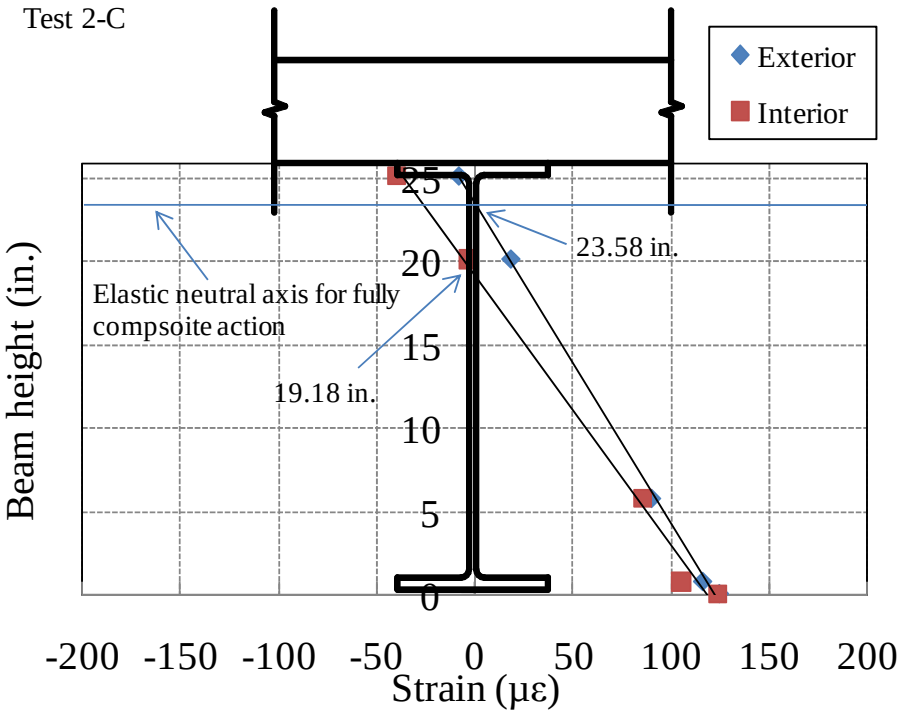

(c) Test 2-C

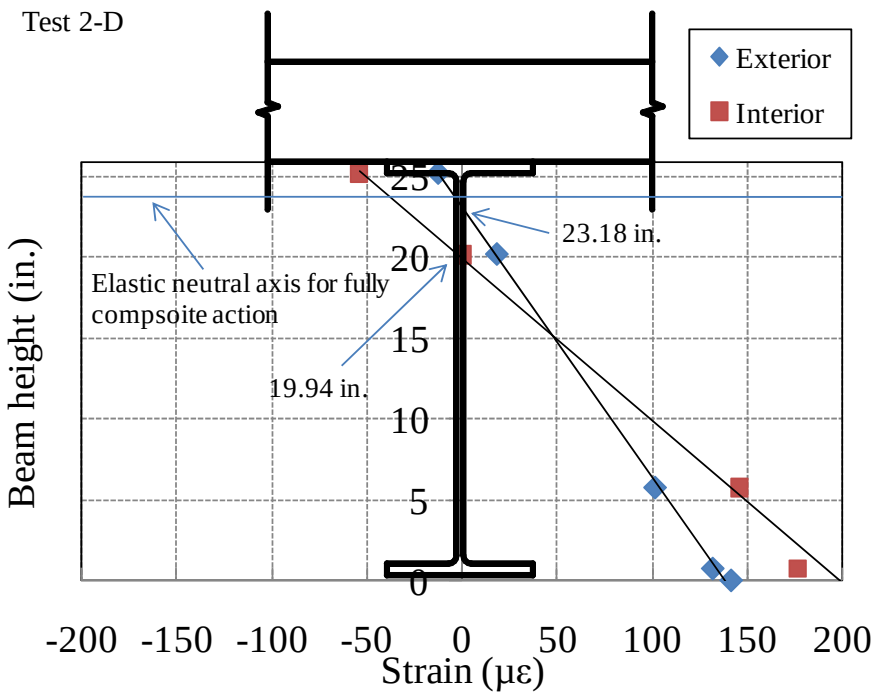

(d) Test 2-D

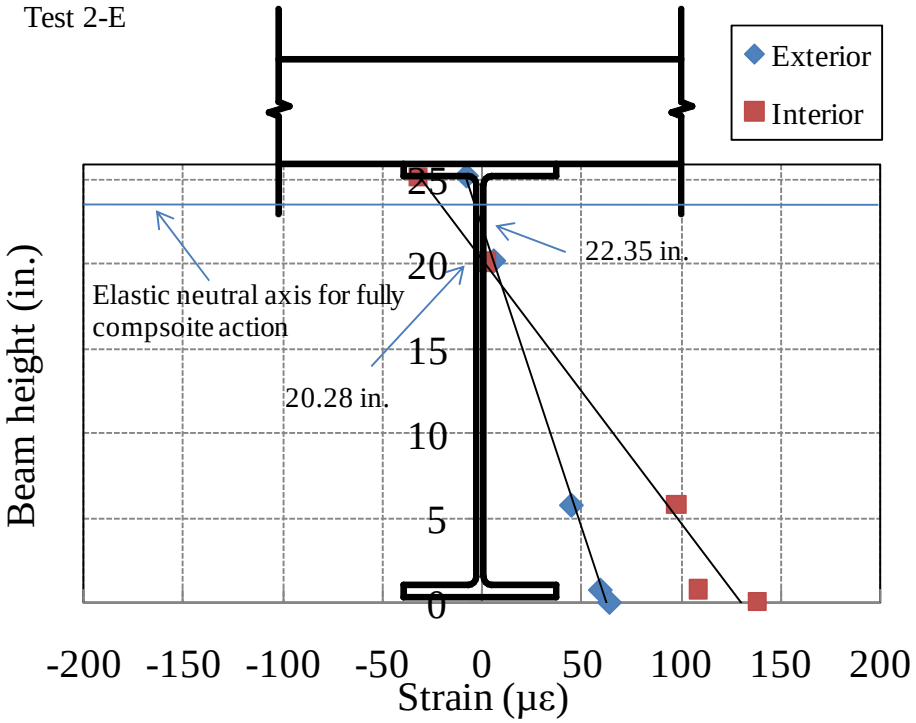

(e) Test 2-E

Figure 4.8: Strain profile in the girder (Test No. 2)

4.3.3 Discussion of Field Tests

Neutral axis location

Composite action between the concrete slab and the steel girder can be evaluated by neutral axis locations. The neutral axis of a completely non-composite beam is located at the mid-height of the steel beam. The elastic neutral axis location for a composite beam can be calculated using the transformed section assuming full composite action without any slip at the steel-concrete interface. The theoretical neutral axis location of the beam section of the Hondo Bridge is 12.94 in. from the bottom of the beam, assuming no composite action. The location of the elastic neutral axis of the section assuming complete composite action is 23.37 in. from the bottom of the beam.

Before the retrofit, as shown in Figure 4.7, most test runs show the neutral axis somewhat above mid-height of the section. As noted earlier, for the interior girder, the neutral axis was higher than the theoretical location by only a small amount. However, for the exterior girder, the measured neutral axis location was significantly higher than the theoretical location. This is attributed to unintended composite action at the steel-concrete interface due to friction or adhesion at the steel-concrete.

Note that the maximum live load stress in the bottom flange of the interior girders prior to retrofit was only about 5 ksi. Even with this low stress level, the unintended composite action was minimal and the bridge girders were acting in a largely non-composite manner. The test results suggest that unintended composite action at the steel-concrete interface of non-composite bridge floor systems should not be relied on for the calculation of the strength of the bridge floor system, as the unintended composite action may be present only at low load levels. As the bridge reaches its ultimate capacity, it is doubtful that unintended composite action due to friction or adhesion can be relied upon. Similar conclusions resulted from an earlier study of non-composite bridge floor systems by Bowen and Engelhardt (2003).

After the retrofit, it is clear that the neutral axis locations moved up in the section due to composite action between the concrete slab and the steel girder. The exterior girders show neutral axis locations very close to the theoretical values for a fully composite beam. For the interior girders, the neutral axes were located somewhat lower than in the exterior girders. It is considered that the higher loads on the interior girder caused slip at the steel-concrete interface, resulting in a lower neutral axis location, as would be expected for a partially composite beam. In summary, the neutral axis locations measured after the retrofit showed that significant composite action was developed in the girders, as expected.

Deflection

Table 4.3 shows measured deflections of the bridge girders before and after the retrofit. As shown in the table, deflection of the girders decreased after the retrofit. Note that the test trucks did not have the same weights for the two tests.

Table 4.3 also shows normalized deflections of Test No. 2, computed as the product of the measured deflection and the ratio of the truck weight of Test 1 to the truck weight of Test 2. These normalized deflections provide a better basis for comparing deflections before and after the retrofit. Some of the test results show a significant decrease in deflection after the retrofit. However, some of the test results showed less decrease in the deflection compared to that expected from Figure 3.13. Figure 3.13 shows a significant increase in stiffness of the bridge girders after retrofit under the AASHTO HS20 design truck loads. It is believed that the

oversized holes used for the HASAA connectors reduced the stiffness of the retrofitted girders at low load levels, as demonstrated by the finite element analysis described in Section 5.3.2. Also, the exterior girders were likely significantly stiffened by the presence of the concrete barriers on the bridge, thereby reducing the impact of the shear connectors.

Table 4.3: Deflections of the bridge girders (Unit: in.)

Test Run	Test A		Test B		Test C		Test D		Test E	
	Ext.	Int.	Ext.	Int.	Ext.	Int.	Ext.	Int.	Ext.	Int.
Test 1 (Measured)	0.16	0.13	0.18	0.25	0.14	0.14	0.15	0.26	0.07	0.16
Test 2 (Measured)	0.13	0.11	0.15	0.19	0.13	0.12	0.15	0.21	0.07	0.14
Test 2 (Normalized)	0.12	0.09	0.13	0.16	0.12	0.11	0.13	0.18	0.06	0.12

4.4 Summary

Field live load test results for the Hondo Bridge were described in this chapter. Two tests were conducted to compare the behavior of the bridge before and after retrofit with post-installed shear connectors. Two TxDOT dump trucks loaded with gravel were used for the tests. For each test, five test runs were conducted with different truck locations. Strain data over the depth of the girder sections were measured to locate the neutral axis. Deflections were also measured to compare the stiffness of the bridge after the retrofit with the stiffness before the retrofit.

Before the retrofit, the Hondo Bridge showed some degree of unintended composite action, likely due to friction and adhesion at the steel-concrete interface. However, the friction was overcome even at low stress levels in the steel girder. After the friction was overcome, the girders behaved in la largely non-composite manner.

After the retrofit, the neutral axis locations moved up significantly in the girders, indicating the development of composite action between the steel girder and the concrete slab. Deflections of the bridge girders also decreased after retrofit. In summary, the results of the field load tests indicate that the post-installed shear connectors were effective in developing a significant degree of composite action, as intended by this retrofit technique.

Chapter 5. Parametric Finite Element Studies

5.1 Introduction

In the previous research on TxDOT Project 0-4124, full-scale composite beams were constructed in the laboratory and retrofitted with post-installed shear connectors. The behavior of the full-scale composite beams was investigated under static loading. Based on the test results along with single shear connector tests and analytical studies, design recommendations were developed, and formed the basis for the retrofit of the Hondo Bridge.

Full-scale composite beam tests give valuable insight into the structural behavior of the beams retrofitted with post-installed shear connectors. However, given the practical limits on laboratory testing, it is not possible in the laboratory to test a wide range of variables that are needed for complete design recommendations (Lam *et al.* 2000). In this study, the finite element method was adopted to further study the behavior of many composite beams with different geometries, and to investigate the effects of various parameters on the behavior of composite beams.

Beam depth, span length, and shear connection ratio were selected as the main variables for the parametric study, along with the effects of oversized holes in the steel beam flange. Results from the parametric studies, combined with laboratory test results from project 0-4124, combined with the experiences of the Hondo Bridge retrofit, were used to develop design recommendations reported in Chapter 6.

5.2 Parametric Study of Composite Beams

5.2.1 Analysis Modeling Parameters

Using the finite element program ABAQUS, parametric studies were conducted to evaluate the effects of beam depth, span length, and shear connection ratio. Sixty composite beams were modeled with steel beam depths from W27 to W36, span lengths from 30 ft to 50 ft, and shear connection ratios from 10 to 50 percent. The beams were simply supported, and were intended as variants on the full-scale beam specimens tested in TxDOT Project 0-4124 (Kwon et al. 2007). The beam sections and span lengths were determined based on an evaluation of typical older TxDOT bridges conducted by Hungerford (2004). In that investigation, typical span lengths of continuous steel girder bridges ranged from 50 ft to 60 ft. Since the parametric study involved simply supported beams, it was desired to use simply supported spans equal in length to the approximate distance between the points of inflection of continuous girders. For end spans of multi-span continuous bridges, the distance between points of inflection is about 75 percent of the span. Relatively low shear connection ratios were selected for the composite beam design because the high fatigue strength of post-installed shear connectors permits the use of significantly fewer shear connectors than conventional welded shear studs for new construction.

From the analysis of composite beams using the finite element program ABAQUS, the maximum strength, stiffness, and deformation capacity were evaluated and the maximum strength and stiffness were compared with the results from current design equations in the AASHTO and AISC provisions. Deformation capacities were compared in terms of an equivalent ductility factor (defined later in this chapter), and that ductility factor was also used to

recommend a minimum shear connection ratio for strengthening existing bridge girders using post-installed shear connectors.

To evaluate the effect of oversized holes in the steel beam flange, six additional composite beams were modeled in this study. In the single shear connector tests and full-scale beam tests in Kwon (2008), 15/16-in. diameter holes were drilled through the steel beam flange to install 7/8-in. diameter shear connectors. Field personnel from TxDOT recommended the use of 1-in. diameter holes in the steel beam flange for the HASAA connector to simplify the installation process, and the 1-in. diameter holes were used for the retrofit of the Hondo Bridge. Although the gap between the oversized hole and the shear connector was filled with adhesive, slip without load may occur due to poor workmanship or weathering of the adhesive. Shear connectors in the six composite beam models were designed to slip without load until the gap closed and then to follow the load-slip curves proposed by Ollgaard et al. (1971). As shown in Figure 5.1, the shear connectors were assumed to fail at 0.23-in. slip after the initial gap closed. For the DBLNB and HTFGB connectors, recall that 7/8-in. diameter holes in the steel beam flange are used for 7/8-in. diameter shear connectors in the Hondo Bridge, so that significant slip without load can be prevented.

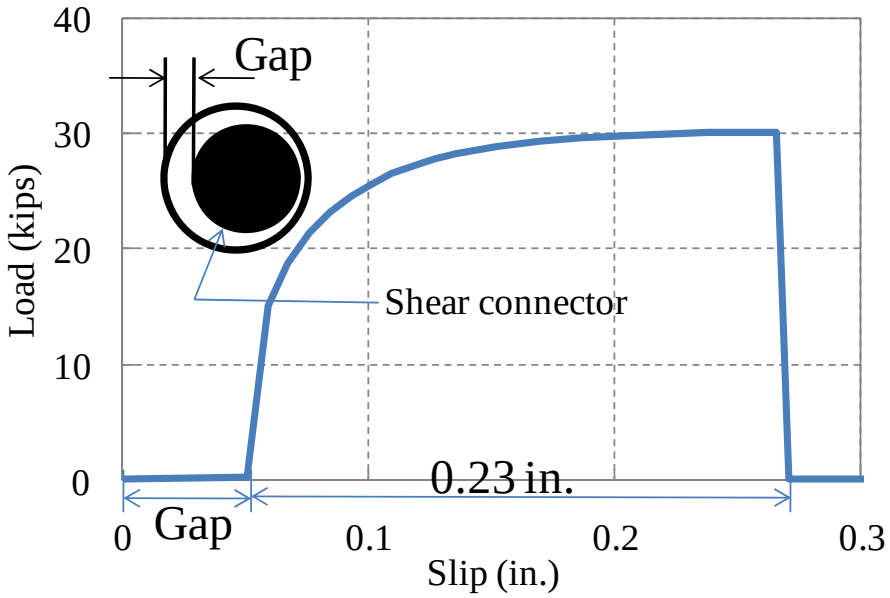

Figure 5.1: Idealized load-slip behavior of a shear connector with an initial gap

In the parametric studies, slab details and material properties were kept constant. The concrete slab, 7-in. deep and 84-in. wide, had the same details as the full-scale beam test specimens in TxDOT Project 0-4124 (Kwon et al. 2007). The yield stress of the steel beam and the ultimate strength of the concrete were taken as 50 ksi and 3,000 psi, respectively. Assuming 7/8-in. diameter shear connectors with 125-ksi ultimate strength and the threads in the shear plane, the shear connectors had an ultimate strength of 30.1 kips. All shear connectors were installed near the supports with 12-in. longitudinal spacing. To impose higher slip demands on the post-installed shear connectors, the self-weight of the steel beam and concrete slab was not considered in the analysis.

5.2.2 Finite Element Model

A three-dimensional finite element model was developed in this study to simulate the behavior of composite beams retrofitted with post-installed shear connectors. To develop the numerical model, various modeling issues were considered including element types, material behavior, numerical solution controls, boundary conditions, and interaction between the concrete slab and steel beam.

Material Modeling

A modified Hognestad (1951) stress-strain relationship was used to model the concrete stress-strain curve in compression. It is assumed that concrete is in the elastic range when f_c is less than $0.45 f_c'$, where f_c is the compressive stress in the concrete and f_c' is the ultimate concrete compressive strength. In this model, the initial modulus of elasticity of the concrete, E_c, is taken as $1.8\times10^3 + 460 f_c'$ (ksi). In tension, a smeared cracking model was used to model the concrete behavior (ABAQUS, 2007). In this model, cracking is assumed to occur when the stress reaches a failure surface. The concrete model, however, does not track individual macro cracks. Instead, the presence of cracks affects the stress and material stiffness of the corresponding integration points. To include the effects of reinforcement on the bottom of the concrete slab (tension side), tension stiffening behavior was defined. In ABAQUS, tension stiffening can be defined by a post-failure stress-strain relationship of concrete material. The concrete material model used in this study is shown in Figure 5.2.

To model the stress-strain relationship of the steel beams and reinforcing bars, an elastic-perfectly plastic model was used. The modulus of elasticity of the steel beams and the reinforcing bars, E_s, is taken as 29,000 ksi. Strain hardening was not included in this model.

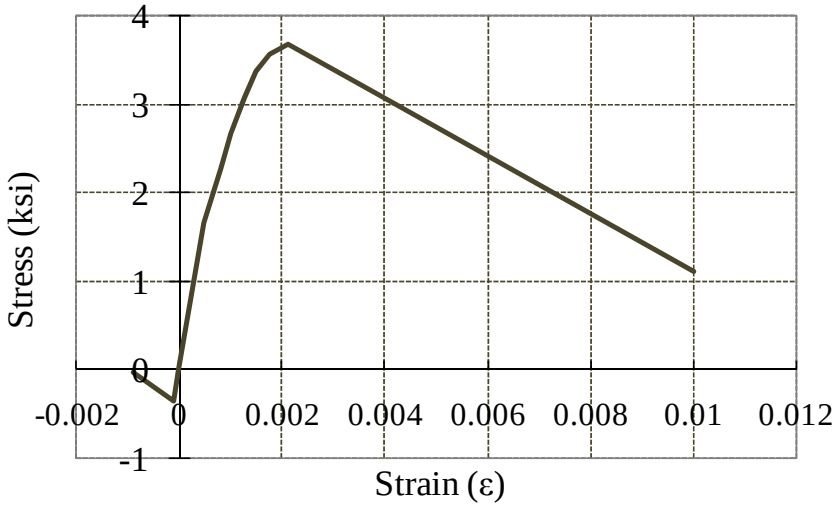

Figure 5.2: Concrete model in ABAQUS

Element Selections

A finite element analysis model developed in this study is shown in Figure 5.3. A 4-node shell element (S4) was selected for both the steel beam and the concrete slab. Element type S4 in ABAQUS is a fully integrated, finite membrane strain shell element. Simpson's rule is used to calculate the cross-sectional behavior of the shell elements (ABAQUS 2007). In ABAQUS, one or multiple layers of reinforcement can be specified in the shell element. The reinforcing bar layers are smeared in the shell element.

Connector elements were used to model the shear connectors. ABAQUS provides several types of connector elements to impose constraints between two elements. Among these various types of connectors, CARTESIAN connectors were used to simulate the behavior of the shear connectors. This connector is a "spring-like" element defined in a local Cartesian coordinate system, and capable of deforming in the coordinate system. Elastic and inelastic behavior can be defined for the element. Connector failure can also be specified with limit values for force or relative displacement. If the specified failure criterion is met, the connector is removed and is no longer effective in the analysis.

Figure 5.3: Finite element model for full-scale beam specimen

Contact interactions in ABAQUS were defined to simulate the interaction between the steel beam and the concrete slab. There is no limit on the magnitude of pressure that can be transmitted between the two surfaces. Separation of contacted surfaces was not allowed after contact occurs, since separation of the steel beam flange and the concrete slab was not detected for the full scale beam tests, except for one specimen at a large deflection. Bond and friction at the interface was not considered in the finite element model.

The connector elements were connected to the shell elements that represent the concrete slab and the steel beam. The stiffness of the connector element is affected by the stiffness of the shell elements to which the connector element is attached. To obtain load-slip relations of

individual shear connector in composite beams, the single shear connector specimen described in Kwon (2008) was modeled in ABAQUS. In the finite element model, slip was measured at the same location as in the single shear connector test specimens. The finite element model for the single shear connector tests is shown in Figure 5.4.

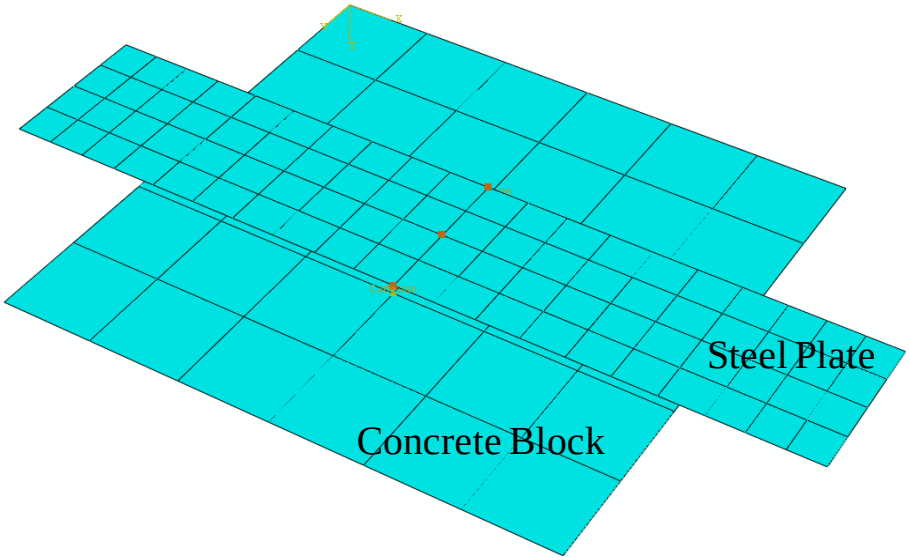

Figure 5.4: Finite element model for single shear connector specimen

Analysis Procedure

A pressure load was applied at mid-span of the beam to simulate the point load applied during the full-scale beam tests. Both geometric and material nonlinearities were considered during the analysis. Local buckling and lateral torsional buckling of the steel beam were not considered in this model.

The General Static method in ABAQUS is not appropriate to predict negative stiffness during the analysis. To simulate possible negative stiffness during the analysis, the Riks method was used for the static analysis (ABAQUS 2007). This method is generally used for predicting nonlinear collapse and post-buckling analysis including strain softening. This method uses load as unknown and seeks load and displacement simultaneously (ABAQUS 2007).

5.3 Results of Parametric Study

5.3.1 Composite Beams with Different Geometries

Load-deflection relations of composite beams with a W36x160 steel beam and 50-ft long span are shown in Figure 5.5. As expected, the strength, stiffness, and deformation capacity of the composite beams increased with increasing shear connection ratio. Load-deflection curves of all of the sixty composite beams modeled in ABAQUS are shown in Appendix C. Failure of the composite beams was taken as coinciding with the failure of the first shear connector. For some composite beams, the solution did not converge before the first shear connector failure. These composite beams were used only for evaluation of strength and stiffness, not for evaluation of

deformation capacity. The maximum strength and initial stiffness of the composite beams from the finite element method are listed in Table 5.1 to 5.3, along with the values computed from current design provisions (AASHTO 2007, AISC 2005).

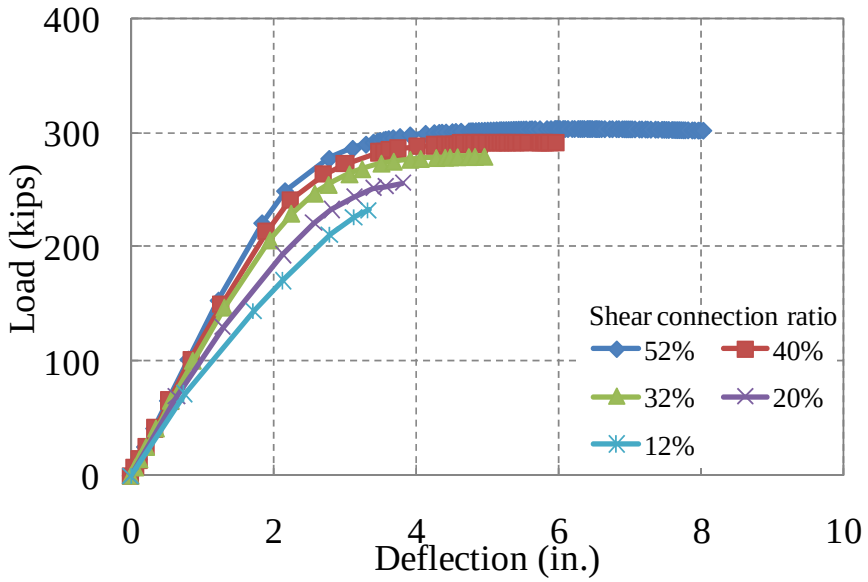

Figure 5.5: Load-deflection relations of composite beams (W36x160 beam, 50-ft span)

Table 5.1: Analysis results for composite beams with 30-ft span

Section	Shear connection ratio (%)	Number of connectors in a shear span	Max. load (kips)		Initial stiffness (kips/in.)		Ductility
			AASHTO AISC	ABAQUS	AISC	ABAQUS	
W27x94	47	22	244	252	217	213	7.6
	39	18	237	245	206	208	5.2
	30	14	226	235	193	199	4.2
	22	10	210	222	178	187	3.3
	13	6	191	201	160	169	2.8
W30x99	50	24	280	292	266	266	*
	41	20	272	285	253	261	4.7
	29	14	252	266	231	246	3.6
	21	10	235	248	214	230	3.0
	12	6	213	226	193	209	2.3
W33x130	48	24	385	398	405	388	*
	40	20	373	388	387	381	4.0
	32	16	357	373	367	369	3.4
	20	10	327	342	332	340	2.7
	12	6	302	317	303	311	2.1
W36x160	52	26	495	513	567	517	*
	40	20	473	491	533	507	*
	32	16	454	473	507	492	2.8
	20	10	420	439	462	455	2.4
	12	6	393	413	423	418	2.2

*: Convergence was not achieved before shear connector failed.

Table 5.2: Analysis results of composite beams with 40-ft long span

Section	Shear connection ratio (%)	Number of connectors in a shear span	Max. load (kips)		Initial stiffness (kips/in.)		Ductility
			AASHTO AISC	ABAQUS	AISC	ABAQUS	
W27x94	47	22	183	190	92	98	*
	39	18	178	185	87	94	4.9
	30	14	169	178	82	89	3.2
	22	10	158	166	75	84	2.5
	13	6	143	151	68	74	2.1
W30x99	50	24	210	216	112	119	*
	41	20	204	212	107	116	4.5
	29	14	189	197	98	108	3.0
	21	10	176	184	90	101	2.5
	12	6	160	168	81	93	2.2
W33x130	48	24	289	297	171	176	*
	40	20	279	287	163	171	3.4
	32	16	268	276	155	165	2.8
	20	10	245	253	140	152	2.2
	12	6	227	235	128	140	1.9
W36x160	52	26	371	386	239	238	3.9
	40	20	355	366	225	230	2.6
	32	16	341	352	214	222	2.5
	20	10	315	325	195	206	1.9
	12	6	295	300	179	190	1.6

*: Convergence was not achieved before shear connector failed.

Table 5.3: Analysis results of composite beams with 50-ft long span

Section	Shear connection ratio (%)	Number of connectors in a shear span	Max. load (kips)		Initial stiffness (kips/in.)		Ductility
			AASHTO AISC	ABAQUS	AISC	ABAQUS	
W27x94	47	22	147	151	47	50	*
	39	18	142	147	44	48	4.5
	30	14	135	141	42	46	2.9
	22	10	126	132	39	44	2.4
	13	6	115	117	35	41	1.7
W30x99	50	24	168	172	57	62	*
	41	20	163	168	55	60	4.4
	29	14	151	157	50	56	2.6
	21	10	141	146	46	53	2.2
	12	6	128	132	42	49	1.9
W33x130	48	24	231	235	87	92	*
	40	20	224	228	84	89	2.8
	32	16	214	219	79	86	2.1
	20	10	196	199	72	80	1.7
	12	6	182	180	65	74	**
W36x160	52	26	297	304	122	126	3.4
	40	20	284	291	115	121	2.5
	32	16	272	279	110	117	2.1
	20	10	252	256	100	108	1.6
	12	6	236	232	91	97	**

*: Convergence was not achieved before shear connector failed.
**: Max. load was less than simple plastic analysis result.

Comparisons with Current Design Provisions (Strength and Stiffness)

The post-installed shear connection methods introduced in this study are unconventional, and the shear connectors are recommended to be installed only near the supports or zero-moment regions. This is in contrast to conventional welded shear studs which are typically installed along the entire span of composite beams. Therefore, it is necessary to determine whether the equations used to calculate the maximum strength and initial stiffness of composite beams in the current design provisions (AISC 2005, AASHTO 2007) can also be used to determine the maximum strength and initial stiffness of composite beams retrofitted with post-installed shear connectors.

For this purpose, the maximum load-carrying capacity of the composite beams modeled in ABAQUS was compared with the results from simple plastic analysis. Figure 5.6 shows the maximum strength of the sixty composite beams from ABAQUS along with the maximum strength from simple plastic analysis. The straight line at 45 degrees indicates complete agreement between the two sets of predicted capacities. Analysis results lying below the straight line correspond to cases in which the strength computed from simple plastic analysis is less than the strength predicted by the ABAQUS model; that is, where simple plastic analysis provides a conservative estimate of strength. As shown in Figure 5.6, the strength predicted by simple plastic analysis agreed very well with the strength predicted by ABAQUS, for all of the analytical models with various span lengths, beam depths, and shear connection ratios. In cases where there were discrepancies, simple plastic analysis gave conservative results, except for two composite beams. The composite beams with W33x130 and W36x160 beam sections, 50-ft span length, and 10-percent shear connection ratio did not reach their maximum strengths based on the current design provisions. Those specimens did, however, reach over 98 percent of the maximum strength from simple plastic analysis.

Stiffness of the composite beams retrofitted with post-installed shear connectors in the elastic range, as predicted by ABAQUS, were also compared with stiffness predictions based on the commentary of the *AISC Specification* (2005). The commentary of *AISC Specification* provides an equation for the effective moment of inertia for a partially composite beam. As shown in Figure 5.7, the ABAQUS-predicted stiffness of most of the composite beams were generally within 10 percent or less of the values given by the AISC equation. The ABAQUS-predicted stiffness values were usually greater than the AISC values. Because the ABAQUS-predicted stiffnesses were based on analytical models calibrated against the full-scale tests described here, they are presumably more accurate than the AISC values. This implies that using the AISC equations, which give slightly smaller stiffness and hence greater deflections, would be conservative for the composite beams studied here. Some beams with short spans, large beam depths, and high shear connection ratios showed slightly lower stiffness in ABAQUS than that predicted by the equation in the *AISC Specification*.

The post-installed shear connectors investigated in this study are intended for use in strengthening existing non-composite steel bridge girders. Due to the high fatigue strengths of these post-installed shear connectors, partially composite design is possible. Further, because of the high cost of post-installing shear connectors, there is a strong incentive to minimize the number of connectors. For this reason, the shear connection ratios used in this study are lower than the ratios typically used for new construction in building applications (AISC 2005). In the commentary of *AISC Specification*, partially composite beams with a shear-connection ratio less than 25 percent are not recommended. As shown in Figure 5.6 and Figure 5.7, however, even with very low shear connection ratios, the strength and stiffness of composite beams retrofitted

with post-installed shear connectors can be determined quite accurately by the equations widely used for new constructions in the AISC and AASHTO provisions.

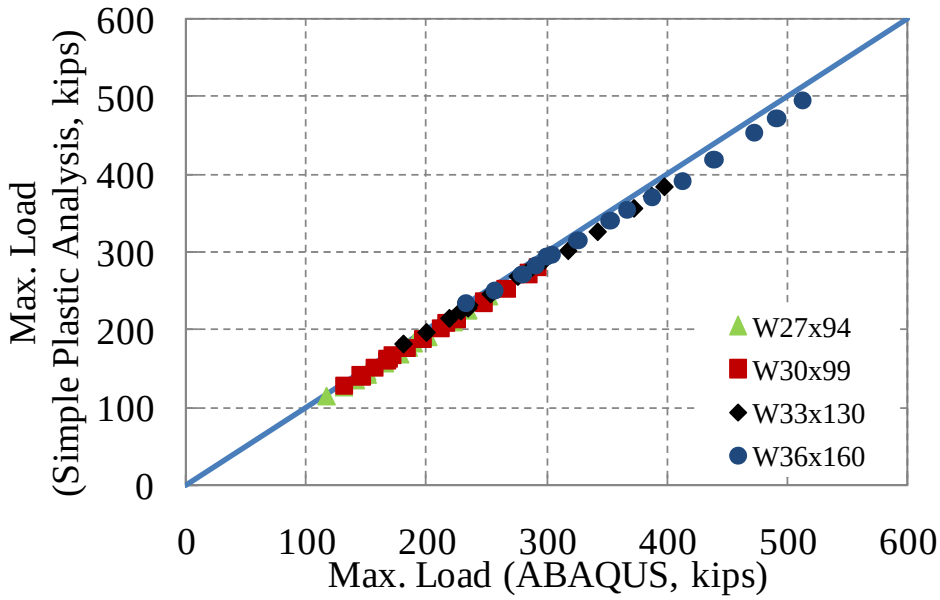

Figure 5.6: Comparison of strength of composite beams (ABAQUS versus simple plastic analysis)

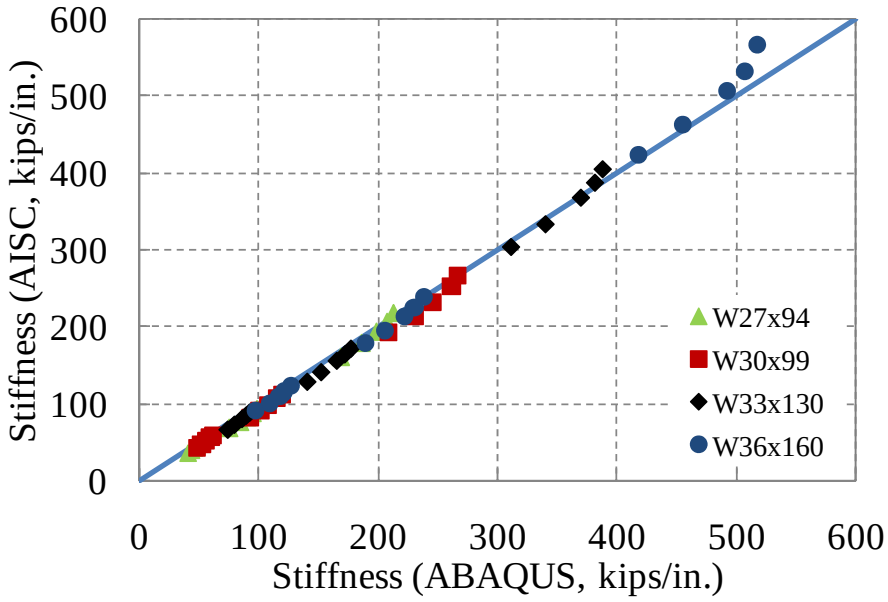

Figure 5.7: Comparison of stiffness of composite beams (ABAQUS versus simple plastic analysis)

Deformation Capacity of Composite Beams with Post-Installed Shear Connectors

Current AASHTO and AISC design provisions have no specific requirements for inelastic deformation capacity of composite beams. These provisions provide quantitative design criteria only for stiffness and strength of composite beams. Although not specifically addressed by AASHTO or AISC, some degree of inelastic deformation capacity, i.e. ductility, is desirable. Ductility enhances safety by providing warning of impending failure, and by allowing redistribution of loads to adjacent beams. The load-deformation response curves of the sixty composite beams modeled using the finite element program ABAQUS provides the opportunity to assess the ductility of these beams. From the response curves, the ductility of the beams was evaluated using a ductility factor, μ, defined in terms of an equivalent elasto-plastic load-deflection curve, as shown in Figure 5.8. The analytically predicted load-deflection curve of a composite beam was idealized by two straight lines representing the initial stiffness calculated using ABAQUS and the maximum strength calculated using simple plastic analysis. The intersection of those two lines was taken as an equivalent yield displacement, Δ_y. The maximum deflection, Δ_{max}, was defined as the deflection at which the first shear connector failed. The corresponding ductility factor was then calculated as Δ_{max} / Δ_y.

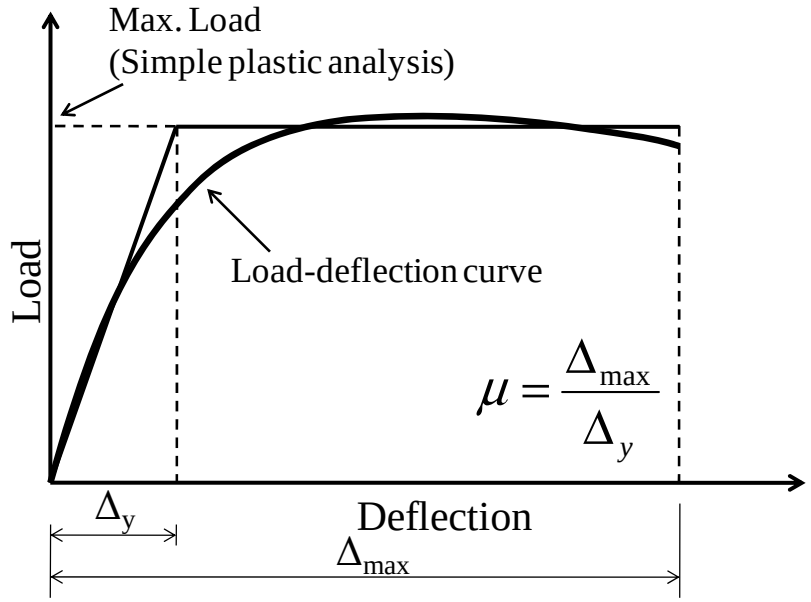

Figure 5.8: Definition of ductility factor

The calculated ductility factor for each composite beam is plotted in Figure 5.9, and listed in Tables 5.1 to 5.3. Composite beams for which the analysis stopped before shear connector failure are not plotted in the figure, nor are composite beams which did not reach the maximum load calculated from simple plastic analysis. As shown in Figure 5.9, the ductility factor of composite beams increases with increasing shear connection ratio. It is also clear that deep steel beam sections develop less ductility. Increased span length increases the slip demand at the steel-concrete interface at M_{max}. As expected, the increased slip demand at the steel-concrete interface

causes composite beams with long spans to have lower ductility than composite beams with short spans.

In general, ductility is desirable from the point of view of permitting redistribution of overloads to adjacent girders and for providing warning of failure. However, as discussed earlier, current AASHTO and AISC design provisions have no minimum required level of ductility. For the purposes of designing safe bridge retrofits, it was judged useful to select a minimum acceptable ductility factor. Examination of the full scale composite beam tests of the TxDOT Project 0-4124 (Kwon et al. 2007) shows that all full-scale composite beam specimens in this study had a ductility factor of at least 2.0. All specimens showed substantial deflection, over 4 in., before any shear connector failed. Therefore, that value was selected as a lower ductility limit for partially composite beams retrofitted with post-installed shear connectors. That is, a ductility factor of 2 was taken as the minimum allowable ductility factor.

Most composite beams investigated in this parametric study had ductility factors higher than 2. Some composite beams with low shear connection ratios, deep beam sections, and long spans had the ductility factors less than 2 (Figure 5.9). In this study a minimum shear connection ratio 30 percent is recommended for strengthening of existing non-composite steel bridge girders using post-installed shear connectors. All composite beams modeled in ABAQUS with shear connection ratios exceeding 30 percent showed ductility factors higher than 2. In these parametric studies, the post-installed shear connectors were concentrated near the support to reduce slip at the steel-concrete interface as recommended in Kwon (2008).

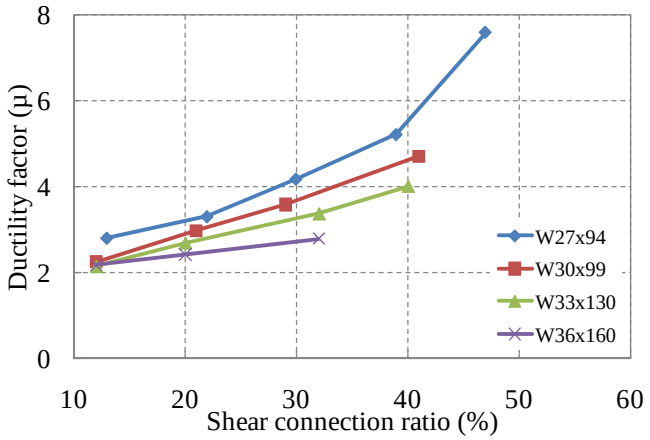

(a) Span: 30 ft

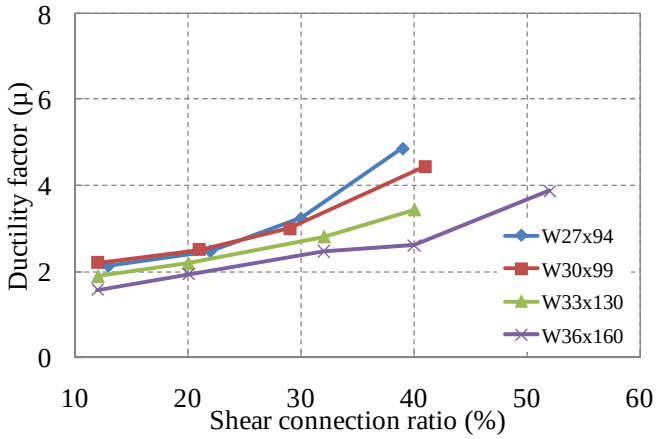

(b) Span: 40 ft

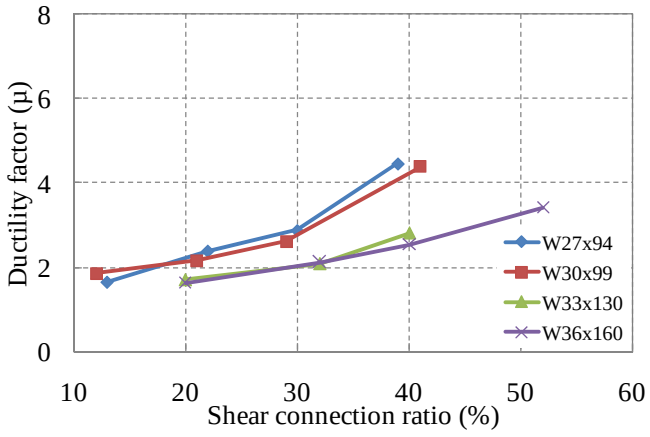

(c) Span: 50 ft

Figure 5.9: Ductility of composite beams

5.3.2 Effect of Oversized Holes

The effect of oversized holes in the steel beam flange was evaluated for composite beams having a W30x99 steel beam section and 38-ft long span, which has the same geometry as the full-scale test specimens in TxDOT Project 0-4124. Figure 5.10 shows the ABAQUS load-deflection curves for six composite beams with 38-ft spans, along with the analysis results for an otherwise identical non-composite beam. The composite beams that were analyzed had connection ratios of 30 percent, corresponding to 16 shear connectors in a shear span. Composite beam Model HASAA-30BS2 in Figure 5.10 had no gap between the holes in the steel beam flange and the connectors. That model showed the highest stiffness, strength, and ductility factor of all the composite beams in Figure 5.10. In the other composite beam models, slip occurred in the shear connectors without any load, using the load-slip relationship shown in Figure 5.1. The designations used in Figure 5.10 start with the type of shear connectors, followed by shear connection ratio (30 percent). The "BS" stands for Beam Static analysis. A numeral at the end of the specimen name added to distinguish each from the others.

Model HASAA-30BS3 was designed so that the two shear connectors near the support would resist load immediately (no gap between the connectors and the beam flange), and the other 14 shear connectors in the same shear span would have the maximum gap of 0.125 in., assumed to be unfilled with adhesive, so that these shear connectors would not resist load until 0.125-in. slip was reached. This model was developed because shear connectors near a support have the maximum slip demand, and generally govern the deformation capacity of the composite beam. Because the other shear connectors would not begin to resist load until experiencing a slip of 0.125 in., lower initial stiffness was expected for this composite beam. It did in fact have lower initial stiffness and lower deformation capacity than Model HASAA-30BS2. It still showed higher strengths than computed from simple plastic analysis, however, and its ductility factor was still higher than 2.

The other four analytical models, Models HASAA-30BS4 to HASAA-30BS7, had shear connectors with initial gaps that were assumed to vary randomly. For each composite beam, 32 random numbers between 0 and 1 were generated, and those numbers were multiplied by 0.125 in. which is the maximum slip that shear connectors can experience without any load. This method was considered to be a realistic reflection of the gaps associated with shear connectors in real construction. The four composite beam models with arbitrary shear-connector gaps at oversized holes in the beam flange differed little with each other with respect to initial stiffness and maximum strength. As shown in Table 5.4, initial stiffness of these composite beams is lower than that of Model HASAA30BS2 which had no gaps. Their maximum strength, however, differs little from that of Model HASAA-30BS2. These four composite beam models also show ductility factors higher than 2.

From the finite element analysis involving different shear connector locations in oversized holes, it can be concluded that oversized holes in the steel beam flange do not significantly affect the strength of partially composite beams retrofitted with post-installed shear connectors. Consequently, for the HASAA connector, it is acceptable to use a 1-inch diameter hole in the beam flange for a 7/8-inch diameter connector, as was done for the Hondo Bridge. The use of oversize holes has a more significant impact on initial elastic stiffness, as indicated by the finite element analysis (Figure 5.10) and from the live load test measurements at the Hondo Bridge. However, as long as the primary requirement of the retrofit is to increase the strength of a bridge rather than the stiffness, as was the case at the Hondo Bridge, the reduced stiffness resulting from the use of oversize holes has little practical significance. In cases where post-

installed shear connectors are added to a bridge with the primary purpose of increasing stiffness, then the use of oversize holes should be avoided, or their effect on stiffness be considered in the design of the retrofit.

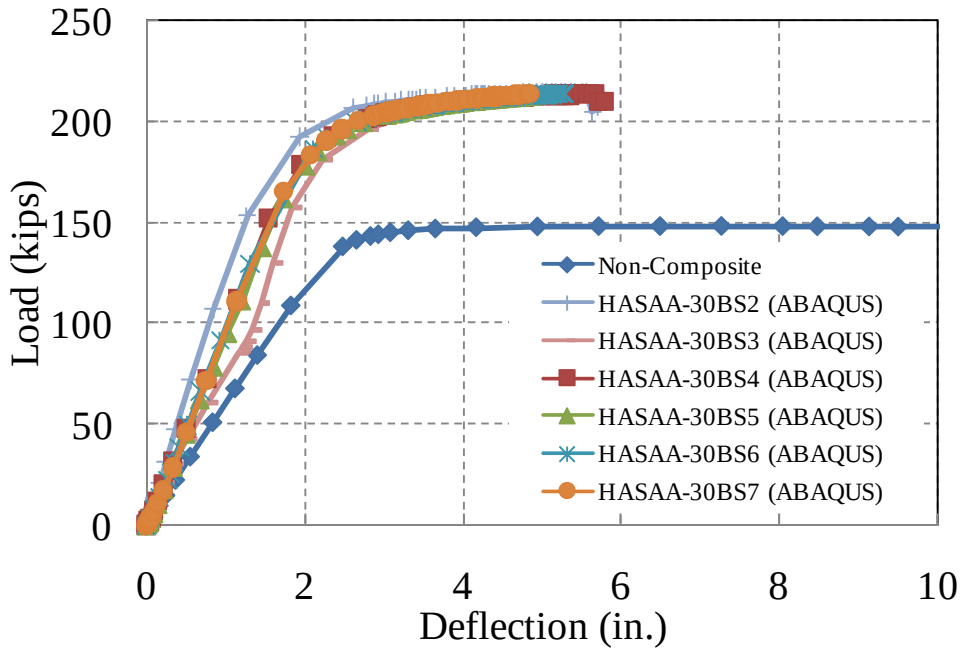

Figure 5.10: Load-deflection graphs considering the effects of oversized holes

Table 5.4: Analysis results of composite beams with oversized holes in the beam flange

Model	Max. load (kips)		Ductility factor
	AISC, AASHTO	ABAQUS	
HASAA-30BS2	205	214	3.3
HASAA-30BS3	205	211	2.3
HASAA-30BS4	205	213	2.8
HASAA-30BS5	205	212	2.2
HASAA-30BS6	205	214	2.5
HASAA-30BS7	205	213	2.3

5.4 Summary

In this chapter, results are described for parametric studies conducted to supplement the full-scale beam test results obtained in Project 0-4124, and to investigate the behavior of composite beams retrofitted with post-installed shear connectors with various beam depths, span lengths, and shear connection ratios. The effect of oversized holes in the steel beam flange was also investigated.

From the analytical study of 60 composite beam models, it was concluded that current design equations (AASHTO 2007, AISC 2005) accurately predict the maximum strength and elastic stiffness of partially composite beams with post-installed shear connectors concentrated near the supports or the zero-moment regions.

The deformation capacity of the composite beams was also evaluated using a ductility factor, defined in terms of an elasto-plastic approximation to calculated load-deflection curves. Based on previous experimental results, a minimum acceptable value of 2 was suggested for the ductility factor. Based on the finite element analysis results, a minimum shear connection ratio of 30 percent is recommended for composite beams retrofitted with post-installed shear connectors. Because the behavior of real, multi-girder bridges is more complex than that of the single-girder bridges addressed by this parametric study, more research would be desirable to investigate the relationship between ductility demands and available ductility for bridges made of composite beams with partial composite design.

The parametric study shows that the gap between the oversized holes in the steel beam flange and the shear connector does not significantly affect the strength of partially composite beams constructed with post-installed shear connectors. Nonetheless, it is beneficial to eliminate such gaps if possible, because doing so increases stiffness and ductility.

Chapter 6. Summary, Conclusions, and Design Recommendations

6.1 Introduction

This project was an implementation of research conducted under TxDOT Research Project 0-4124 on the use of post-installed shear connectors to develop composite action in existing non-composite steel bridge girder systems. Previous work in TxDOT Project 0-4124 identified various post-installed shear connectors, conducted tests on these connectors, and evaluated their performance. Based on single shear connector tests, full-scale beam tests, and analytical studies, three types of post-installed shear connectors were recommended, which are referred to as the Double-Nut Bolt (DBLNB), the High-Tension Friction-Grip Bolt (HTFGB), and the Adhesive Anchor (HASAA).

In this implementation study, an existing non-composite bridge in the San Antonio District was retrofitted with these three types of post-installed shear connectors to increase the load-carrying capacity of the bridge girders. The bridge is located near the town of Hondo, Texas, and is referred to herein as the Hondo Bridge. A detailed design for strengthening the Hondo Bridge was undertaken in this study. Potential design and construction difficulties were identified and solutions to these difficulties were suggested. The bridge consists of three identical simple spans and each span was retrofitted with a different type of post-installed shear connector. For the spans retrofitted with the DBLNB and HTFGB connectors, 28 shear connectors per girder were adequate to achieve the load-rating requested by TxDOT. For the HASAA connectors, 52 shear connectors were installed per girder. The required number of post-installed shear connectors was significantly less than the number of conventional welded shear studs that would have been needed to satisfy AASHTO fatigue requirements.

Field live load tests were conducted using loaded TxDOT dump trucks. Five different truck locations were selected for the tests. Deflections and strain profiles in steel girder sections were measured during the tests. Tests were conducted both before and after the retrofit. The test results showed clearly that significant composite action was developed in the retrofitted girders, as expected.

To supplement the field studies, a finite element model was developed and parametric studies were conducted using the finite element model to evaluate the effects of various parameters including beam depth, span length, and shear connection ratio on the overall stiffness, strength, and ductility of the composite beams with post-installed shear connectors. These supplemental studies were conducted to assist in the design of the retrofit for the Hondo Bridge and to contribute to the development of design recommendations.

6.2 Summary and Conclusions

Overall, the results of this study indicate that the addition of post-installed shear connectors can significantly increase the strength of existing non-composite bridge girders. By using partial composite design, the addition of a relatively small number of post-installed shear connectors can increase the flexural capacity of an existing girder in positive moment regions by 40 to 50 percent. The use of post-installed shear connectors can therefore provide an effective means for strengthening existing non-composite bridges. Some specific observations and conclusions from this implementation project are as follows:

- A complete design process to strengthen the Hondo Bridge using post-installed shear connectors was developed in this study, and can be used as a model for future strengthening projects. This design process resulted in a recommendation to install 28 shear connectors per girder for the DBLNB and HTFGB connectors, and 52 shear connectors per girder for the HASAA connector. A larger number of HASAA connectors were needed due to the lower fatigue strength of this connector. Shear connectors were installed at 12-in. spacing near the ends of each girder. No shear connectors were installed in the center portion of the girders. Locating the shear connectors near the beam ends enhances the ductility of the retrofitted girders.
- A load rating was conducted for the Hondo Bride prior to retrofit, showing an HS10.6 inventory level rating and an HS17.6 operating level rating. With the addition of the post-installed shear connectors, the load rating for the bridge increased to HS17.4 inventory level and HS29.1 operating level. Thus, both the inventory level and operating level load ratings increased 65-percent as a result of the installation of post-installed shear connectors.
- The effect of fatigue on the required number of shear connectors was evaluated in this case study. The results of this evaluation showed that fatigue did not control the required number of connectors for the DBLNB and HTFGB connectors. For these cases, the required number of connectors was controlled by static strength requirements, and the 28 post-installed shear connectors per girder, based on partial composite design, were adequate to achieve the load-rating increase noted above.
- In the case of the HASAA connectors, fatigue controlled the required number of connectors. This is because the fatigue life of the HASAA connector is less than that for the DBLNB and HTFGB connectors, although it is still substantially better than for conventional welded studs. In the case of the HASAA connector, satisfying fatigue design requirements, 52 connectors were needed, as compared to 28 based on static strength requirements. Note that for conventional welded studs, approximately 120 shear studs per girder would be needed to satisfy AASHTO fatigue requirements. Also, as described in Chapter 3, finite element analysis indicated that 28 HASAA connectors per girder would actually have been satisfactory for fatigue. The increase from 28 to 52 was needed as a result of using conservative hand calculation methods to compute the stress range in the connectors.
- Load tests were conducted on the Hondo Bridge before and after the retrofit. Composite behavior after the retrofit was verified by measuring deflections and strain profiles in steel beam sections. The load tests showed that significant composite action was developed in the retrofitted bridge girders, as expected.
- A finite element model was developed and parametric studies were conducted to investigate the effects of steel beam depth, span length, and shear connection ratio on the overall system performance of the strengthened partially composite beams. The analysis results showed that an increase in beam depth and span length resulted in reduced deformation capacity of composite beams. Composite beams with a high shear-connection ratio showed better deformation capacity than composite beams with a low shear-connection ratio. All of the composite beams with a shear-

connection ratio of at least 30 percent showed a global ductility factor of at least two. Based on this analysis, a minimum shear connection ratio of 30 percent is recommended. Based on the analysis results, it was also shown that the strength and stiffness of composite beams retrofitted with post-installed shear connectors can be accurately calculated using current AASHTO and AISC design equations. The parametric study also showed that the gap between the oversized holes in the steel beam flange and the shear connector does not significantly affect the strength of partially composite beams constructed with post-installed shear connectors. Consequently, oversize holes (hole diameter is 1/8-inch greater than fastener diameter) can be used to facilitate construction. Nonetheless, it is beneficial to eliminate such gaps if possible, because doing so increases stiffness and ductility of the retrofitted girder.

- The actual installation of the post-installed shear connectors on the Hondo Bridge proved considerably more difficult than anticipated prior to construction and based on the connector installation experiences in Project 0-4124. Problems encountered during the construction are described in Chapter 3, along with suggestions for mitigating these problems in future installations.

6.3 Preliminary Design Recommendations

The results of this study and the previous TxDOT Project 0-4124 clearly demonstrate that the strength and stiffness of existing non-composite steel bridge girders can be increased significantly by post-installing shear connectors. Based on the research results from laboratory tests and analytical studies, a preliminary design approach for strengthening existing steel bridge girders by using post-installing shear connectors can be proposed. Preliminary design recommendations are as follows:

- Three types of post-installed shear connectors are recommended for use in strengthening existing non-composite bridge girders. The three types of post-installed shear connectors are the Double-Nut Bolt (DBLNB), the High-Tension Friction-Grip Bolt (HTFGB), and Adhesive Anchor (HASAA). These connectors consist of high strength bolts or threaded rods placed in holes that are drilled in the concrete slab and top flange of the steel girder. The holes are filled with high strength grout (double-nut bolt and high tension friction grip bolt) or structural adhesive (adhesive anchor). Installation of the double-nut bolt and high tension friction grip bolt require construction operations on both the top and bottom sides of the concrete slab. The adhesive anchor, in contrast, can be completely installed from underneath the slab, thereby minimizing traffic disruptions on the bridge.
- Use of either 3/4-in. or 7/8-in. diameter shear connectors is recommended, as these are the diameters tested in this research project and the previous laboratory tests (Kwon et al. 2007). The use of larger diameter shear connectors can reduce the number of shear connectors needed to achieve the same level of shear connection ratio. 7/8-inch diameter shear connectors were used on the Hondo Bridge. Other diameters may be suitable, although test data would be desirable to evaluate their performance.

- For the DBLNB and HASAA connectors, the use of ASTM A193 B7 threaded rods is suggested. For the HTFGB connector, the use of ASTM A325 high-strength bolt or equivalent is suggested.
- The use of partial composite design is recommended as an overall basis for strengthening steel bridge girders with post-installed shear connectors. Use of a shear connection ratio less than 30 percent is not recommended to avoid non-ductile behavior of the strengthened girder. The flexural strength and elastic stiffness of retrofitted partial composite beams can be computed using current AASHTO and AISC design provisions (AASHTO 2007, AISC 2005).
- The use of Equation 2.1 is recommended for computing the static strength of post-installed shear connectors. This equation can be applied to all three types of post-installed shear connectors.
- Pending the availability of additional fatigue tests, it is recommended to use 35 ksi as a fatigue endurance limit for the DBLNB and HTFGB connectors (Equation 2.2) . Equation 2.3 is recommended to calculate the fatigue strength of the HASAA connector.
- It is recommended that general requirements concerning clear cover, edge distance, and minimum transverse spacing between shear connectors in the AASHTO provisions be followed.
- It is recommended that post-installed shear connectors be concentrated near zero moment regions, rather than being distributed uniformly along the length of the beam. This increases the overall ductility of the strengthened partially composite beams (Kwon 2008). The minimum longitudinal spacing of the shear connectors used for the full-scale beam tests and in the Hondo Bridge was 12 in.
- Installation procedures used for the post-installed shear connectors in the full-scale beam tests are described in detail in Appendix B, and can be used as a guide for actual field installation. Modifications to these procedures should be considered based on the construction difficulties encountered in the Hondo Bridge, as described in Chapter 3.

6.4 Recommendations for Future Research

Following are recommendations for further research related to strengthening existing non-composite beams using post-installed shear connectors:

- Additional single shear connector tests under fatigue loading are needed to better characterize the S-N relationship for the post-installed shear connectors, as well as to characterize the variability in fatigue performance.
- Further studies are needed to develop methods for computing the forces on post-installed shear connectors under service level loading, for purposes of fatigue design. For conventional fully composite bridge girders, shear flow at the steel-concrete interface is computed based on a transformed fully composite cross-section. In the case of a partially composite girder, the use of a transformed cross-section may not provide an accurate estimate of shear flow. Further, the post-

installed shear connectors are installed near the girder ends only, with no connectors in the center portion of the girder. For this arrangement of connectors, it is unclear how to compute connector shear force from the shear flow. For the Hondo Bridge, a simple and conservative approach was developed for checking the stress range on the post-installed shear connectors. This simple method may be too conservative for the HASAA connectors. For the Hondo Bridge, the simple method showed 52 shear connectors per girder were needed to satisfy fatigue requirements, whereas only 28 shear connectors per girder were needed to satisfy static strength requirements. However, more exact finite element analysis showed that, in fact, fatigue did not control the required number of HASAA connectors, and 28 connectors per girder would have been sufficient.

- This study investigated the use of post-installed shear connectors for increasing the positive moment capacity of girders, and is most useful for simple spans. Additional research is needed to extend the results of this study to continuous multi-span steel girders that have inadequate flexural capacity in negative moment regions. Possible approaches may include post-installing shear connectors in negative moment regions to develop composite action in these regions. Alternatively, post-installed shear connectors could be added to positive moment regions, with an increase in load capacity achieved through plastic redistribution of moment from the negative moment regions to the strengthened positive moment regions.

Appendix A: Load Rating For Hondo Bridge

A.1. Non-Composite Beam Load Rating

A.1.1 Geometry

- Span length: 39.33 ft (bearing length deducted)
- Materials: Steel $F_y = 33\,ksi$ (year built: 1950) AASHTO Manual 6.6.2.1
  Concrete $f_c' = 2.5\,ksi$ AASHTO Manual 6.6.2.4

Steel section dimensions are shown in Figure A.1.

For the bare steel beam,
$\bar{y} = 12.94\,in.$
$I_x = 2782.7\,in.^4$
$S_t = S_b = 215\ in^3$

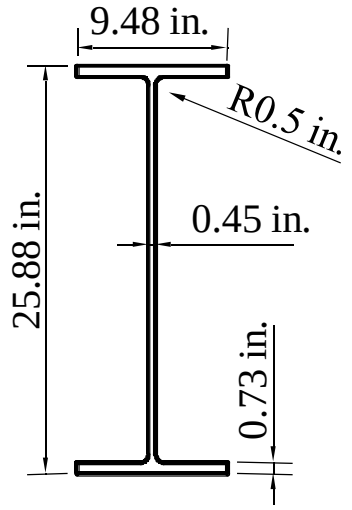

Figure A.1: Steel beam section

A.1.2 Load Calculation

- Dead loads

Deck: $7 \times \frac{6.25}{12} \times 0.15 = 0.547\,kips/ft$

Stringer: $0.085\,kips/ft$ Diaphragm: $0.012\,kips/ft$

Moment due to dead load, M_{DL}

$$M_{DL} = \frac{wL^2}{8} = \frac{(0.547 + 0.085 + 0.012) \times 39.33^2}{8} = 124.52\ ft - kips$$

- Superimposed dead loads

In AASHTO, it is specified that "Curbs, railings, and wearing surface, if placed after the slab has cured, may be distributed equally to all roadway stringer beams."

Curb: $1\times\frac{10}{12}\times 0.15/2 = 0.063 kips/\ ft$

AASHTO Specifications 3.23.2.3.1.1

Railing: $\frac{20 lb/\ ft}{2} = 0.01 kips/\ ft$

Wearing surface: $7\times\frac{0.5}{12}\times 0.144 = 0.042\ kips/\ ft$

Moment due to superimposed dead load

$$M_{SDL} = \frac{wL^2}{8} = \frac{(0.0625+0.010+0.042)\times 39.33^2}{8} = 22.14\ ft-kips$$

$$M_{DL} + M_{SDL} = 146.66\ ft-kips$$

- Live Loads

$M_L = 219\ ft-k$ (without impact and distribution factor)

AASHTO Manual Appendix A3

Impact factor $I = \frac{50}{L+125} \le 0.3$ AASHTO Specifications 3.8.2.1

$$= \frac{50}{39.33+125} = 0.304 \quad \therefore I = 0.3$$

Distribution factor $DF = \frac{S}{5.5} = \frac{7}{5.5} = 1.273$ AASHTO Specifications 3.23.2.3.1.5

$M_{L+I} = 219\times 1.3\times 1.27 = 371\ ft-kips$ (with impact and distribution factor)

A.1.3 Section Capacity

- Check compact section criteria AASHTO Specifications 10.48.1.1

Compression flange: $\frac{b}{t} \le \frac{4110}{\sqrt{F_y}}$ O.K.

Web thickness: $\frac{D}{t_w} \le \frac{19230}{\sqrt{F_y}}$ O.K.

$Z = 245\ in.^3$

$M_u = F_y Z = 3085\ in.-kips = 673.75\ ft-kips$

A.1.4 Load Rating

$$RF = \frac{C - A_1 D}{A_2 L(1+I)}$$ AASHTO Manual 6.5.1

For the Load Factor Method, $A_1 = 1.3$ for both Inventory and Operating level, $A_2 = 2.17$ for Inventory level and 1.3 for Operating level.

- Strength criterion

Inventory level $RF = \frac{673.75 - 1.3 \times 146.66}{2.17 \times 371} = 0.60$

Operating level $RF = \frac{673.75 - 1.3 \times 146.66}{1.3 \times 371} = 1.00$

- Serviceability criterion ($f_s \le 0.8F_y$) AASHTO Specifications 10.57.1

AASHTO Specifications require that bridge girders remain elastic for overload vehicles.

Inventory level $RF = \frac{0.8 \times 33 \times 215/12 - 146.66}{1.67 \times 371} = 0.53$ Control

$\therefore RT = 0.53 \times HS20 = HS10.6$

Operating level $RF = 0.53 \times 1.67 = 0.88$ Control

$\therefore RT = 0.88 \times HS20 = HS17.6$

A.2. Load Rating for Strengthened Composite Beam

A.2.1 Geometry

Composite beam section is shown in Figure A.2.

Modular ratio $n = \frac{29000}{1820\sqrt{2.5}} = 10.08$

Effective slab width $b_{eff} = 75\ in.$ AASHTO Specifications 10.38.3.1

Partial composite design is used for the retrofit of the currently non-composite steel bridge girders. Fourteen shear connectors in a shear span (total 28 shear connectors in a beam) are used to retrofit the bridge. As a reference, 56 post-installed shear connectors in a beam are required for fully composite beam design.

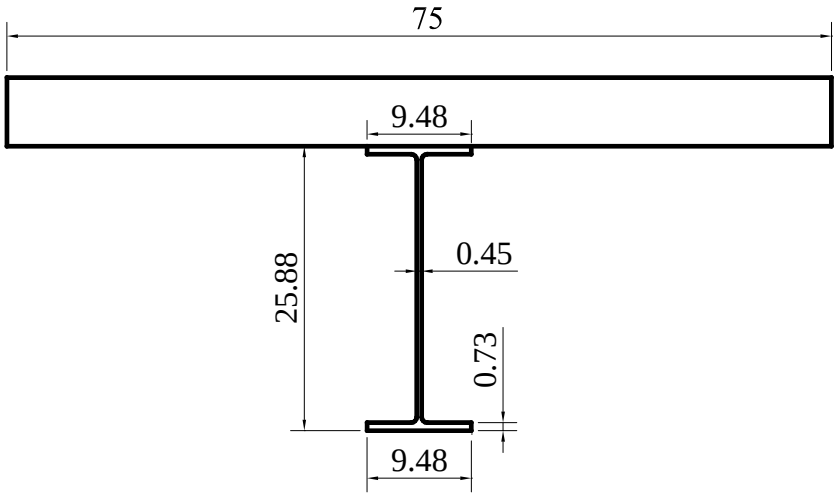

Figure A.2: Composite beam section (unit: in.)

A.2.2. Ultimate Strength

The ultimate strength of individual shear connectors can be calculated using the equation below.

$$Q_n = 0.5 A_{sc} F_u = 0.5 \times 0.8 \times \pi \times \left(\frac{0.875}{2}\right)^2 \times 125 = 30.07\, kips$$

The effective shear area, A_{sc}, of the threaded part of the connectors can be calculated as 80% of the unthreaded area.

$$\sum Q_n = 30.07 \times 14 = 420.92\, kips$$

Simple plastic analysis is used to determine the ultimate strength of the partial composite beam retrofitted with post-installed shear connectors.

Plastic N.A. $\bar{y} = 6.58\, in.$ from the top of the slab

$$M_{ult} = 1056.73\ ft - kips$$

- Strength criterion

Inventory level: $RF = \dfrac{1056.73 - 1.3 \times 146.66}{2.17 \times 371} = 1.08$

Operating level: $RF = \dfrac{1056.73 - 1.3 \times 146.66}{1.3 \times 371} = 1.80$

- Serviceability criterion ($f_s \le 0.95 F_y$) AASHTO Specifications 10.57.2

For overload vehicles, the bridge girders are required to behave elastically. *AASHTO Specifications* do not address any methods to determine the beam stress for partial composite bridge girders. The effective section modulus of a partially composite beam, as given in the commentary of the *AISC Specification*, is used to calculate stress in the beam flange.

$$S_{eff} = S_s + \sqrt{\left(\sum Q_n / C_f\right)} \cdot \left(S_{tr} - S_s\right) = 215 + \sqrt{420.92 / 829.95} \cdot \left(\frac{7147.03}{23.37} - 215\right)$$

$$= 279.68\, in^3$$

AISC Specification Commentary I3

Inventory level: $RF = \dfrac{33 \times 0.95 - \dfrac{146.66 \times 12}{215}}{1.67 \times \dfrac{371 \times 12}{279.68}} = 0.87$ Controls

$\therefore RT = 0.87 \times HS20 = HS17.4$

Operating level: $RF = 0.87 \times 1.67 = 1.45$ Controls

$\therefore RT = 1.45 \times HS20 = HS29.1$

A.2.3 Fatigue Strength

Shear connectors are numbered as shown in Figure A.3. The HS20 design truck, including impact factor and distribution factor, was moved from the left support to the right support and the right to the left. The shear force in each shear connector was calculated at each location of the truck and the maximum stress range was determined for each connector. Two examples are shown below. It was assumed that horizontal shear force where shear connectors are installed is resisted by the connectors at the section. The horizontal shear force where shear connectors are not installed was assumed to be resisted equally by the shear connectors in the shear span.

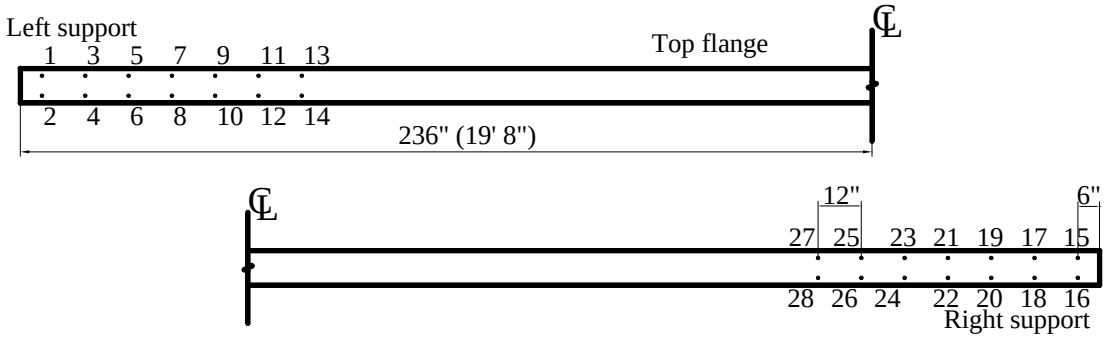

Figure A.3: Shear connector numbering

- Case I: Rear wheel is located 4 ft from the left support

Figures A.4 and A.5 show truck wheel locations and the corresponding shear force diagram.

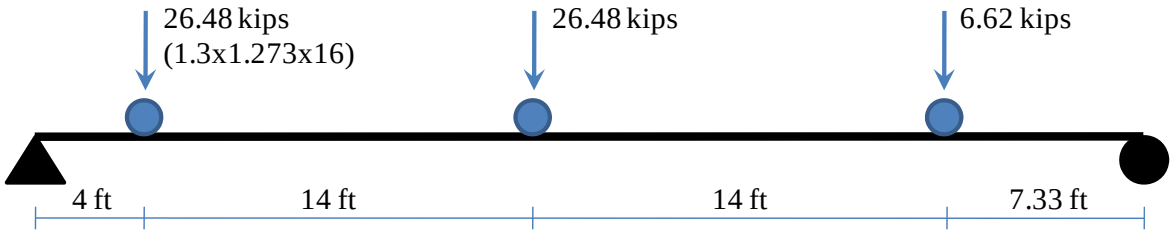

Figure A.4: Truck wheel locations

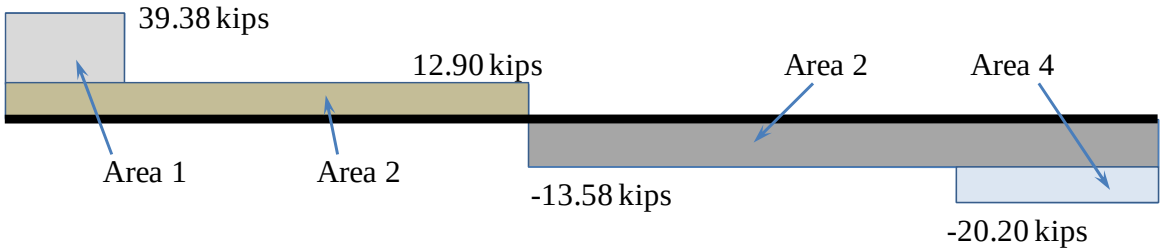

Figure A.5: Shear force diagram

For Area 1

$V = 39.38 - 12.90 = 26.48\,kips$, $I_{tr} = 7147.03\,in^4$, $Q = 262.03\,in^3$

Shear flow $f = \frac{VQ}{I_{tr}} = \frac{26.48 \times 262.03}{7147.03} = 0.97 kips/in = 11.65 kips/ft$

Total horizontal shear force, V_h, can be obtained by multiplying the shear flow with the applied span length in the beam.

$V_h = 11.65 kips/ft \times 4\,ft = 46.6 kips$

The number of shear connectors loaded in the span is 8.

$Q_1 = Q_2 \cdots = Q_8 = 46.6 kips/8 = 5.825 kips$

For Area 2

$V = 12.90\,kips$

Shear flow $f = \frac{12.90 \times 262.03}{7147.03} = 0.47 kips/in = 5.68 kips/ft$

Total horizontal shear force V_h

$V_h = 5.68 \times 18 = 102.16 kips$

The number of shear connectors loaded is 14.

$Q_1 = Q_2 = \cdots = Q_{14} = 102.16 kips/14 = 7.30 kips$

For Area 3

$V = -13.58 kips$

Shear flow $f = \frac{13.58 \times 262.03}{7147.03} \times 12 = 5.97 kips/ft$

Total horizontal shear force V_h

$V_h = 5.97 \times 21.33 = 127.34 kips$

The number of shear connectors loaded is 14.

$Q_{15} = Q_{16} = \cdots = Q_{28} = 127.34/14 = 9.10 kips$

For Area 4

$V = -20.20 + 13.58 = -6.62 kips$

Shear flow $f = \frac{6.62 \times 262.03}{7147.03} \times 12 = 2.91 kips/ft$

Total horizontal shear force V_h

$V_h = 2.91 \times 7.33 = 21.33 kips$

The number of shear connectors loaded is 14.

$Q_{15} = Q_{16} = \cdots = Q_{28} = 1.52 kips$

The shear connector forces for Case I loading are shown in Table A.1.

Table A.1: Connector shear forces for Case I loading

Connector	1	3	5	7	9	11	13
	2	4	6	8	10	12	14
Shear force (kips)	13.13	13.13	13.13	13.13	7.30	7.30	7.30

27	25	23	21	19	17	15	Connector
28	26	24	22	20	18	16	
10.62	10.62	10.62	10.62	10.62	10.62	10.62	Shear force (kips)

- Case II: Rear wheel is located 36 ft from the left support

Figure A.6 and Figure A.7 show truck wheel locations and the shear force diagram for Case II loading.

Figure A.6: Truck wheel locations

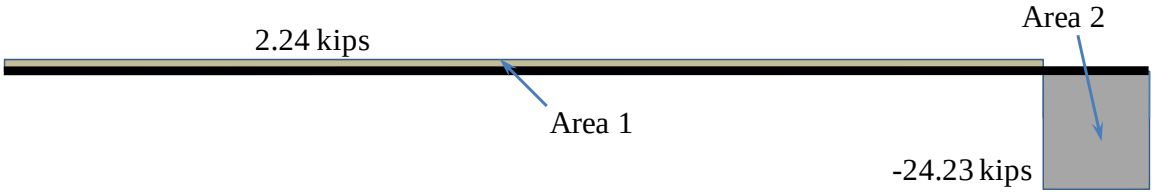

Figure A.7: Shear force diagram

For Area 1

$V = 2.24\,kips$

Shear flow $f = \frac{2.24 \times 262.03}{7147.03} \times 12 = 0.9872 kips/ft$

Total horizontal shear force V_h

$V_h = 0.9872 \times 36 = 35.54 kips$

The number of shear connectors loaded is 22 (14 in the left shear span and 8 in the right shear span)

$Q_5 = Q_2 = \cdots = Q_{14} = 1.62 kips$

$Q_{21} = Q_{22} = \cdots = Q_{28} = -1.62 kips$

Connector force is positive when the connector head deforms toward the nearest support.

For Area 2

$V = -24.23 kips$

Shear flow $f = \dfrac{24.23 \times 262.03}{7147.03} \times 12 = 10.66 kips / ft$

Total horizontal shear force V_h

$V_h = 10.66 \times 3.33 = 35.54 kips$

The number of shear connectors loaded is 6.

$Q_{15} = Q_{16} = \cdots = Q_{20} = 5.92 kips$

Connector shear forces are summarized in Table A.2 for Case II loading.

Table A.2: Connector shear forces for Case II loading

Connector	1	3	5	7	9	11	13
	2	4	6	8	10	12	14
Shear force (kips)	1.62	1.62	1.62	1.62	1.62	1.62	1.62

27	25	23	21	19	17	15	Connector
28	26	24	22	20	18	16	
-1.62	-1.62	-1.62	-1.62	5.92	5.92	5.92	Shear force (kips)

The HS20 truck load was moved to the both directions. Table A.3 shows shear connector force for several truck locations. Truck locations in Table A.3 are the distance from a support to the rear wheel location.

- Check maximum stress range

Connector 7 and 8 experienced the maximum stress range for the truck loadings.

$$\frac{13.12+1.61}{0.8\times\pi\times(0.875/2)^2}=30.62ksi\le 35ksi \quad \therefore O.K.$$

Table A.3: Shear connector force for several truck locations (kips)

Distance from left support (ft)	Shear connector number (near left support)							Shear connector number (near right support)						
	1, 2	3, 4	5, 6	7, 8	9, 10	11, 12	13, 14	27, 28	25, 26	23, 24	21, 22	19, 20	17, 18	15, 16
0	8.34	8.34	8.34	8.34	8.34	8.34	8.34	8.34	8.34	8.34	8.34	8.34	8.34	8.34
2	14.49	14.49	8.01	8.01	8.01	8.01	8.01	9.68	9.68	9.68	9.68	9.68	9.68	9.68
4	13.12	13.12	13.12	**13.12**	7.30	7.30	7.30	10.63	10.63	10.63	10.63	10.63	10.63	10.63
10	11.19	11.19	11.19	11.19	11.19	11.19	11.19	10.92	10.92	10.92	10.92	10.92	10.92	12.85
16	11.06	11.06	11.06	11.06	11.06	11.06	11.06	11.06	11.06	11.06	11.06	11.06	11.06	11.06
20	10.44	10.44	10.44	10.44	10.44	10.44	10.44	6.00	6.00	12.20	12.20	12.20	12.20	12.20
30	5.92	5.92	5.92	5.92	5.92	5.92	5.92	5.92	5.92	5.92	5.92	5.92	5.92	5.92
36	1.61	1.61	1.61	1.61	1.61	1.61	1.61	-1.61	-1.61	-1.61	-1.61	5.92	5.92	5.92
38	0.63	0.63	0.63	0.63	0.63	0.63	0.63	-0.63	-0.63	-0.63	-0.63	-0.63	9.37	9.37

Distance form right support(ft)	Shear connector number (near left support)							Shear connector number (near right support)						
	1, 2	3, 4	5, 6	7, 8	9, 10	11, 12	13, 14	27, 28	25, 26	23, 24	21, 22	19, 20	17, 18	15, 16
0	8.34	8.34	8.34	8.34	8.34	8.34	8.34	8.34	8.34	8.34	8.34	8.34	8.34	8.34
2	9.68	9.68	9.68	9.68	9.68	9.68	9.68	8.01	8.01	8.01	8.01	8.01	14.49	14.49
4	10.63	10.63	10.63	10.63	10.63	10.63	10.63	7.30	7.30	7.30	13.12	13.12	13.12	13.12
10	12.85	10.92	10.92	10.92	10.92	10.92	10.92	11.19	11.19	11.19	11.19	11.19	11.19	11.19
16	11.06	11.06	11.06	11.06	11.06	11.06	11.06	11.06	11.06	11.06	11.06	11.06	11.06	11.06
20	12.20	12.20	12.20	12.20	12.20	6.00	6.00	10.44	10.44	10.44	10.44	10.44	10.44	10.44
30	5.92	5.92	5.92	5.92	5.92	5.92	5.92	5.92	5.92	5.92	5.92	5.92	5.92	5.92
36	5.92	5.92	5.92	**-1.61**	-1.61	-1.61	-1.61	1.61	1.61	1.61	1.61	1.61	1.61	1.61
38	9.37	9.37	-0.63	-0.63	-0.63	-0.63	-0.63	0.63	0.63	0.63	0.63	0.63	0.63	0.63

Appendix B: Recommended Installation Procedures for Post-Installed Shear Connectors

May 21, 2008 (June 08, 2008, revised)
Gunup Kwon, Michael Engelhardt, Richard Klingner
University of Texas at Austin Ferguson Laboratory

B1. Shear Connection Methods and Connector Locations

This document presents recommended installation procedures for post-installed shear connectors to increase the load-carrying capacity of the bridge on FM 462 over the Live Oak Creek near Hondo (herein referred to as the "Hondo Bridge"). The bridge consists of three simply supported spans and each span is 40 ft, 7 in. long. Three types of post-installed shear connectors were selected to strengthen the bridge and a different shear connection method will be applied to each span. Figure B.1 shows a schematic drawing of the bridge in Hondo and the shear connection methods which will be applied to each span.

For the first and second span from the left, a total of 28 shear connectors will be installed for each girder and the location of the shear connectors is shown in Figure B.2(a). These two spans will be retrofitted with the DBLNB and HTFGB connectors. A total 52 shear connectors will be installed for the third span which will be strengthened with the HASAA connectors [see Figure B.2(b)]. The longitudinal spacing of the shear connectors is 12 in. and two shear connectors will be installed in a row. The location of the shear connectors can be adjusted to minimize cutting of reinforcement in the concrete slab. A rebar locator may be useful for identifying the approximate location of reinforcing bars.

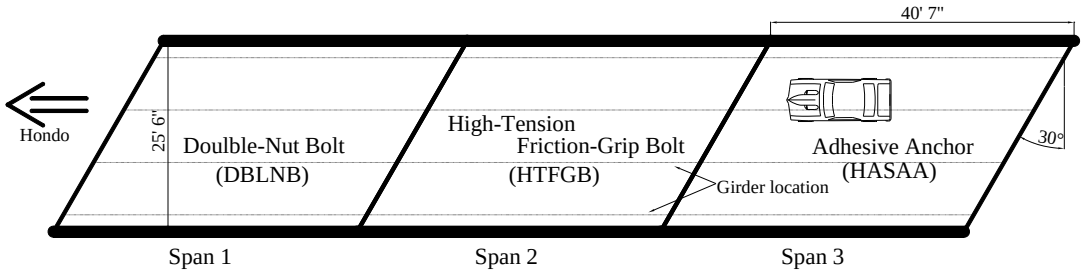

Figure B.1: Overall layout of the Hondo Bridge

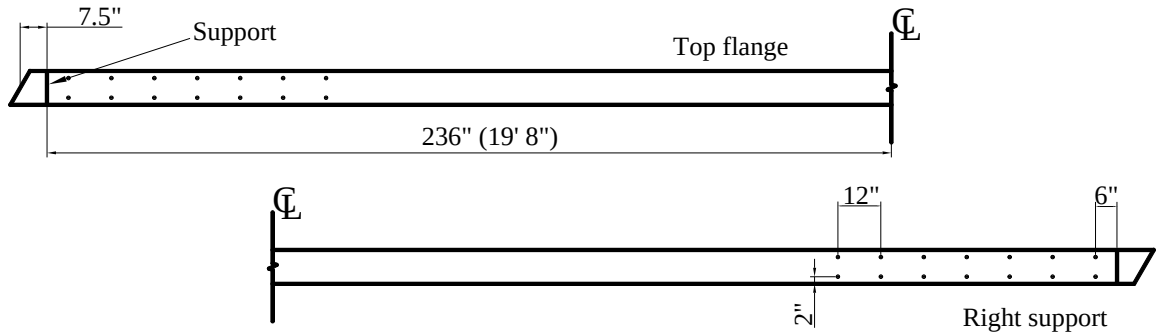

(a) Shear connector locations for the DBLNB and HTFGB connectors

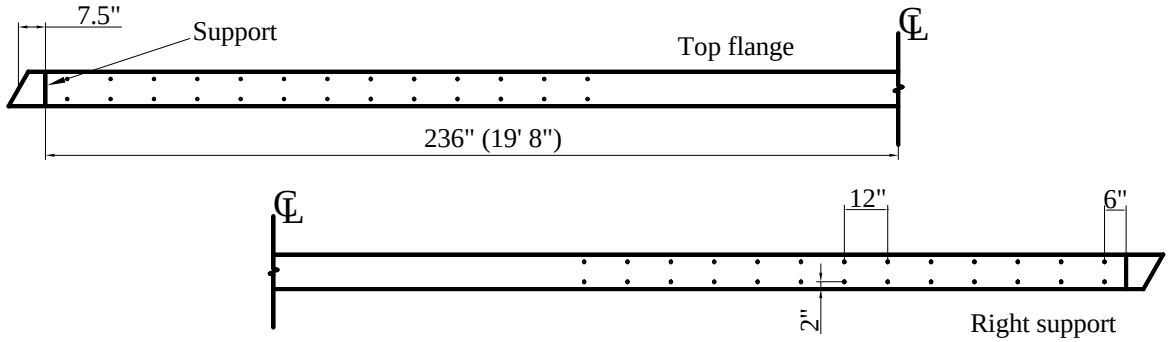

(b) Shear connector locations for the HASAA connectors

Figure B.2: Typical shear connector locations in each girder

B2. Installation of the Double-Nut Bolt (DBLNB) Connectors

7/8-inch diameter ASTM A193 B7 threaded rod is used for this method. Installation of the DBLNB connectors (Figure B.3) requires access from both the top and the bottom of the slab. Drilling through both the concrete slab and the steel beam flange is completed from the top and tightening of the connector is done underneath the slab using an impact wrench to reach the required pretension in the connector. Listed below is the procedure used to install the DBLNB connectors.

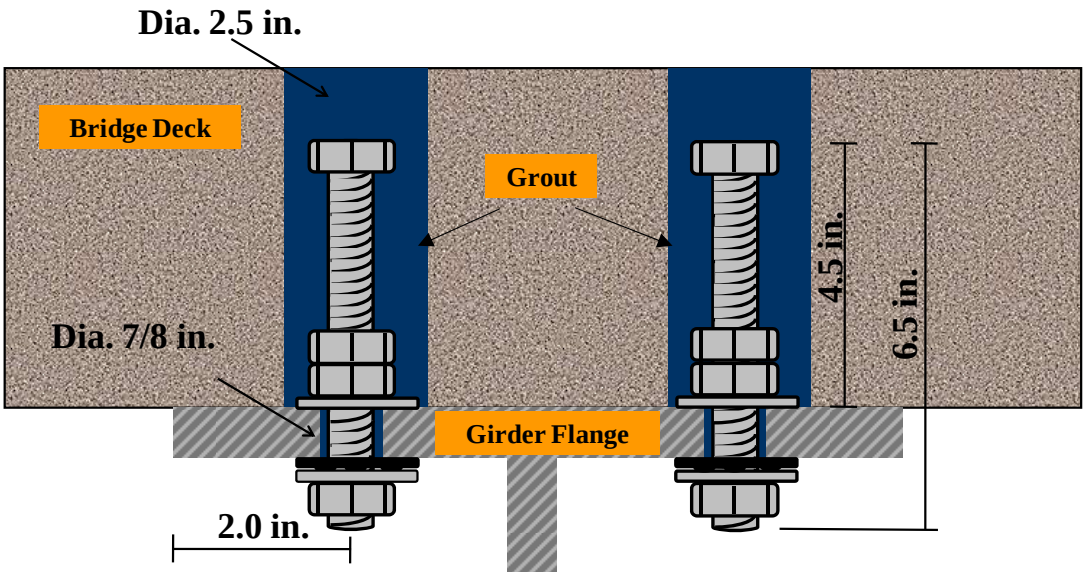

Figure B.3: Double–nut bolt connector

1) A 2.5-in. diameter hole is drilled into the concrete slab from the top using a Hilti DD200 coring machine (Figure B.4). A DD-BL U4 diamond core bit can be used for the coring operation. A constant water supply is needed to keep the drill bit cool.

2) A 7/8-in. diameter hole is drilled through the steel beam top flange from the top side of the slab using a portable magnetic drill. A 10-in. long drill bit is recommended to drill the holes from the top of the slab. A hollow round bar can be placed inside of the cored hole in the concrete to serve as a guide for the steel drill bit. This guide also helps to keep the inside surface of the concrete clean from cutting oil (Figure B.5).

3) A 6.5-in long ASTM A193 B7 threaded rod is placed from the top to provide a 4.5-in. embedment depth. Three nuts and a washer should be inserted in the rod before the rod is placed in the hole as shown in Figure 3. Next, the connector is tightened to a pretension of 39 kips using an impact wrench. “Squirter” Direct Tension Indicating (SDTI) washers can be used to confirm the required pretension. This washer has several bumps on the surface. Under this bump, orange-color silicone is embedded. As a bolt is tightened, the silicone material comes out and gives a visual indication of the bolt tension (Figure B.6).

4) Grout is poured to fill the gap. High-strength, fast-setting grout is recommended to minimize traffic disruption (Five Star Highway Patch or similar).

Figure B.4: Coring using Hilti DD200 coring machine

Figure B.5: Drilling through the beam flange

Figure B.6: Use of "Squirter" Direct Tension Indicating (SDTI) washer

B3. Installation of the High-tension Friction-Grip Bolt (HTFGB) Connector

The 7/8-inch diameter ASTM A325 high-strength bolts are used for this connection method. Figure shows a schematic drawing of the HTFGB connectors and the detailed installation procedure is as follows.

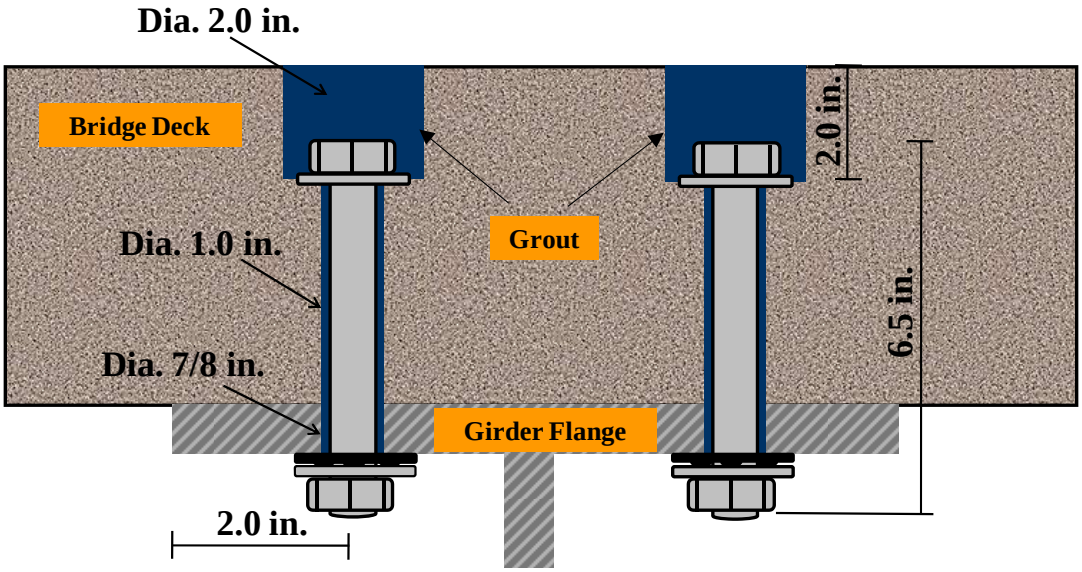

Figure B.7: High-tension friction-grip bolt connector

1) A 2-in. deep and 2-in. diameter hole is drilled into the concrete from the top using a Hilti TE-55 rotary hammer drill as shown in Figure B.8.

2) A 1-in. diameter, concentric hole with the 2-in. diameter hole is drilled through the concrete slab from the top using a Hilti DD200 coring machine.

3) A 7/8-in. diameter hole is drilled through the steel beam flange from the top side of the slab using a portable magnetic drill. The drill bit should be handled carefully not to touch the concrete surface inside the 1-in. diameter hole to minimize wear of the bit. Figure B.9 shows the concrete slab after the drilling.

4) A 6.5-in. long ASTM A325 high strength bolt with a washer is inserted from the top of the slab into the hole. The connector is tightened to a pretension of 39 kips using an impact wrench from the bottom of the slab. A SDTI washer should be used to confirm the required pretension. The turn-of-the-nut method is not accurate for the installation of the HTFGB connectors due to the presence of the concrete within the grip of the bolt.

5) Grout is poured to fill the hole on the concrete surface.

Figure B.8: Drilling into the concrete slab

Figure B.9: Concrete slab surface before connector installation

B.4. Installation of the Adhesive Anchor (HASAA) Connector

7/8-inch diameter ASTM A193 B7 threaded rod is used for the HASAA connectors. No drilling or coring is required from the top of slab (Figure B.10), so the HASAA shear connector can be completely installed from underneath the bridge. Following is the procedure used to install the HASAA connectors.

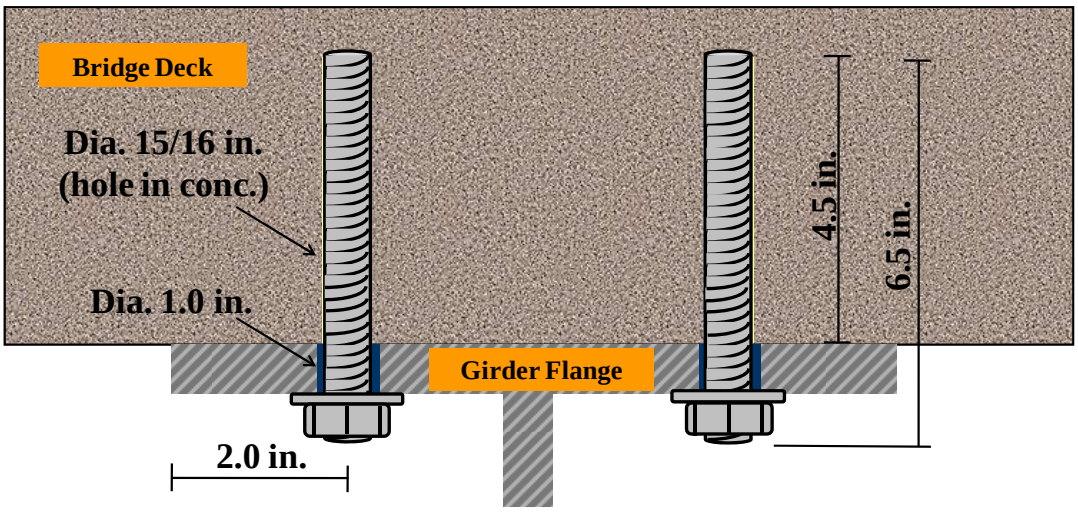

Figure B.10: Adhesive anchor (HASAA) connector

1) A 1-in. diameter hole is drilled through the steel beam flange from the bottom of the slab. A portable Jancy Slugger Cutter Mag Drill with magnetic base can be used to drill the hole (Figure).

2) A 4.5-in. deep hole is drilled into the concrete slab from the bottom using a 15/16-in. drill bit and a Hilti TE-55 rotary hammer drill (Figure B.12).

3) The drilled hole is cleaned using a wire brush and compressed air before injecting adhesive.

4) Hilti HIT HY 150 adhesive is injected into the hole using HIT-MD 2000 manual dispenser. Eight to nine holes can be completed with an 11.1-fluid ounce cartridge pack.

5) The 7/8-inch diameter ASTM A193 B7 threaded rod is inserted with a twisting motion. The rod can be adjusted during the specified gel time, but should not be disturbed between the gel time and cure time. For HIT HY 150 adhesive, the gel time and the cure time are 6 min. and 50 min. at $68^{\circ}F$, respectively. The cure time of HIT HY150 MAX is 30 min. at $68^{\circ}F$. Adhesive that overflowed is wiped off, leaving adhesive filling the gap between the oversized hole in the steel flange and the anchor. The adhesive is viscous enough to hold the connector in the hole, so the connector is not required to be held in place during the cure time to prevent from falling.

6) After the cure time, the nut is installed with a 150 lb-ft torque using a torque wrench.

Figure B.11: Drilling through the beam flange using a slugger drill

Figure B.12: Drilling into the concrete slab using a rotary hammer drill

Appendix C: Analysis Results of Composite Beams

C.1. Composite Beams with W27x94 Section

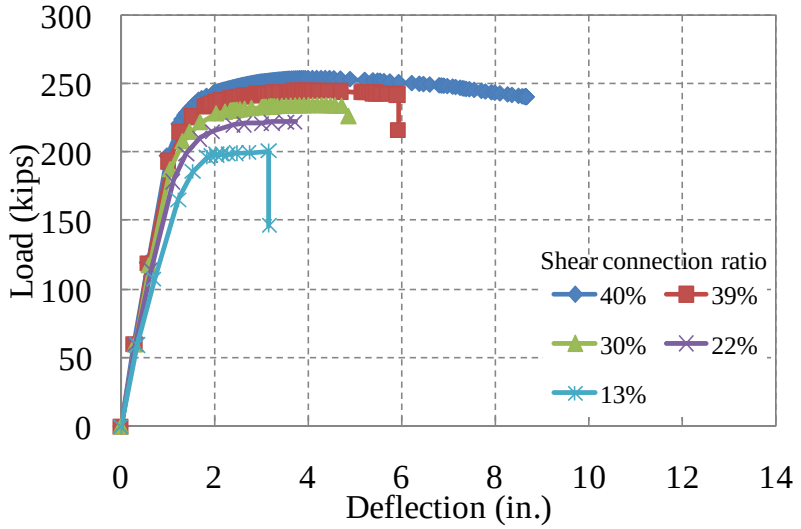

Figure C.1: Load-deflection relations of composite beams (W27x94, 30-ft span)

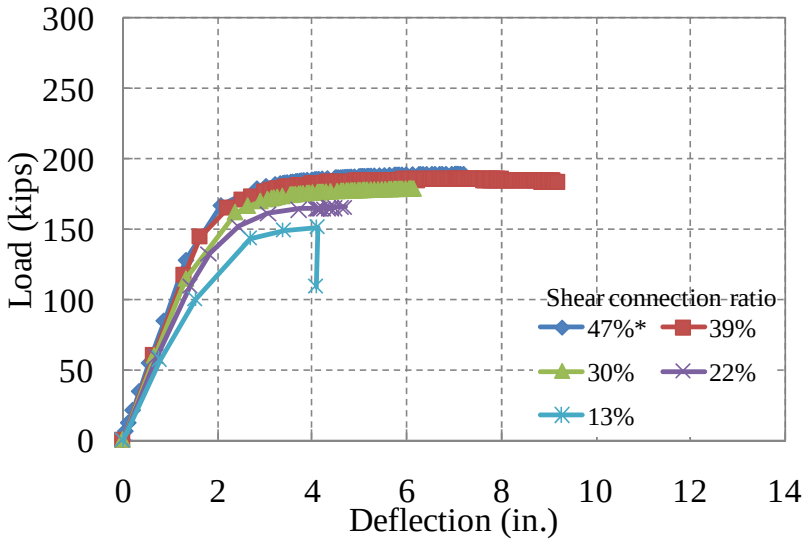

*: Convergence was not achieved before shear connector failed.

Figure C.2: Load-deflection relations of composite beams (W27x94, 40-ft span)

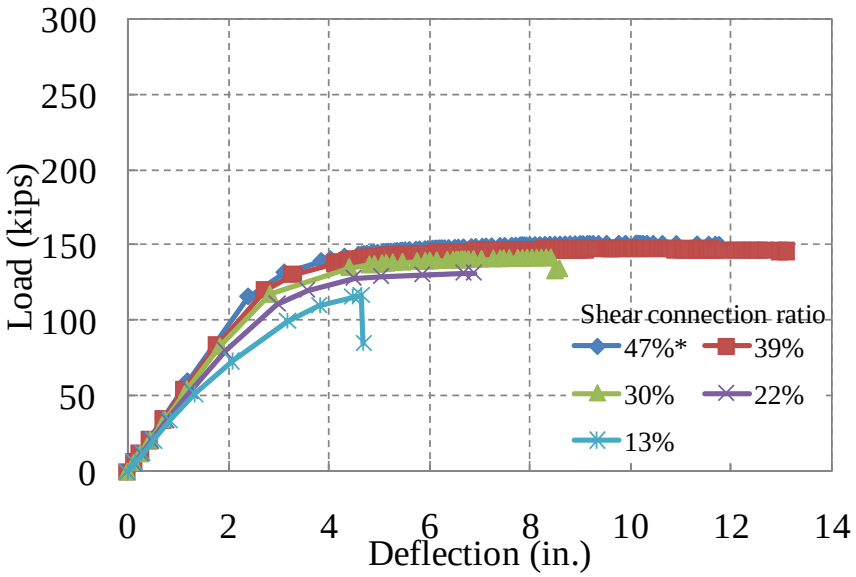

*: Convergence was not achieved before shear connector failed.

Figure C.3: Load-deflection relations of composite beams (W27x94, 50-ft span)

C.2. Composite Beams with W30x99 Section

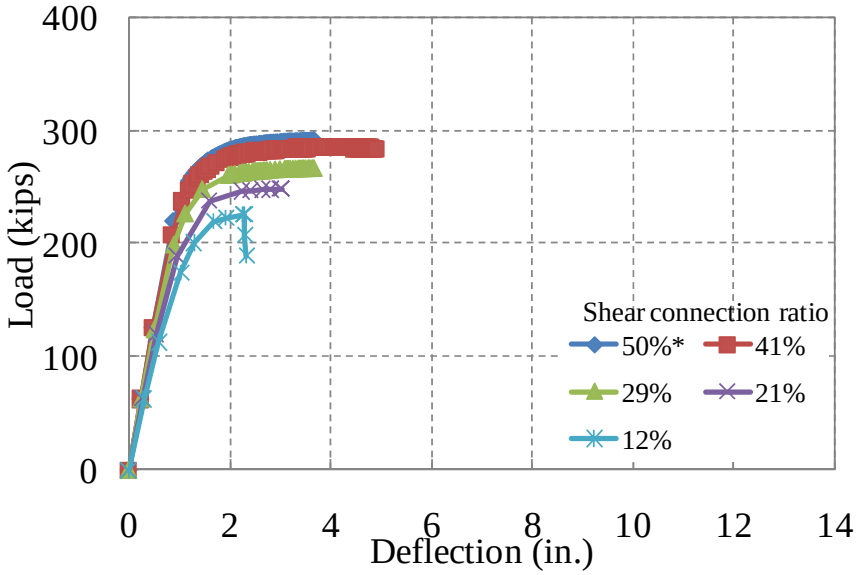

*: Convergence was not achieved before shear connector failed.

Figure C.4: Load-deflection relations of composite beams (W30x99, 30-ft span)

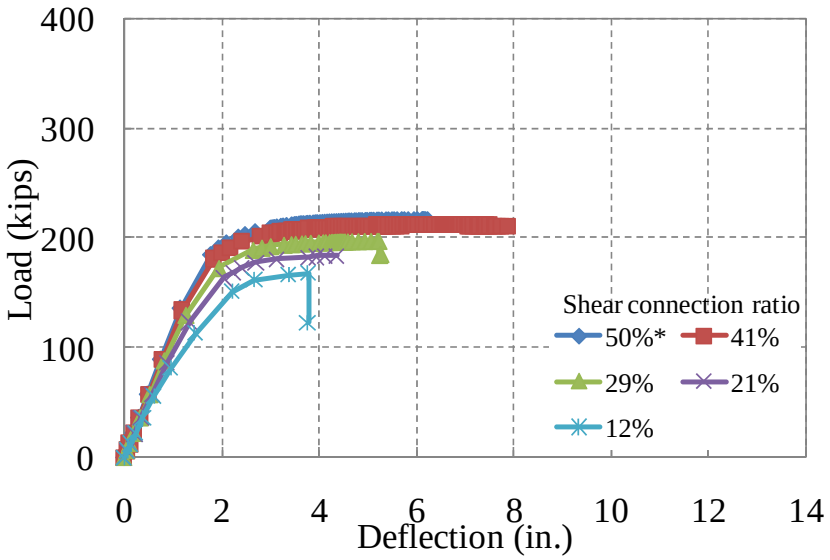

*: Convergence was not achieved before shear connector failed.

Figure C.5: Load-deflection relations of composite beams (W30x99, 40-ft span)

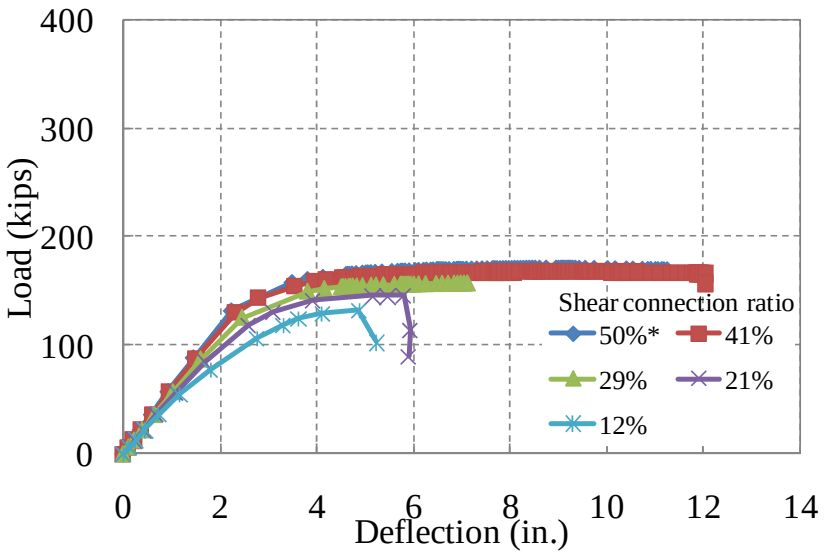

*: Convergence was not achieved before shear connector failed.

Figure C.6: Load-deflection relations of composite beams (W30x99, 50-ft span)

C.3. Composite Beams with W33x130 Section

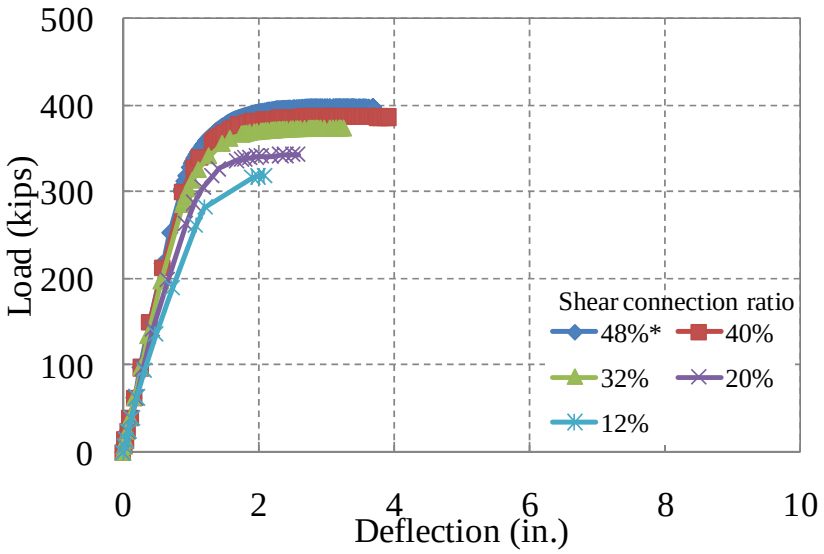

*: Convergence was not achieved before shear connector failed.

Figure C.7: Load-deflection relations of composite beams (W33x130, 30-ft span)

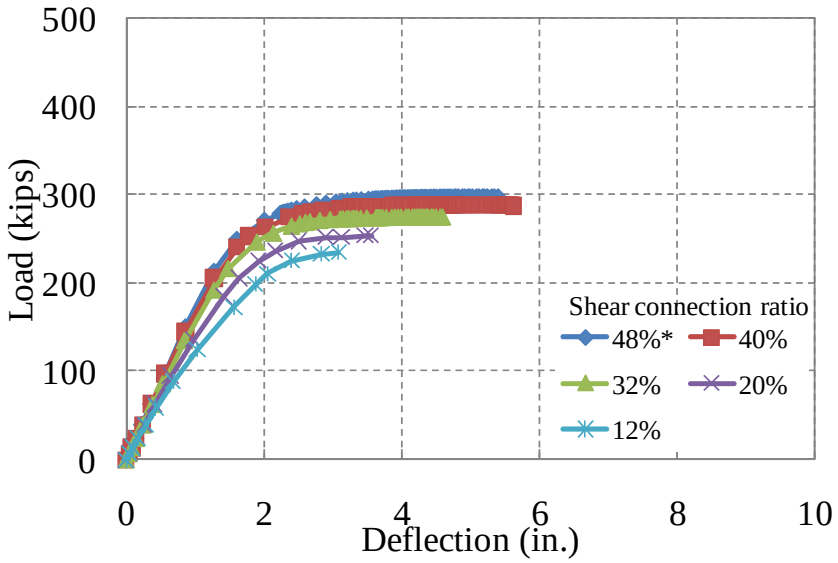

*: Convergence was not achieved before shear connector failed.

Figure C.8: Load-deflection relations of composite beams (W33x130, 40-ft span)

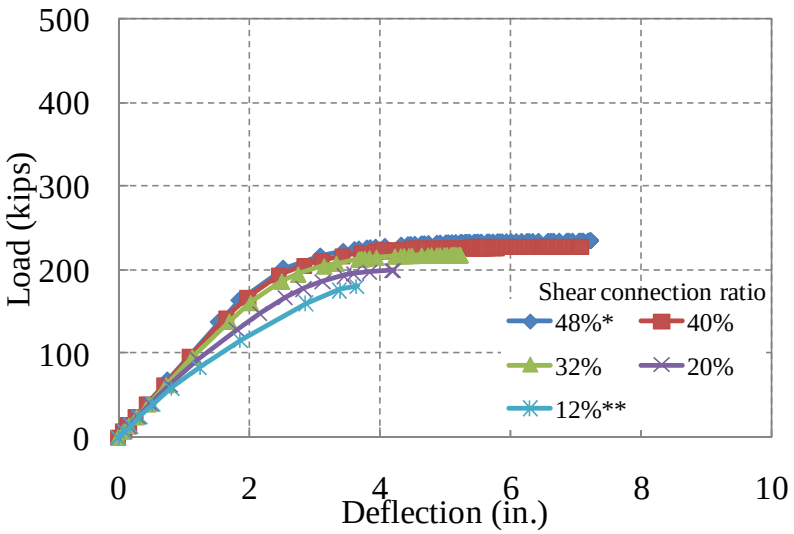

*: Convergence was not achieved before shear connector failed.
**: Max. load was less than simple plastic analysis result.

Figure C.9: Load-deflection relations of composite beams (W33x130, 50-ft span)

C.4. Composite Beams with W36x160 Section

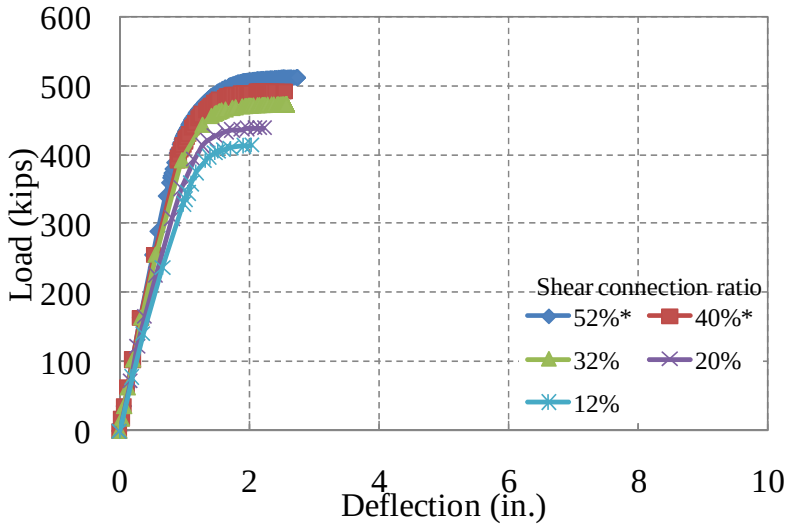

*: Convergence was not achieved before shear connector failed.

Figure C.10: Load-deflection relations of composite beams (W36x160, 30-ft span)

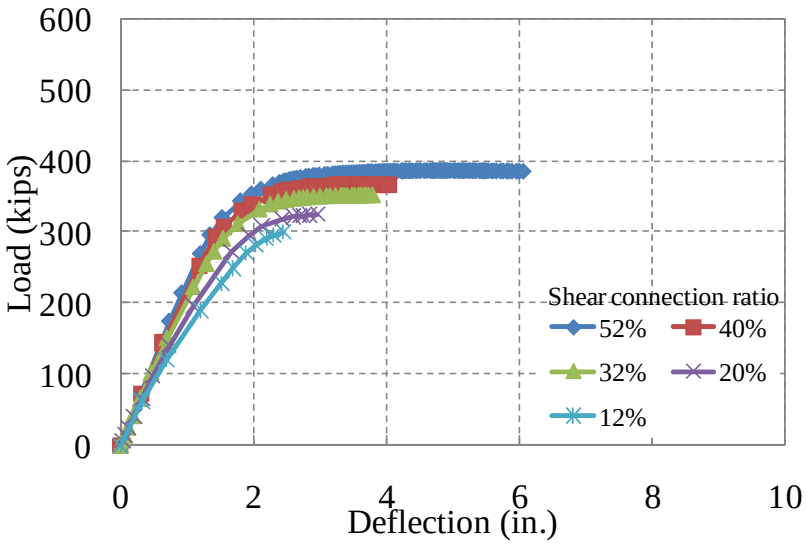

Figure C.11: Load-deflection relations of composite beams (W36x160, 40-ft span)

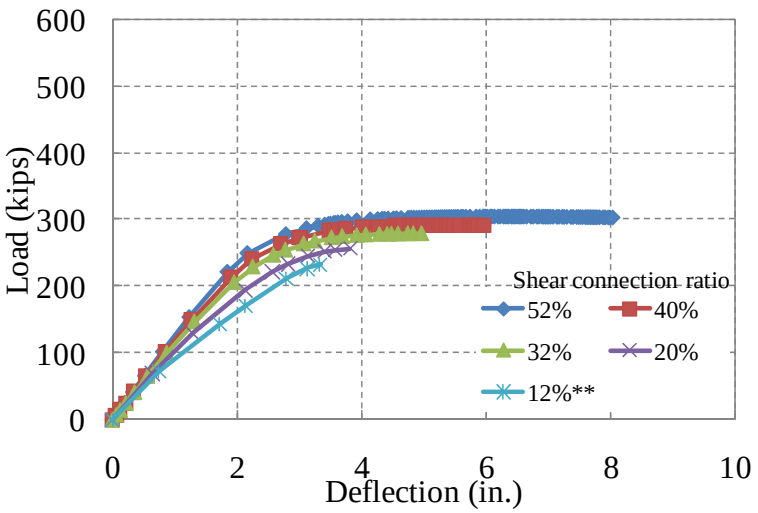

**: Max. load was less than simple plastic analysis result.

Figure C.12: Load-deflection relations of composite beams (W36x160, 50-ft span)

References

AASHTO (2007). "LRFD Bridge Design Specifications Interim Customary U.S. Units, 4th Edition." American Association of State Highway and Transportation Officials, Washington, D.C.

AASHTO (2002). "Standard Bridge Design Specifications (2002) 17th Edition." American Association of State Highway and Transportation Officials, Washington, D.C.

AASHTO (2005). "Guide Manual for Condition Evaluation and Load and Resistance Factor Rating (LRFR) of Highway Bridges." American Association of State Highway and Transportation Officials, Washington, D.C.

AASHTO (2003). "Manual for Condition Evaluation of Bridges, Second Edition." American Association of State Highway and Transportation Officials, Washington, D.C.

ABAQUS (2007). "ABAQUS Analysis User's Manual (Ver. 6.7)." ABAQUS, Inc, Pawtucket, RI.

ACI (2005). "Building Code Requirements for Structural Concrete (ACI 318-05) and Commentary (ACI 318R-05)." American Concrete Institute, Farmington Hills, Michigan, 2005.

AISC (2005). "Steel Construction Manual Thirteenth Edition." American Institute of Steel Construction, U.S.A., 2005.

Benac, D. J. (2007). "Technical Brief: Avoiding Bolt Failures." Journal of Failure Analysis and Prevention, Vol. 7, No. 2, pp79-80.

Bowen, C.M. and Engelhardt, M.D. (2003). " Analysis, Testing, and Load Rating of Historic Steel Truss Bridge Decks." Center for Transportation Research Report, CTR 1741-2, University of Texas at Austin.

Hungerford, B.E. (2004). "Methods to Develop Composite Action in Non- Composite Bridge Floor Systems: Part II." MS Thesis, Department of Civil, Architectural and Environmental Engineering, University of Texas at Austin.

Johnson, R.P., May, I.N. (1975). "Partial-Interaction Design of Composite Beams." The Structural Engineer 53(8), 305-311.

Kayir, H. (2006). "Methods to Develop Composite Action in Non-Composite Bridge Floor Systems: Fatigue Behavior of Post-Installed Shear Connectors." MS Thesis, Department of Civil, Architectural and Environmental Engineering, University of Texas at Austin.

Kwon, G. (2008). "Strengthening Existing Steel Bridge Girders by the Use of Post-Installed Shear Connectors." Ph.D. Dissertation, Department of Civil, Architectural and Environmental Engineering, University of Texas at Austin.

Kwon,G., Hungerford, B., Kayir, H., Schaap, B., Ju, Y.K., Klingner, R. and Engelhardt, M. (2007). "Strengthening Existing Non-Composite Steel Bridge Girders using Post-Installed Shear Connectors," Report No. FHWA/TX-07/0-4124-1, Center for Transportation Research, University of Texas at Austin, July.

Lam, D., Elliott, K.S., and Nethercot, D.A. (2000). "Parametric Study on Composite Steel Beams with Precast Concrete Hollow Core Floor Slabs." Journal of Constructional Steel Research, Vol 54, pp283-304.

McGarraugh, J.B., Baldwin, J.W. (1971). "Lightweight Concrete-Steel Composite Beams." Engineering Journal, American Institute of Steel Construction, 8(3), 90-98.

Ollgaard, J.G., Slutter, R.G., Fisher, J.W. (1971). "Shear Strength of Stud Shear Connectors in Lightweight and Normal-Weight Concrete." AISC Engineering Journal, 8, 55-64.

Schaap, B. A. (2004). "Methods to Develop Composite Action in Non-Composite Bridge Floor Systems: Part I." MS Thesis, Department of Civil, Architectural and Environmental Engineering, University of Texas at Austin.

Taly, N. (1998). "Design of Modern Highway Bridges." McGraw-Hill, New York, NY.

Viest, I.M. et al. (1997). "Composite Construction: Design for Buildings." McGraw-Hill, New York, NY.

Viest, I.M., Fountain, R. S., Siess, C.P. (1958). "Development of the New AASHO Specification for Composite Steel and Concrete Bridges." HRB Bull. 174, 1-17.